5-2014

Mechanisms Underlying Distinct Egfr Versus Fgfr-3 And -1 Dependency In Human Bladder Cancer Cells

Tiewei Cheng

MECHANISMS UNDERLYING DISTINCT EGFR VERSUS FGFR-3 AND -1 DEPENDENCY IN HUMAN BLADDER CANCER CELLS

by

Tiewei Cheng, M.D.

Approved:

_____

David J. McConkey, Ph.D.
Chairman, Supervisory Committee

_____

William Plunkett, Ph.D.

_____

Varsha Gandhi, Ph.D.

_____

Gary E. Gallick, Ph.D.

_____

Michael Ittmann, M.D. Ph.D.

Approved:

_____

Dean, The University of Texas
Graduate School of Biomedical Science at Houston

MECHANISMS UNDERLYING DISTINCT EGFR VERSUS FGFR-3 AND -1 DEPENDENCY IN HUMAN BLADDER CANCER CELLS

A

DISSERTATION

Presented to the Faculty of
The University of Texas Health Science Center at Houston and
The University of Texas M.D. Anderson Cancer Center
Graduate School of Biomedical Sciences

in Partial Fulfillment
of the Requirements
for the Degree of

DOCTOR of PHILOSOPHY

by

Tiewei Cheng, M.D.
Houston, Texas
May, 2014

DEDICATION

I would like to dedicate this dissertation to my parents, who have supported me over the course of my entire educational journey. Thank you for your love and understanding. To my uncle and aunt, who encouraged me to pursue graduate education and motivated me to complete this work. To my sweet girlfriend, you came to my life and brought me love and fun for the last three years. Thank you for your unconditional love. I love all of you, and this work is dedicated to you.

ACKNOWLEDGEMENTS

There are many people who helped me to achieve the completion of this work, and I couldn't have done this without any of them. First, my greatest appreciation is to my advisor Dr. David McConkey, who trained me to be a scientist in his laboratory. I sincerely appreciate all that he has done to guide me throughout my doctoral research. Thank you for demonstrating the scholarship, enthusiasm for science, leadership, integrity and creativity for the last five years. I couldn't say enough as a person how much I appreciate what you have invested in me. You are a great mentor.

I would also like to thank the faculty members who have served on my advisory and supervisory committee and tremendously impacted my graduate training. Dr. William Plunkett, thank you for serving on all of my committees for such a long time and providing me a research tutorial at you lab. It was a great experience. Dr. Varsha Gandhi, thank you for organizing and serving as director for such an exceptional ETAP program. I am so proud that I am part of it. Dr. Garry Gallick, thank you for leading my candidacy exam committee and serving on all of my committees. Your input to my research project is extreme valuable and helpful. Dr. Michael Ittmann, thank you for serving on my supervisory committee. Your comments and suggestion on my doctoral research helped me navigate

through the hard days. Special thanks to Dr. Walter Hittelman for his instruction to set up electronic microscope based invasion assay. Last but not least, Dr. Jeffery Myers, thank you for accepting me for research tutorial in your lab.

To my fellow students and lab mates, past and present, thank you for sharing the great experiences in the lab, both successful and miserable ones. I would also like to thank you for all of the advice and help over the last five years. I owe a large portion of my graduate training to all of you. Special thanks to Dr. Beat Roth, it was wonderful and exciting to work with you for the last two years. I am grateful to our close collaboration and friendship.

Lastly, I would like to thank all of my family and friends. Mom and Dad, thank you all for the support. Carly, thank you for being there for me and lending me a hand during the bad days. To my extended family, thank you all for your support and love over the last five years.

MECHANISMS UNDERLYING DISTINCT EGFR VERSUS FGFR-3 AND -1 DEPENDENCY IN HUMAN BLADDER CANCER CELLS

Tiewei Cheng, M.D.
Supervisory Professor: David J. McConkey, Ph.D.

The epidermal growth factor receptor (EGFR) and fibroblast growth factor receptor (FGFR) are activated by gene amplification, mutation and overexpression in bladder cancer, which drives tumor development and progression. Both EGFR and FGFR inhibitors are currently being tested in clinical trials. However, bladder cancer (BC) cells show remarkably heterogeneous sensitivities to both inhibitors, and the molecular determinants of this heterogeneity are presently unclear. Therefore, in this study, using selective EGFR and FGFR inhibitors in BC cells, we demonstrated that FGFR3 and FGFR1 play largely non-overlapping roles in mediating proliferation and invasion in the distinct “epithelial” and “mesenchymal” subsets of human BC cells. Furthermore, we examined the sensitivities to FGFR3 and EGFR inhibition in a panel of human BC cells, and found that FGFR3 and EGFR dependency are mutually exclusive biological phenotypes controlled by PPARγ-FABP4 pathway. This study significantly extends and complements our knowledge of molecular mechanism that mediates growth receptor dependent proliferation in BC.

TABLE OF CONTENTS

LIST OF FIGURES

CHAPTER 1

CHAPTER 3

CHAPTER 4

LIST OF TABLES

CHAPTER 1

CHAPTER 3

CHAPTER 4

CHAPTER 1. INTRODUCTION

1.1. Fibroblast growth factor family and its receptors in cancer

1.1.1. The FGF-FGFR signaling system

FGFs. The fibroblast growth factor (FGF) family is composed of 18 ligands that bind to four homologous high-affinity fibroblast growth factor receptors (FGFR1-4) [1]. The ligands can be classified into 6 subfamilies based on sequence similarity: FGF1-2; FGF3, FGF7, FGF10 and FGF22; FGF4-6; FGF8, FGF17 and FGF18; FGF9, FGF16 and FGF20; and FGF19, FGF21 and FGF23 [1]. There are also 4 “FGFs” that are numbered (FGF11-FGF14) but are not assigned to any subfamilies. Although these ligands share similar amino acid sequence with the FGF family, they do not activate FGFRs and therefore are not generally grouped into the FGF family [2]. Typically, FGFs can be classified as intracrine, paracrine and endocrine ligands respectively. Intracrine FGFs are intracellular molecules independent of FGFR and they mediate the function of voltage gated sodium channels [3]. However, paracrine FGFs, which is the major type of ligand, regulates physiological and pathophysiological functions by binding with and activating FGFRs at cell surface [4]. Recently, FGF19, FGF21 and FGF23 have been shown to function via endocrine route and are thought to medicate biological response via FGFRs. These ligands function over long distances, and are dependent on co-existence of klotho, a nuclear receptor binds to FGFRs to increase its binding affinity to specific endocrine FGFs, which then regulate vitamin D, bile acid, cholesterol, and glucose homeostasis [5].

FGFRs. The FGF ligands function by binding to the FGFR family and activating it through an HSGAG dependent manner. So far, four receptors (FGFR1, FGFR2, FGFR3 and FGFR4) have been identified in this family. FGFRs are comprised of three extracellular immunoglobulin domains (D1, D2, D3), a single-pass trans-membrane domain and a cytoplasmic tyrosine kinase domain (Figure 1.1) [6]. A distinct character of FGFRs is the presence of an acidic, serine-rich sequence between D1 and D2 domains, named the acid box. The D2 and D3 domains of FGFRs are required for ligand binding and are used to determine ligand specificity. However, the D1 domain and the acidic box are believed to play a vital role in receptor auto-inhibition. There are several FGFR isoforms generated by multiple mechanisms, and alternative exon splicing of the D3 domain is the most important one. For instance, alternative splicing at the second half of the FGFR1-3's D3 domain produces b and c (i.e. FGFR1b and FGFR1c) isoforms that carry out discrete FGF binding specificities (Figure 1.1) [7]. Specifically, b isoforms are generally produced in epithelial tissue while c isoforms are generated in mesenchymal tissue [8]. Therefore, the FGF family ligand-receptor binding specificity (Table 1.1) is partially mediated through the primary sequence differences among the 18 FGFs and 7 FGFR isoforms that are produced by alternative splicing. The ligand-receptor binding specificity is also

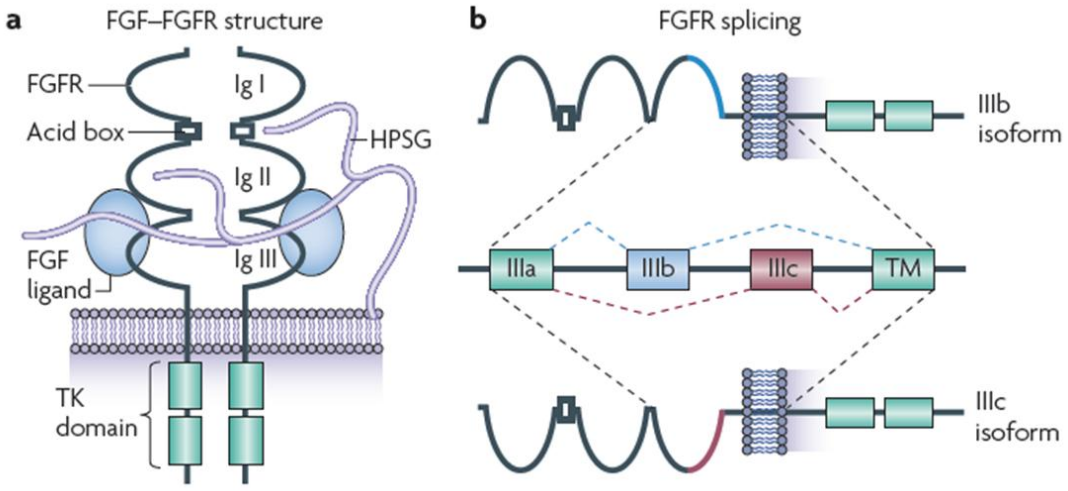

Figure 1.1 FGFR structure and alternative splicing. a. The basic structure of the fibroblast growth factor (FGF) –FGF receptor (FGFR) complex comprises two receptor molecules, two FGFs and one heparan sulphate proteoglycan (HSPG) chain. **b.** Ligand-binding specificity is generated by alternative splicing of the Ig III domain. The first half of Ig III is encoded by an invariant exon (IIIa), which is spliced to either exon IIIb or IIIc, both of which splice to the exon that encodes the transmembrane (TM) region. *Adapted from Turner N, Grose R, Nat Rev Cancer. 2010 Feb;10(2):116-29 with the permission from Nature Publishing Group.*

Receptor	ligands
FGFR1 IIIb	FGF1, FGF2, FGF3, FGF10, FGF22
FGFR1 IIIc	FGF1, FGF2, FGF4, FGF5, FGF6, FGF8, FGF9, FGF16, FGF17, FGF18, FGF20, FGF21, FGF23
FGFR2 IIIb	FGF1, FGF3, FGF7, FGF10, FGF22
FGFR2 IIIc	FGF1, FGF2, FGF4, FGF5, FGF6, FGF8, FGF9, FGF16, FGF17, FGF18, FGF20, FGF21, FGF23
FGFR3 IIIb	FGF1, FGF9, FGF16
FGFR3 IIIc	FGF1, FGF2, FGF4, FGF5, FGF6, FGF8, FGF9, FGF16, FGF17, FGF18, FGF20, FGF21
FGFR4	FGF1, FGF2, FGF4, FGF5, FGF6, FGF8, FGF9, FGF16, FGF17, FGF18, FGF19, FGF20, FGF21, FGF23

Table 1.1 FGF-FGFR binding specificity.

regulated by temporal and spatial expression patterns of FGFs, FGFRs and HSGAGs.

HSGAG binding and FGF-FGFR dimerization and activation. A functional FGF-FGFR complex is comprised of two FGF-FGFR-HSGAG (on a 1:1:1 basis) symmetrical units [9]. HSGAG binds to a basic canyon at the distal end of the membrane to facilitate and bolster protein to protein interactions. Ligands, shuttled by FGF-binding protein that releases FGFs from the extracellular matrix [10], bind to both receptors, and the two receptors interact with each other through a subdomain at the base of D2 [11]. HSGAG binding serves two primary purposes to promote the FGFR signaling. First, HSGAG promotes ligand-receptor dimerization by facilitating and strengthening protein-to-protein interaction between FGF and FGFR both inside and outside the complex through simultaneously binding to both ligand and receptor. Second, HSGAG binding to ligands stabilizes FGFs against degradation, and serves as a storage for ligands which also control the rate of ligand diffusion [12].

Downstream signaling and its negative regulation. Ligand dependent dimerization results in a structural shift in the FGFR receptor to activate the intracellular kinase domain that leads to an intermolecular trans-phosphorylation of the tyrosine kinase domains of the receptor. The phosphorylated tyrosine residues serve as docking site for the adaptor proteins [13], such as FGFR substrate 2 (FRS2), which are phosphorylated by FGFRs, resulting in the activation of multiple signaling

pathways. Among all of the adaptor proteins, FRS2 is the primary adaptor highly unique to FGFR signaling instead of other growth factor receptors. FRS2 binds to the intracellular domain of FGFRs using its phosphorylation-binding domain (PTB), and is then phosphorylated by the activated FGFRs. The activated FRS2 recruits its own adaptor proteins, SOS) and GRB2 to activate the downstream signaling pathway [13]. In addition, GRB2 associated binding protein 1 acts downstream of FGFR separately from FRS2 to activate an PI3K/AKT-dependent pathway [14].

Independent of FRS2 binding, a separate site in the intracellular portion of the activated FGFR binds to the SH2 domain of phospholipase Cγ (PLCγ). The activation of PLCγ facilitates protein kinase C (PKC) signaling [15,16], which partially augments the activation of MAPK pathway (Figure 1.2).

Following activation of FGFR signaling, signal attenuation and negative pathway feedback control could take places. First, FGFRs are internalized and then degraded, which is partially mediated by CBL-mediated mono-ubiquitylation [17]. Second, MAPK phosphatases such as MAPK phosphatase 3 and others phosphatases from Sprouty and SEF family are activated followed by FGFR activation to reduce the level of downstream signaling [18-21]. These proteins modulate the MAPK signal transduction cascade at multiple points [22].

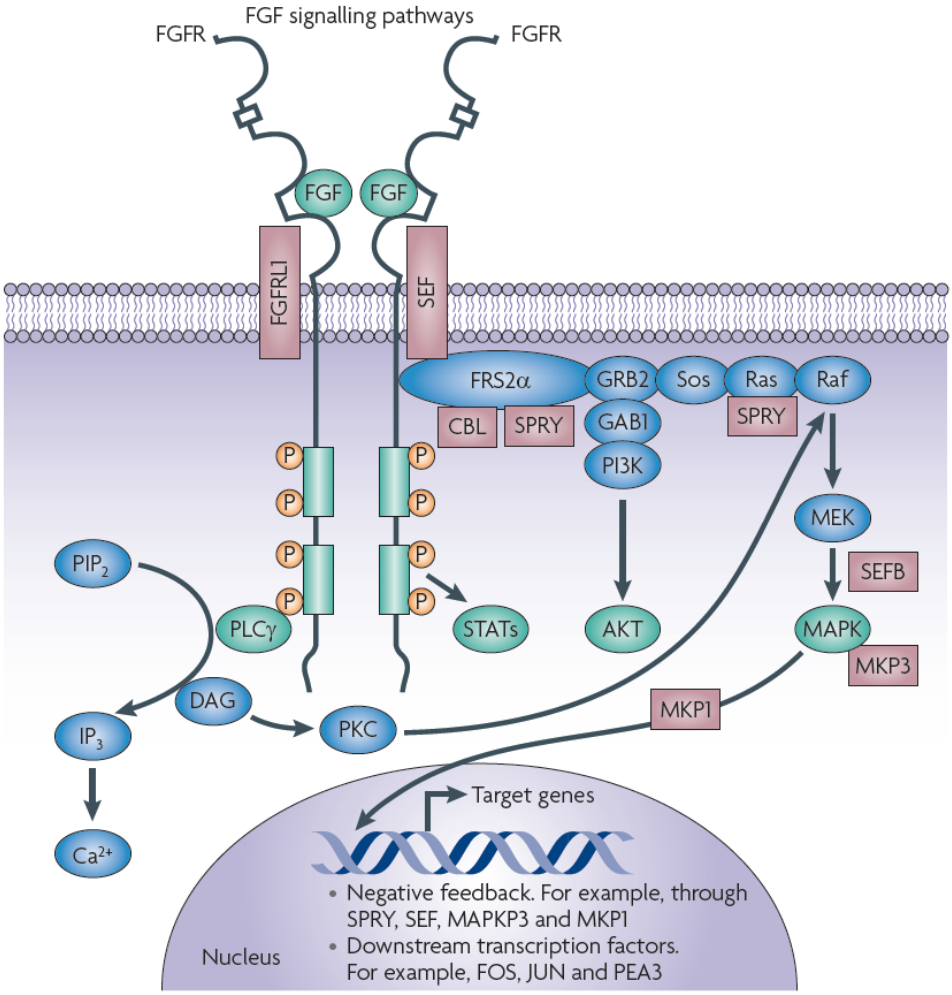

Figure 1.2 FGFR signaling network. The signal transduction network downstream of fibroblast growth factor (FGF) receptors (FGFRs), along with negative regulators. Following ligand binding and receptor dimerization, the kinase domains transphosphorylate each other, leading to the docking of adaptor proteins and the activation of four key downstream pathways: RAS–RAF–MAPK, PI3K–AKT, signal transducer and activator of transcription (STAT) and phospholipase Cγ (PLCγ) (green). Signaling can be negatively regulated at several levels by receptor internalization or the induction of negative regulators, including

FGFR-like 1 (FGFRL1), SEF, Sprouty (SPRY), CBL, MAPK phosphatase 1 (MKP1) and MKP3 (brown). *Reprinted from Turner N, Grose R, Nat Rev Cancer. 2010 Feb;10(2):116-29 with the permission from Nature Publishing Group.*

Physiological function of FGF-FGFR signaling. FGF-FGFR signaling plays a vitally essential role in embryonic development, wound healing, and tissue cross-talk.

Several of the 18 FGFs expressed in human cells are vital for embryonic development due to their essential roles in stimulating cell growth and migration. Specifically, extensive studies in mouse genetic models and human pathologies have indicated a pivotal role of FGFs in embryology from gastrulation to organogenesis [13,23,24]. For instance, FGF8 knockout mice display defects in gastrulation [25], and FGF9 and FGF10 knockout mice die at birth due to their inabilities to develop functional lungs [26,27]. In humans, FGF3 and FGF10 are associated with hereditary aplastic syndromes [28,29]; FGF20 is involved in Parkinson's disease [30,31]. In addition, defects of FGFRs mostly cause skeletal and growth defects in mouse models [32,33].

FGF-FGFR signaling also functions in wound healing and tissue repair in adults. In the process of wound healing, several FGFs, including FGF1, 2, 7 and 10, are released from the extracellular matrix to stimulate proliferation and migration in both mesenchyme and epithelium to accomplish wound closure and re-epithelialization [34,35]. FGF2 also has been shown to stimulate neovascularization, which is an essential component of the overall wound healing [36]. In parallel, endothelial cells express the IIIc isoforms of FGFR2 and FGFR3 in response to FGFs

stimulation [37].In addition, previous studies have shown the involvement of FGF16 and FGF18 in angiogenesis in cardiac tissue [38].

The cellular process of epithelial-mesenchymal tissue cross-talk plays an essential role in both embryonic development and wound healing. The interaction between these two tissue types is achieved by tissue specific FGFR variants generated by alternative splicing corresponding to FGFs produced in the respective tissue microenvironment [39,40]. As a result, the IIIb isoform of FGFR2 is predominately expressed in epithelia, whereas the IIIc isoform primarily exists in mesenchyme [8].

1.1.2. Deregulation of FGF-FGFR signaling in cancer

There is substantial evidence that supports the presence of aberrant FGF signaling in multiple types of malignancies. The underlying mechanisms of deregulation are manifold and largely tumor specific, but they can be divided into two groups. One group is genomic FGFR alterations including activating mutation, FGFR gene amplification and chromosomal translocation that result in ligand-independent receptor signaling. In contrast, the other group is alterations that drive ligand dependent activation including deregulation of autocrine and paracrine signaling and germline single nucleotide polymorphisms (Figure 1.3).

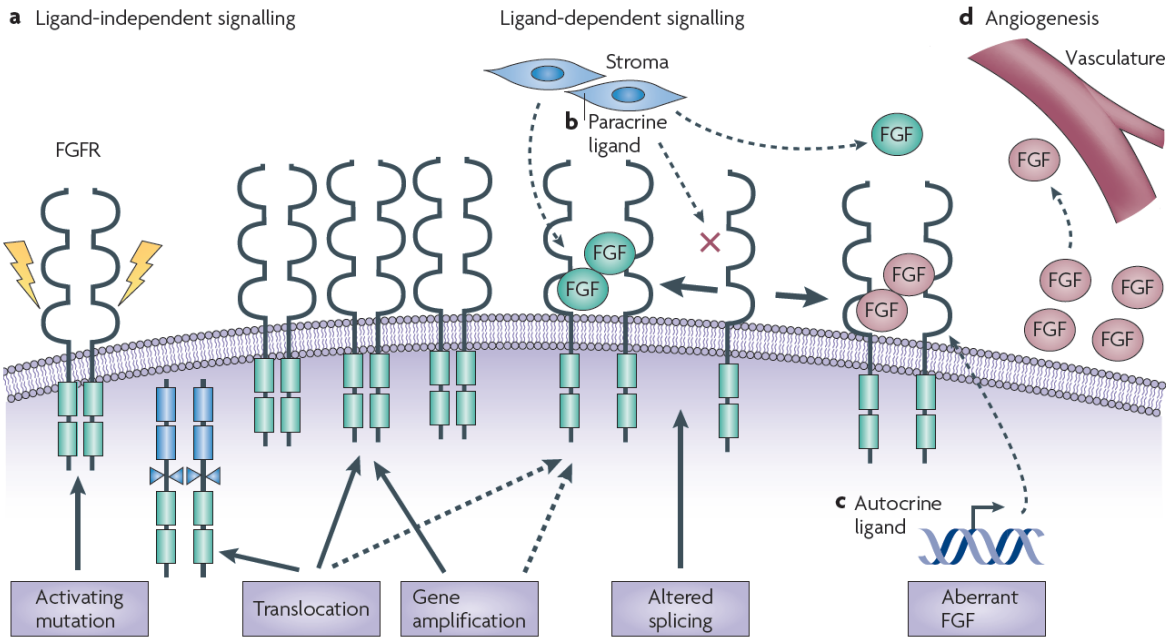

Figure 1.3 Mechanisms of pathogenic cancer cell FGF signalling. The ways in which fibroblast growth factors (FGFs) and FGF receptors (FGFRs) can be altered in cancer fall into four main groups. **a.** Genomic alteration of FGFR can occur through three mechanisms, leading to ligand-independent signalling. First, activating mutations can result in ligand-independent dimerization or constitutive activation of the kinase (shown by yellow lightning). Second, chromosomal translocations can also lead to ligand-independent signalling. Intragenic translocations generate fusion proteins, usually with the amino terminus of a transcription factor fused to the carboxy-terminal FGFR kinase domain, resulting in dimerization of the fusion protein and constitutive signalling. **b.** Establishment of a paracrine loop. Altered FGFR expression on a cancer cell can potentially occur by splicing, which alters FGFR specificity, or by amplification of an FGFR gene to express FGFR out of context, which is

activated by FGF (green) expressed by a stromal component. Tumour cells can stimulate stromal cells to release FGF ligands and increase the release of ligands from the extracellular matrix. **c.** Establishment of an autocrine loop. FGF ligands are produced in an autocrine fashion by a cancer cell (brown). The autocrine loop can be established by FGFR expression out of context or by the increased expression of FGF ligands. **d.** FGF stromal effects, including angiogenesis. FGF released from stromal cells or cancer cells can act on endothelial cells to promote angiogenesis. *Reprinted from Turner N, Grose R, Nat Rev Cancer. 2010 Feb;10(2):116-29 with the permission from Nature Publishing Group.*

Activating mutations. A profile of kinase gene mutation status from 210 different human cancers highlights the importance of FGFR mutation in tumor pathogenesis [41]. Substantial evidence suggests that FGFR mutations are most frequently associated with the development of urothelial cancer [42], although this type of mutation is identified in other types of cancers including multiple myeloma, prostate cancer and cervical cancer [43,44]. In addition, ~60% of urothelial cancers overall have somatic mutations in the FGFR3 coding region, and mutations are predominantly associated with non-muscle invasive urothelial cancers, whereas only 10-15% of muscle invasive urothelial cancers carry FGFR3 mutations [45]. The most common FGFR3 mutation (>50%) occurs in the extracellular domain named S249C, where this point mutation leads to constitutive receptor dimerization and activation independently of ligands [46,47]. Mutations also occur in the transmembrane domain such as S371C, and in the kinase domain such as K652E, but less frequently. Both mutations lead to constitutive activation of the receptors [48].

Interestingly, recent studies indicated that FGFR3 mutations more commonly co-exist with PIK3CA mutations in urothelial cancer, whereas FGFR3 mutations do not co-exist with HRAS mutation [49,50]. In addition, FGFR2 mutations do not coincide with KRAS mutations in endometrial cancer [51].

Gene amplifications. In general, amplification of FGFR1 and FGFR2 are identified more frequently than FGFR3 amplification [52], and FGFR3

amplification occurs much less frequently than activating mutation of FGFR3. FGFR1 amplification has been mostly studies in breast cancer which occurs at ~10% of all breast cancer cases, largely in estrogen receptor positive type [53,54]. In addition, amplification of FGFR1 was observed in ovarian cancer, lung cancer and bladder cancer but to a lesser extent [55-57]. However, it is still debatable whether higher level of FGFR1 leading to tumorigenesis by aberrantly responding to paracrine FGF ligands or by ligand independent activation of the signaling pathway. In general, FGFR2 amplification was reported in ~10% of gastric cancers [58,59]. Strong evidence suggests that FGFR2 amplification in gastric cancer cells results in ligand independent signaling, although paracrine secretion of FGF7 may partially promote cellular proliferation *in vivo* [60].

Chromosomal translocations. A good example of FGFR chromosomal translocation come from the study of multiple myeloma, where 15% of cancers harbor a t(4:14) translocation that directly connects FGFR3 at 4p16.3 to the immunoglobulin heavy chain IGH locus at 14q32 [61]. The intergenic translocation with the breakpoints at ~70kb upstream of FGFR3, renders the FGFR3 gene to be controlled by highly active IGH promoter. Ultimately, the consequence of the translocation is to cause high level overexpression of FGFR3, which leads to aberrant ligand dependent or independent signaling [62]. It is also important to note FGFR3 mutations exist in a fraction (~5% cases) of the t(4:14) multiple myeloma, which would possibly further reinforce the FGFR3 signaling [63]. The importance

of this t(4:14) translocation in multiple myeloma has been modeled using transgenic mice [61], and is associated with poor prognosis. Studies also demonstrated the t(4:14) myeloma cells are highly sensitive to FGFR3 inhibition [64,65]. In addition, several FGFR intragenic translocations have been discovered, which typically results in a fusion protein comprised of the N terminus of a transcription factor fused onto an FGFR kinase domain which leads to constitutive FGFR dimerization and activation [66-68].

In urothelial cancer, a recent study identified a new FGFR3-TACC3 translocation, where FGFR3 at 4p16.3 is re-arranged to form a t(4:7) translocation that results in a FGFR3-BAI1-associated protein 2-like 1 (BAIAP2L1) fusion at RT112, RT4 and SW780 [69]. The fusion receptor causes high levels of ligand independent activation of FGFR3. Several other studies have demonstrated that these cells exhibited a high level of dependency on FGFR3 signaling and were extremely sensitive to FGFR inhibition [47,49,70], which suggested that this translocation might be the determinant of FGFR dependency in RT112, RT4 and SW780. It is still unclear which mechanism causes the activation of FGFR signaling by the FGFR3-TACC3 fusion protein. However, William *et al* [69] suggested that the loss of the C-terminus of the FGFR3 in this translocation was not sufficient to cause the activation of FGFR signaling, which implicates that presence of fusion partners in this FGFR3-TACC3 translocation.

1.2. Epidermal growth factor receptor in cancer

1.2.1. The EGFR signaling system

The epidermal growth factor receptor (EGFR) is a transmembrane tyrosine kinase receptor of the ErbB family [71,72]. The ErbB family is consist of four related receptors: EGFR (Erb1/HER1), ErbB2 (HER2/neu), ErbB3 (HER3), and ErbB4 (HER4) [73,74]. EGFR activation engages three major downstream signaling pathways including MAPK/Erk pathway, PI3K/AKT and PKC pathway. These three pathways are cross-connected at multiple points that lead to signal interaction, integration and ultimately pathway cascade. As a result, the activation of EGFR in a particular cell results in a variety of biological consequences [74]. Specifically, receptor activation recruits and phosphorylates multiple intracellular substrates, which leads to pathway cascade that engage cellular functions including cell proliferation, growth and survival, cell migration and invasion, angiogenesis and tumor metastasis.

EGFR signaling. Similar to FGFR signaling, the EGFR signal cascade is comprised of three phases that are ligand binding and sub-sequential receptor dimerization and activation, phosphorylation of cytoplasmic substrate to initiate intracellular signaling cascade, and finally various cellular responses driven by diverse gene transcription activities [73]. EGFR is comprised of an extracellular region (ectodomain), a transmembrane domain, and an intracellular kinase domain with a

regulatory carboxyl terminal segment [75]. The ectodomain is composed of two types of sub-domains, namely the L domain and a cysteine-rich (CR) domain [73], where only the L type of domain is used for ligand binding. A variety of ErbB family ligands bind to EGFR and drive homo- or hetero-dimerization with the other three ErbB receptors [76-78]. However, EGF and transforming growth factor-α (TGFα) are believed to be the most important ligands for EGFR [79]. Following ligand binding, EGFR extracellular domains undergo substantial structure re-configuration that leads to homo- and hetero-dimerization of receptors [77], which activate the intrinsic EGFR tyrosine kinase domain and sub-sequential autophosphorylation of the receptor intracellular kinase domain. Followed by the activation of EGFR tyrosine kinase, multiple intracellular substrates including SOS and GRB2 are recruited to specific phosphotyrosine sites on the receptor [80]. There are 3 major downstream signaling pathways induced by EGFR activation. One of them is Ras/Raf/MAPK pathway. The activation of Ras by adaptor molecules Grb2/SOS initiates the activation of mitogen-activated protein kinases (MAPKs) and ERK1/2 through multiple steps of signal cascade, which in turn regulate transcription factors linked to cell proliferation and survival [81]. The second signaling route in EGFR activation is the PI3K/AKT pathway [82,83], which transduces a signal cascade to trigger cellular responses ranging from cell proliferation and survival to migration and invasion. The third downstream signaling is through protein kinase C and Stat. The activation of this route

initiates distinct transcriptional events that regulate a variety of cellular responses including cell survival, invasion and DNA repair [73].

1.2.2. Deregulation of EGFR in cancer

Similar to FGFR deregulation in cancer, deregulation of tightly controlled EGFR signaling drives the development of malignancy (oncogene addiction) in multiple types of cancer. Among them, non-small cell lung carcinoma (NSCLC) is the mostly investigated due to its higher occurrence of EGFR deregulation and relative favorable response to EGFR targeted therapy compared to other types of cancer.

Several mechanisms of EGFR alteration, including EGFR gene amplification and activating mutation, overexpression of receptor and ligands, and/or loss of negative feedback regulation[84], could lead to the abnormal receptor activation, which ultimately drives the tumor development and progression. Below we will discuss the two most extensively studied EGFR alterations: EGFR gene amplification and activating mutation.

EGFR gene amplification. One of the most investigated EGFR alternations is activation of EGFR signaling through increased gene copy number through amplification. EGFR is frequently overexpressed in many human tumors including breast and lung cancer, head and neck cancer, urothelial cancer, colorectal cancer, ovarian cancer, prostate cancer, and glioblastoma [85]. The increased expression can exceed a threshold,

which results in ligand independent constitutive activation of its tyrosine kinase and signal cascade that drives EGFR oncogene addiction [74,86]. Elevated EGFR expression is a strong prognostic marker in head and neck cancer, ovarian cancer and bladder cancer [87]. Specifically, a great number of studies indicated that the increased EGFR expression highly correlated with poor clinical outcomes in multiple types of cancer, including breast, lung, head and neck, and urothelial cancers [88,89]. Furthermore, elevated EGFR gene copy number is associated with increased clinical response to EGFR TKI erlotinib and mAbs cetuximab in NSCLC [90].

Activating mutation. EGFR activating mutations were first reported in NSCLC through retrospective studies of EGFR mutation status in early clinical trials of gefitinib or erlotinib [91]. It was then discovered that EGFR activating mutations are strongly predictive of benefit from EGFR targeted therapy [91] mainly because the gain-of-function mutation drives continued oncogenic signaling (oncogene addiction). Up to date, there are two most common mutation types that account for >90% of EGFR mutations revealed in NSCLC. Mutations in exon 19 that account for 45-50% of EGFR mutation incidence result in small in-frame deletions [92]. The second most common mutation locating in exon 21 (activation loop of EGFR) is a point mutation L858R that comprise about 45% of EGFR mutation [92]. Overall, the activating mutations cause ligand independent

activation of EGFR signaling and simultaneously result in EGFR oncogene addiction.

Additionally, EGFR mutations can be accompanied by gene amplification. For example, EGFRvIII, a deletion variant that lacks exon 2-7 (extracellular domain), forming a constitutively active receptor was found predominantly in malignant gliomas (20%-30%), where 50%-60% of patients bearing the mutation also showed amplification of wild type EGFR [93]. Follow up studies revealed that EGFRvIII was also expressed in head and neck cancer, lung cancer and breast cancer, although the occurrence rate was not as high as it is in malignant gliomas [94].

1.3. Role of FGFR and EGFR signaling in the development of bladder Cancer

1.3.1. Bladder cancer stratification and management

Bladder cancer occurs with a very high incidence worldwide. Each year, ~400,000 new cases are diagnosed and ~ 150,000 disease-related deaths occur [95]. In United States, BC was ranked as the fourth most common malignancy and eighth most common cancer-related death in men in 2012 [96]. The most frequent histologic type of BCs is urothelial carcinoma (UC) (~90%), whereas squamous cell carcinoma and adenocarcinoma combined accounts for <10% of BCs [97]. BCs are diagnosed using the TNM classification system along with tumor grade, which helps surgical

and medical oncologist to determine the treatment regimens and to predict the prognosis. The TNM classification system describes the depth of tumor penetrating into the bladder tissue (T), the status of regional lymph node (N) and the presence or absence of distant metastases (M).

Bladder cancer can be separated into two major phenotypic variants: superficial non-muscle-invasive UCs and muscle invasive UCs [98]. Up to 80% of the BCs are superficial non-muscle-invasive tumors at the time of diagnosis [97]. These tumors arise from hyperplastic urothelium and tend to localize within the bladder lining and connective tissues, therefore only a small portion (~20%) will eventually progress to become invasive tumors. The non-muscle-invasive BCs are normally managed by cytoscopic resection with or without intravesical instillation of immunotherapy agents including bacillus Calmetee-Guerin (BCG) [99]. However, up to ~70% of these tumors recur as non-muscle-invasive disease, which results in the need for long-term surveillance and frequent tumor resection and disease management, therefore making BC one of the most expensive malignancies to manage [99]. On the other side, ~20% of BCs are muscle-invasive tumors at the time of diagnosis [97]. These tumors arise from severe dysplasia or carcinoma in situ (CIS) and tend to invade into bladder muscle layer and finally metastasize to regional lymph nodes and distant organs. Therefore, muscle-invasive BCs are highly lethal. The standard care for muscle invasive BCs is radical cystectomy, with or without adjuvant or neoadjuvant chemotherapy [99].

Regardless of recent advance in radical cystectomy, chemo-radiation therapy, chemotherapy and targeted therapy, 50% of the muscle-invasive BC patients die after 5 within of diagnosis [99]. Therefore, it is very important to identify the molecular mechanisms underlying the metastatic profile of muscle-invasive BC and progressive profile of superficial BC into muscle invasive phenotype.

1.3.2. Role of FGFR and EGFR signaling in bladder caner

Multiple mechanisms of FGFR activation in bladder cancer have been identified in recent studies. For example, ~70% of low grade non-muscle-invasive BCs carry FGFR3 mutations which drive ligand independent activation of FGFR3 [100]. Furthermore, several studies have provided direct evident to support the cause-effect link between the present of FGFR3 activating mutations and bladder cancer tumorgenesis [101,102]. Moreover, overexpression of FGFR3 and FGFR1 accounts for ~25% and 15% of this disease respectively [97,103]. Experimental studies have identified FGFR1 activation as the underlying mechanism that drives cell proliferation and invasion [103,104]. Overall, FGFR signaling is showed to mediate cell proliferation, cell migration and invasion and tumor growth and metastasis in bladder cancer [70,104,105]. Moreover, FGFR inhibitors showed substantial inhibitory effects against proliferation, invasion and tumor metastasis in preclinical models both *in vivo* and *in vitro* [70,103,104]. In summary, FGFR signaling is activated in bladder cancer

to drive tumor development and progression, which provides a rationale for FGFR targeted therapy in bladder cancer patients.

Similarly, EGFR signaling has long been implicated in bladder cancer though the molecular mechanism by which EGFR regulates bladder cancer biology are still not very clearly defined. For example, EGFR overexpression in bladder cancer is reported by several studies [106,107] and the overexpression of its ligands in bladder cancer is also revealed by other studies [108,109] . Overall, EGFR signaling is found to regulate cell proliferation and tumor growth, cell migration and invasion, and angiogenesis in bladder cancer [110]. Additionally, the overexpression of EGFR highly correlates with not only tumor grade and stage [111], but also patient survival [112]. Furthermore, previous work showed that transgenic overexpression of EGFR in bladder cancer cells promotes tumor development and progression in xenograft [113], which directly supported the role of EGFR in driving tumor biology of bladder cancer. Moreover, clinically relevant EGFR antagonists and inhibitors showed significant anti-proliferative and anti-angiogenic effects in preclinical research [114,115]. In summary, all of the evidence provides direct rationale to clinically target EGFR in bladder cancer patients.

1.4. FGFR and EGFR targeted therapy

As discussed above, manifold experimental evidence suggested the role of deregulated FGFR and EGFR in certain cancers including bladder cancer, lung cancer, head and neck cancer, colon cancer and multiple myeloma. Moreover, preclinical studies found significant anti-tumor activities of FGFR and EGFR antagonists both *in vitro* and *in vivo*. Therefore, investigating clinical utilization of FGFR and EGFR targeted therapy has become the frontier of translational and clinical research, and there is high level of enthusiasm to develop promising novel agents for FGFR and EGFR targeted therapy given the urgent needs to seek better treatment paradigms to improve patient outcome in clinic.

Although several approaches have been tested to target FGFR and EGFR, the two most extensively studied and advanced approaches are monoclonal antibodies [116] (mAbs) directly against the receptors extracellular region and low-molecular-weight tyrosine kinase inhibitors (TKIs) [117] that interfere with intracellular tyrosine kinase domain (Figure 1.4). The antibodies bind to the extracellular region of the receptors and compete with ligands, whereas the TKIs compete intracellularly with ATP for binding sites at receptor's tyrosine kinase domain. However, at the downstream level of signaling pathways, antibodies and TKIs have similar effects because both of the approaches lead to an effective blockade of the primary downstream signal transduction including the MAPK pathway [118], the PI3K/Akt pathway [119], and the PKC/Stat pathway [120]. In

contrast, there may be two differences between mAbs approach and TKIs approach. Firstly, mAbs instead of TKIs are able to form a complex containing receptor that leads to receptor internalization [95], which in turn cause signal attenuation. Secondly, mAbs but not TKIs also have the capability to induce antibody-dependent cellular cytotoxicity (ADCC) [96]. Below, we will separately discussed FGFR and EGFR targeted therapy and their clinical development.

1.4.1. FGFR targeted therapy

Currently, FGFR targeted therapy is still at an early stage of clinical development where most of the development efforts are focus on anti-FGFR TKIs. Two FGFR specific TKIs are being evaluated in clinical trials despite the fact that multiple other FGFR antagonists have showed anti-tumor activity in preclinical research [121,122]. One of them is BGJ-398 (Figure 1.5 for structure, Table 1.2 for *in vitro* IC_{50}) that is developed by Novartis and is evaluated in advanced solid tumor with FGFR1 or FGFR2 amplification or FGFR3 mutation in phase I clinical trial on does escalation studies (NCT01004224). Another one is AZD4547 (Figure 1.5 for structure, Table 1.2 for *in vitro* IC_{50}), developed by AstraZeneca that just finished its phase I clinical trial with advanced solid tumors (NCT01213160). The drug is currently tested in phase II clinical trials in solid tumors (NCT01795768) as single drug or in combination with hormonal therapy for breast cancer patients (NCT01202591) or in combination with

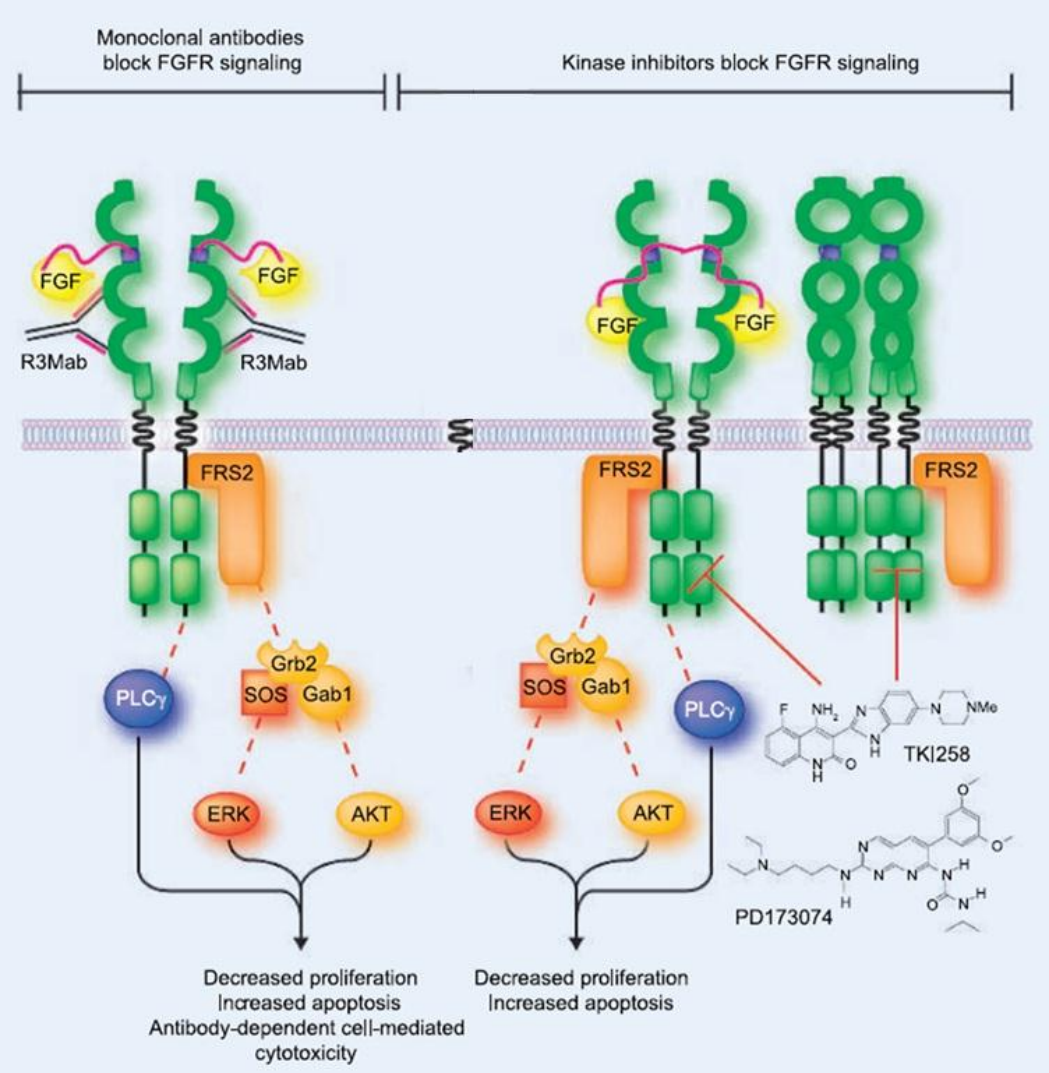

Figure 1.4 Schematic diagram depicts two approach for targeted therapy. Left panel, FGFR-specific monoclonal antibodies bind the extracellular domain of the receptor and inhibit FGFR signaling, causing changes in tumor cell proliferation and survival.

Right panel, treatment of tumor cells with TKIs such as PD173074 or TKI258 blocks ligand-induced FGFR activity and constitutive FGFR signaling from mutated or amplified receptors. FRS2 Tyr phosphorylation decreases, causing an uncoupling of Grb2 from the adaptor protein and a

decrease in ERK and AKT activity. *Adapted from Nancy E. Hynes et al., 2010, Cancer Res; 70(13); 5199–202 with the permission from American Association for Cancer Research.*

chemotherapy for advanced gastric cancer or NSCLC patients (NCT01824901, NCT01457846). Regarding the mAb approach, a specific inhibitory monoclonal antibody targeting FGFR3 was development by Genentech, R3Mab [64] and is currently tested in preclinical models [64,123]. The preclinical study results provided direct *in vitro* and *in vivo* proof to support the translation of into clinical trials in patients with either bladder cancer or hematologic cancer. Overall, the various biological function of FGFR makes it very attractive therapeutic target, and future clinical development efforts are needed for proof-of-concept and developing successful clinical strategies to target FGFR.

1.4.2. EGFR targeted therapy

Compared to FGFR targeted therapy, EGFR targeted therapy has been in development for years, and there are several successful stories. Cetuximab [88], a chimaeric anti-EGFR mABs, was approved by the FDA for treating patients with advanced colon cancer refractory to irinotecan (CPT-11) in 2004. Other examples are gefitinib (Iressa, ZD1839) (Figure 1.5 for structure, Table 1.2 for *in vitro* profile of IC_{50}) and erlotinib, anti-EGFR TKIs. Gefitinib showed increased patient response rate in non-small cell lung cancer (NSCLC) from multiple phase II clinical trials [124,125], which led to accelerated FDA approval for treatment of advanced NSCLC refractory to

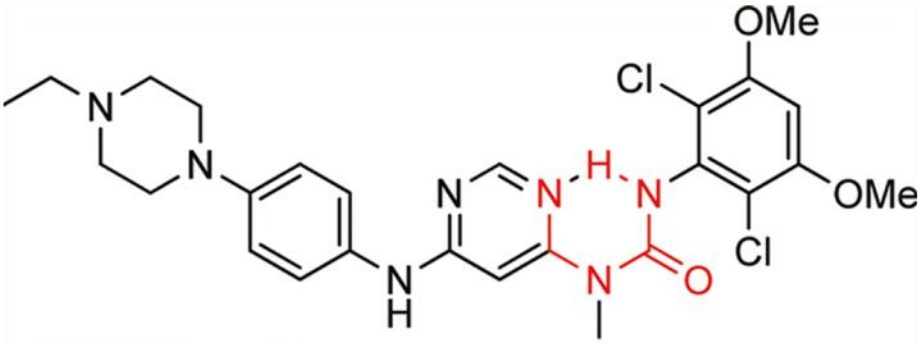

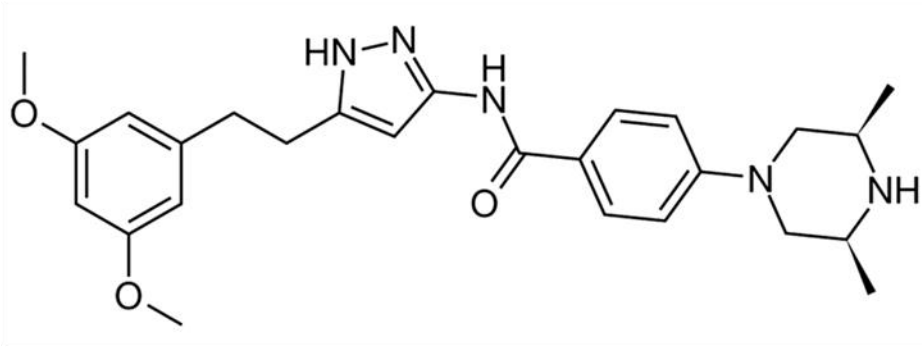

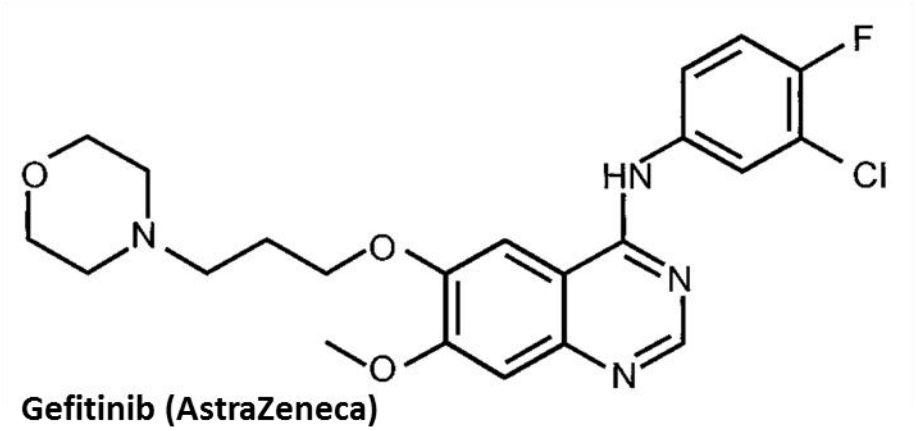

Figure 1.5 Structure of BGJ-398 [126]**, AZD4547** [127] **and Gefitinib** [128]**.**

A. *in vitro* profile of BGJ-398 and AZD4547

Kinase	Enzyme IC_{50} (μM)		Cellular IC_{50} (μM)	
	BGJ-398	AZD4547	BGJ-398	AZD4547
FGFR1	0.0009	0.0002	0.0029	0.012
FGFR2	0.0014	0.0025	0.0020	0.002
FGFR3	0.0010	0.0018	0.0020	0.040
FGFR4	0.060	0.165	N/A	0.142
VEGFR2	0.18	N/A	1.449	N/A
IGFR	>10	0.581	N/A	0.828
EGFR	>10	>100	N/A	N/A
erbB2	>10	>100	N/A	N/A
erbB3	>10	>100	N/A	N/A
erbB4	>10	>100	N/A	N/A
AKT	>10	>100	N/A	N/A
PI3K	>10	>100	N/A	N/A

*reference: [126,127]

B. *in vitro* profile of Gefitinib

Kinase	Enzyme IC_{50} (μM)
EGFR	0.027
erbB2	6.8
Raf	>10
MEK-1	>10
ERK-2	>10

*reference: [128]

Table 1.2 selectivity of BGJ-398, AZD4545 and Gefitinib

chemotherapy in 2003. Additionally, FDA approved erlotinib for treatment of metastatic NSCLC patients with EGFR exon 19 deletions or exon 21 substitution mutation in 2013 [129]. However, the follow up studies revealed that anti-EGFR agents, either mAbs or TKIs failed to improve survival benefit (overall survival) although tumor regression was achienved in multiple large clinical trials in NSCLC [130]. These observations reduced enthusiasm for continuous development of EGFR targeted therapy, and led to limited FDA approval for EGFR targeted therapy and restricted use of gefitinib in NSCLC patients. Therefore, it is of pivotal importance to investigate and discover biomarkers that can lead the selection of patients who are predicted to benefit from EGFR targeted therapy.

In bladder cancer, there is continued interest in EGFR targeted therapy. Specifically, multiple clinical trials that evaluate EGFR targeted therapy agents in conjunction with conventional chemotherapy underway. For example, erlotinib is being evaluated in muscle invasive bladder cancer patients both before and after surgery (NCT00380029). Overall, EGFR still remains as an attractive target in bladder cancer and future development efforts should focus on investigating clinical applicable biomarkers to identify the appropriate subset of patients who can benefit from EGFR target therapy strategy.

1.5. Escape mechanism of EGFR and FGFR targeted therapy

Various drugs targeting EGFR, through either mAbs or TKIs, have proven effective in subsets of patients in several types of cancer. Good examples are Cetuximab, a chimeric monoclonal antibody that is specific for the extracellular domain of the receptor, and gefitinib and erlotinib, TKIs competing with ATP for intracellular binding domain of the receptor, which have been approved for the treatment of several cancer types [72,84]. However, the majority of patients do not respond to EGFR targeted therapy and a high rate of acquired resistance to these therapeutic drugs is observed in patients that do respond [131], suggesting both intrinsic and acquired mechanisms of resistance. Recently, a number of studies indicated a secondary mutation of *egfr*, and activities of other tyrosine kinase receptor including cMET, IGF-1R and FGFRs as mechanisms for resistance. Thus, it is necessary to further understand the resistance mechanisms that help the development of novel strategies to overcome such resistance.

In contrast, FGFR targeted therapy is still at its early stage of development. Due to the incidence of FGFRs as oncogenic determinants in certain types of cancer including bladder cancer, there is a growing interest in developing selective FGFRs tyrosine kinase inhibitors. A good example is AZD4547, a pan FGFR1-3 inhibitor, which has recently entered clinical trials [127]. However, the success of FGFR targeted therapy will require knowledge of mechanisms of both intrinsic and

acquired resistance. So far, two individual studies identified the EGFR activation [132] and a gatekeeper mutation in FGFR3 [133] as two separate escape mechanisms of FGFRs target therapy and I will present details below.

1.5.1. Escape mechanisms of FGFR targeted therapy

Secondary V555M gatekeeper mutation of fgfr. Recently, Chell *et al* [133] generated a derivative of the KMS-11 myeloma cell line ($FGFR3^{Y373C}$, originally sensitive to FGFR inhibition) named KMS-11R by long-term exposure to an FGFR inhibitor (AZ8010), and showed that the KMS-11R acquired resistance to AZ8010. The KMS-11R cell line was also cross-resistant to multiple FGFR TKIs (AZD4547 and PD173074). Sequencing of FGFR3 in the KMS-11R cells demonstrated the presence of a heterozygous mutation at the gatekeeper residue, encoding $FGFR3V^{555M}$, which restricts the access of FGFR TKIs to the ATP binding pocket of the FGFR3. That structural change of the FGFR3 intracellular kinase domain enables this particular cell line to become resistant to FGFR antagonist. The resistant KMS-11R cells exhibits a constitutive activation of FGFR signaling regardless of the presence of FGFR TKIs.

Re-activation of EGFR signaling. A recent study by Turner's group [132] demonstrated that intrinsic or acquired activation of the EGFR contributes to the resistance of FGFR TKIs in FGFR3 activated cells. Their study showed that EGFR signaling was up-regulated following FGFR inhibition

though impaired EGFR receptor trafficking and the release from negative feedback in FGFR3 dependent cells, and combining the EGFR TKI with the FGFR TKI produced synergistic growth inhibition compared to the effects of inhibiting either receptor alone. These data suggested re-activation of EGFR signaling compensates for the loss of FGFR signaling that allows the cells to escape from FGFR inhibition. They also investigated mechanisms for the intrinsic resistance to FGFR inhibition, and suggested that dominant EGFR signaling in cell lines otherwise bearing activating FGFR3 mutation which represses the expression of mutant FGFR3 expression and leads to the intrinsic resistance to FGFR TKIs.

1.5.2. Resistance mechanisms of EGFR targeted therapy.

Secondary T790M mutation of *egfr*. The presence of a secondary mutation of the *egfr*, which leads to a change from threonine (T) to methionine (M) at position 790, was first reported in 2005 [134,135]. The occurrence of the point mutation in tumors that were originally sensitive to EGFR TKIs led to development of resistance to EGFR TKIs [135]. Structural studies of the intracellular kinase domain of EGFR revealed that T790M was located in the ATP binding pocket to which EGFR TKIs binds [136]. It was also demonstrated by structure analysis that the T790M point mutation results in a higher affinity to ATP and a relative lower affinity to EGFR TKIs [136]. The T790M mutation presents in approximately 50% of lung adenocarcinoma tissue as reported in the studies using clinical

specimens with acquired resistance to EGFR TKIs [137]. In contrast, tumor cells harboring the T790M mutation only constituted a minority of the cells before EGFR TKIs treatment. Therefore, the T790M point mutation was identified as a marker for acquired resistance to EGFR TKIs. In addition, previous studies indicated that the T790M mutation of *egfr* caused increased kinase activity, while exhibiting higher level of tyrosine phosphorylation as compared to wild-type EGFR, and showing a growth advantage over wide-type cells [138,139].

MET amplification and HGF overexpression. The MET amplification was reported in HG827GR, a human lung adenocarcinoma cell line with acquired resistance to EGFR TKIs, in 2007 [140]. Several studies showed MET amplification caused the autophosphorylation of MET itself, heterodimerization with HER3, and activation of the PI3K/Akt pathway in EGFR TKI resistant cells [140-142]. Thus, the constitutive activation of PI3K/Akt pathway independent of EGFR activation leads to the failure of EGFR TKIs, which results in the acquired resistance to EGFR TKIs. The analysis of clinical lung adenocarcinoma specimens revealed the incidence of MET amplification is approximately 20% in patients with acquired resistance [140]. It was also demonstrated that the MET amplification was independent of T790M point mutation in lung tumors [141]. In parallel, the overexpression of HGF, the main ligand for the MET tyrosine kinase receptor, was identified as another mechanism of resistance to EGFR TKIs [143]. Unlike MET amplification, overexpression

of HGF stimulates the PI3K/Akt pathway through MET phosphorylation that is independent of HER3 activation. Furthermore, it was reported that HGF promotes MET amplification and coexists with T790M mutation in patients with acquired EGFR TKIs resistance [144]. Together, these studies suggested that MET/HGF activation is one mechanism of EGFR resistance.

De-repression of FGFRs. Recently, Ware *et al* [145] reported that increased levels of FGFRs mRNA was observed in non-small cell lung cancer (NSCLC) cells treated with EGFR TKIs, suggesting an activated FGFR signaling after inhibition of EGFR pathway. They further confirmed that FGFR induction could result in FGFR signaling through ERK pathway. The study also demonstrated that either exposure to exogenous FGF2/7 or co-culture of NSCLC cells with human fibroblasts could rescue growth inhibition induced by EGFR TKIs in NSCLC cells via an FGFR dependent manner. In a separate study, Thomson *et al* [146] revealed that NSCLC cells with a mesenchymal phenotype exhibited remarkable reduction in sensitivity to EGFR specific monoclonal antibody, and also a decreased expression and phosphorylation of EGFR. However, these same cells showed aberrantly escalated FGFR expression and autocrine signaling that activates the MAPK and PI3K/Akt pathway. Their data suggested that activated FGFR signaling played a redundant pathway in NSCLC cells leading to the intrinsic resistant to EGFR monoclonal antibody. Together,

these results indicated activation of FGFRs tyrosine kinase signaling as one mechanism of resistance to EGFR inhibition.

1.6. Rationale of the study

It is evident that bladder cancer is one of the leading cancer types with respect to both occurrence and lethality in the US [96]. Therefore, it is critical to understand the biology of bladder cancer progression and metastasis in order to improve the management of the disease with the ultimate purpose to discover a “cure” for bladder cancer. Given the potential FGFRs and EGFR addiction that bladder cancer possesses, which was highlighted by recent publications [103,104,114,115], a great amount of research focuses on developing strategies to target FGFR and EGFR in bladder cancer. However, there exist remarkably heterogeneous responses to both EGFR and FGFR targeted therapy revealed by recent studies [70,115]. Therefore, it is crucial to understand the molecular mechanisms that drive such heterogeneity and to identify clinical biomarkers associated with the subsets patients who can maximally benefit from FGFR and/or EGFR target therapy. Hence, in this dissertation, I seek to better understand the role of FGFRs in driving distinct cell functions proliferation versus invasion, and to dissect the mechanisms that regulate discretely non-overlapping and mutually exclusive FGFR and EGFR dependency.

CHAPTER 2. MATERIALS AND METHODS

2.1. Chemicals and Reagents

BGJ-398, a novel and selective tyrosine kinase inhibitor (TKI) of FGFR1, 2 and 3, was generously provided by Novartis. Astra Zeneca generously provided AZD4547, a novel and selective tyrosine kinase inhibitor (TKI) of FGFR1, 2, and 3 (citation), as well as the EGFR TKI gefitinib (ZD1839, Iressa®, Astra Zeneca Inc.). For *in vitro* studies, all three TKIs were reconstituted in DMSO at a stock concentration of 10 mmol/L, stored at -20°C and diluted in medium just prior to use so that the concentration of DMSO never exceeded 0.1%. For *in vivo* studies, TKIs was dissolved in 1% polyoxyethylenesorbitan monooleate (Tween-80) and 99% deionized water to the desired concentration (12.5 mg/ml).

The antidiabetic drug rosiglitazone, a potent peroxisome proliferator activated receptor γ (PPARγ) agonist, was purchased from Cayman Chemical as were the PPARα activator Wy14643, the PPARγ antagonist GW9662, and the PPARβ antagonist Sulindac. The PPARβ agonist L-165,041 was purchased from Sigma-Aldrich. The PPARα antagonist GW6471 was purchased from Tocris Bioscience. PPAR agonists and antagonists were stored as stock solutions (100mmol/L in DMSO) at -20°C and diluted to the desired concentrations just before use.

Monoclonal antibodies for FGFR1, FGFR3 and bFGF were purchased from Cell Signaling. Monoclonal antibodies specific for CHOP, FABP4, Ki67 and Phospho-FRS2-α (Tyr436) (rabbit) were purchased from Cell

Signaling; antibodies against ERRFI1 and β-Actin (mouse) were from Sigma. Horseradish peroxidase-conjugated secondary antibodies were purchased from Bio-Rad (anti-rabbit) and Promega (anti-mouse).

Small interfering RNA (siRNA) Smartpools for FGFR1, FGFR3, CHOP, PPARα, β, and γ as well as nonspecific control were purchased from Dharmacon. Small hairpin RNAs (shRNA) used for stable FGFR1 (V3LHS_634640), bFGF (V3LHS_263179), CHOP (V3LHS_646287) and FABP4 (V3LHS_407556; V3LHS_407559; V3LHS_353665) knockdown as well as Precision LentiORFs derived from cDNA coding sequences for CHOP (PLOHS_100066517) and FGFR3 (PLOHS_100066410) overexpression were obtained from Open Biosystems.

2.2. Tumor cell lines and culture conditions

Cell lines were obtained from the University of Texas MD Anderson Cancer Center Bladder SPORE Tissue Bank, and their identities were confirmed by DNA fingerprinting using the AmpFlSTR® Identifiler® Amplification (Applied Biosystems) or AmpFlSTR® Profiler® PCR Amplification (Applied Biosystems) protocols. All cell lines were maintained as monolayers in modified Eagle's MEM supplemented with 10% fetal bovine serum, 1% vitamin solution (Mediatech), and 0.5% each of sodium pyruvate, L-glutamine (Life Technologies), penicillin/streptomycin solution, and nonessential amino acids (BioWhittaker) at 37°C in a 5% CO_2 incubator**.**

2.3. MTT assays

Cells (5×10^3) were plated in 96-well plates and allowed to adhere for 24 hours before they were incubated with or without increasing concentrations of BGJ-398 for 48 h or 5 days. MTT (3-(4,5-dimethylthiazol-2-yl)-2,5-diphenyltetrazolium bromide) assays were used to measure relative cell numbers based on conversion of MTT to formazan in viable cells. MTT dissolved in PBS (50µg/ml) was added to each well and plates were incubated for 2 hours. The medium was then removed and 100µl DMSO was added to each well to lyse cells and solubilize the formazan. A standard micro-plate reader (PowerWave 340, BioTek) was used to determine the absorbance (600 nm). Each experimental data point represents average values obtained from six replicates and each experiment was performed at least twice.

2.4. 3H-thymidine assay

BC cells were plated in 96-well plates supplemented with 10% FBS MEM at a density of 5×10^3 cells per well. After 24 hours, the cells were exposed to drugs at the indicated concentrations for 48 hours. The medium was removed and replaced with fresh MEM containing 1% FBS and 10 µCi/mL [Methyl-^{3}H]thymidine (MP Biomedicals) for 2 hours. The media was subsequently removed. 100µl of 0.1mol/L KOH were then added to each well. The cell lysates were harvested onto fiberglass filter membranes and the amount of radioactivity quantified in a scintillation counter (1450

MICROBETA Trilux liquid scintillation and luminescence counter; PerkinElmer life sciences). Each experimental data point represents average values obtained from six replicates and each experiment was performed at least twice.

2.5. Cell cycle analyses

Cells were plated in 6-well plates and maintained in 10% FBS MEM for 24 hours. Cells were then exposed to various concentrations of BGJ-398 for 48 hours or transfected with either FGFR1 or FGFR3 siRNA for 24 hours (reaching ~75% to 85% confluence) before they were harvested by trypsinization and pelleted by centrifugation. The pellets were then resuspended in PI-FACS buffer (50 µg/mL propidium iodide, 0.1% Triton X-100, and 0.1% sodium citrate dissolved in PBS). Propidium iodide fluorescence was measured by fluorescence-activated cell sorting (FL-3 channel, Becton Dickinson) using the instrument's cycle analysis software.

2.6. Anchorage independent growth assay

Human BC cell lines UM-UC3 and UM-UC13 wild type or non-targeted or bFGF/FGFR1 silenced cells were plated at 1×10^4 cells per well in 6-well-plates supplemented with 10% FBS MEM containing 0.6% agar. Cells were allowed to grow for 2 weeks. Images were acquired using an Olympus IX inverted-phase contrast microscope. The total numbers of colonies per random view (100×) and the average diameter of colonies

per random view (100×) were determined using a SliderBook image analyzer.

2.7. FGFR3 mutation analyses

DNA was isolated from BC cell lines using a genomic DNA extraction kit (Qiagen). PCR was performed to amplify exons 7 and 10 using AmpliTaq Gold DNA polymerase (Applied Biosystems) and the primers 5'-CGGCAGTGGCGGTGGTGGTG-3'(sense) and 5'-AGCACCGCCGTCTGGTTGGC-3' (antisense) for exon 7 and 5'-CCTCAACGCCCATGTCTTT-3' (sense) and 5'-AGGCAGCTCAGAACCTGGTA-3' (antisense) for exon 10 (Sigma Genosys). The following cycling variables were used: 95^{o} C for 10 min, 35 cycles of 95^{o} C for 30 s, then 65^{o} C (exon 7) or 58^{o} C (exon 10) for 30 s, and 72^{o} C for 30 s, followed by a final incubation at 72^{o} C for 10 min. Unincorporated primers and deoxynucleotides were removed using shrimp alkaline phosphatase and exonuclease I (U.S. Biochemical). Products were analyzed by Big Dye Terminator Cycle Sequencing (Applied Biosystems), and the data were analyzed with Sequencing Analysis 3.0 software (Applied Biosystems).

2.8. Real-time reverse transcriptase PCR analyses

Cells were harvested at ~75% to 85% confluence and total RNA was isolated using mirVANA^{TM} miRNA Isolation Kit (Ambion, Life Science). FGFRs and other genes of interests were analyzed by Taqman-based

real-time PCR (ABI PRISM 7500; Applied Biosystems). The comparative CT method was used to determine relative gene expression for each target gene; the cyclophilin A gene was used as internal control to normalize the amount of amplifiable RNA. Taqman primers was purchased from Applied Biosystem as follows: E-cadherin, Hs00170423_m1; TP63, Hs00978343_m1; ZEB1, Hs00232783_m1; Vimentin, Hs00185584_m1; FGFR1, Hs00915142_m1; FGFR2, Hs01552926_m1; FGFR3, Hs00179829_m1; FGFR4, Hs01106908_m1; bFGF, Hs00266645_m; FABP4, Hs01086177_m1; CHOP, Hs00358796_g1; PPARa, Hs00947536_m1; PPARb, Hs04187066_g1; PPARg, Hs01115513_m1; GPX2, Hs01591589_m1; CYP2J2, Hs00951113_m1; ERRFI1, Hs00219060_m1; FRS2, Hs00183614_m1; FGFR3, Hs00179829_m1.

2.9. Immunoblotting analyses

Cells were harvested at ~75% to 85% confluence and lysed. Protein concentrations were measured using the Bradford assay (Bio-Rad Laboratories). Lysates were boiled in sample buffer (62.5 mmol/L Tris-HCl (pH 6.8), 10% (w/v) glycerol, 100 mmol/L DTT, 2.3% SDS, 0.002% bromophenol blue) for 5 minutes and cooled on ice for 5 minutes. Lysates were separated on 8% or 12% SDS-PAGE gels at 110 volts in electrophoresis buffer (25 mmol/L Tris-HCl (pH 8.3), 192 mmol/L glycine, 0.1% SDS) and then electrophoretically transferred onto nitrocellulose membranes in transfer buffer (25 mmol/L Tris-HCl, 192 mmol/L glycine,

20% methanol) for 1 hour at 100 volts. The membranes were incubated in blocking buffer (5% nonfat milk in TBS: 10 mmol/L Tris-HCl (pH 8.0), 150 mmol/L NaCl) for 1 hour at room temperature while shaking and then rinsed once briefly with TBS-T (TBS containing 0.1% Tween-20). The membranes were then incubated with primary antibodies diluted 1:1000 in blocking buffer overnight, washed, and then incubated with second antibodies (anti-rabbit immunoglobulin, horseradish peroxidase–linked F(ab)2 fragment from mouse) diluted 1:8,000 in blocking buffer for 1 hour at room temperature while shaking. Immunoreactive proteins were detected using enhanced chemiluminescence (Amersham Biosciences) according to the manufacturer's instructions.

2.10. Boyden chamber invasion assays

Invasion chambers containing Matrigel-coated polyethylene terephthalate membranes with 8μm pores were purchased from BD BioSciences in a 24-well plate format. Cells (2.5×10^5) were released from tissue culture flasks using EDTA (1 mmol/L), centrifuged, suspended in a serum free medium and placed in the upper compartments of invasion chambers. Thirty percent fetal bovine serum medium was placed in the lower compartments as a chemoattractant and invasion assays were carried out for 48 hours. Each cell line or condition was plated in triplicate. To examine cell invasion after exposure to BGJ-398, cells that had not invaded were removed and the cells on the lower surface of the filter were stained with Diff-Quick (American Scientific Products, McGaw Park, IL).

Invasive activity was measured by counting the cells that had migrated to the lower side of the filter. To evaluate invasion after silencing FGFR1 or bFGF, membranes were removed after incubation for 48 hours at 37°C and stained in propidium iodide (Sigma-Aldrich) without removing cells from the upper surfaces of the membranes. The filters were mounted on glass slides and analyzed by confocal microscopy at 100x magnification. The planes of focus were adjusted so that the cells that had not invaded could be distinguished from the invaded cells and counted in 8 independent fields. Invasive activity was measured by calculating ratios of invaded to non-invaded cells.

2.11. Gene silencing and exogenous overexpression

For small interfering RNA (siRNA) silencing, cells were reverse-transfected with siRNA using RNAiMAX (Invitrogen) according to the manufacturer's guidelines and subjected to cell proliferation assays. In a parallel experiment, siRNA transfected cells were harvested at 48 hours. Total RNA and protein lysates were then analyzed for mRNA expression by RT-PCR and protein expression by immunoblotting to confirm target knockdown efficacy.

For stable short hairpin RNA (shRNA) knockdown and Precision LentiORFs (pLOC) overexpression experiments, cells were plated in a 6-well plates (10^5 cells/well) and transfected 24 hours later with the construct of interest. Polybrene (Santa Cruz) was used to increase the

efficiency of infection. Cells were continuously cultured. Five days after transfection, fluorescence-activated cell sorting (FACS) was performed to isolate the GFP-positive transfected cells followed by puromycin or blasticidin selection. Total RNA and protein lysates were then collected to confirm efficacy of knockdown and overexpression respectively.

2.12. Gene expression profiling analyses

All transcriptome data were generated from triplicates. Total RNA of each replicate was isolated independently using mirVANA^{TM} miRNA Isolation Kit (Ambion, Life Technologies) and RNA purity and integrity were measured by NanoDrop ND1000 (Thermo Scientific) and Agilent Bioanalyzer (Agilent Technologies). High quality RNA was then used for the synthesis of biotin-labeled cRNA using the Illumina RNA amplification kit (Ambion) as described previously. Briefly, 500 ng total RNA was converted to cDNA, then to cRNA by *in vitro* transcription, and finally purified. 1.5 µg cRNA was fragmented and hybridized to Illumina human-HT12V4 chips (Illumina). The slides were washed, scanned with Bead Station 500 (Illumina), and the signal intensities were quantified using GenomeStudio (Illumina). Quantile normalization in linear models was used to normalize the data, which were processed by established techniques as described previously (citation).

BRB ArrayTools (version 4.2, National Cancer Institute) was used to analyze the data. A class comparison tool within BRB ArrayTools was

used to identify top genes that were differentially expressed. The software uses a two-sample t test to calculate the significance of the observation with false discovery rate (FDR) ($P < 0.001$). To visualize expression patterns of genes, specific gene expression values were centered and adjusted to a mean of zero and then subjected for clustering with Cluster and TreeView (citation). Functional and pathway analyses were performed using the Ingenuity Pathway Analysis (IPA) software (Ingenuity System). The software contains a database for identifying networks and pathways of interest in genomic data. The “upstream regulator” analysis function was used to interpret the biological properties of gene profiling data.

2.13. Animals study

Female athymic nude mice (NCr-nu) were purchased from the National Cancer Institute. The mice were housed under specific pathogen-free conditions in the Animal Core Facility at The University of Texas M. D. Anderson Cancer Center. The facility has received approval from the American Association for Accreditation of Laboratory Animal Care and in agreement with current regulations and standards of the U.S. Department of Health and Human Services, the U.S. Department of Agriculture, and the NIH. The mice used in these experiments were 6 to 8 weeks old.

2.14. Subcutaneous xenograft experiments

Subcutaneous injections of UM-UC-9 and UM-UC-14 into the right flank were conducted using 10^6 cells/ 50µl Hank’s balanced salt solution

(HBSS) without calcium and magnesium. The tumors' major and minor axes were measured with a caliper twice a week. The tumor volumes (mm^3) were calculated using the formula: $width^2 \times length / 2$. Tumors were allowed to establish for 5 days before being randomized into groups for experiments.

2.15. Orthotopic xenograft experiments

Human BC cell line UM-UC-3 was transduced with a lentiviral vector encoding luciferase (luc) and red fluorescent protein (RFP, mCherry) as described previously (citation). After stable transduction with the luc-RFP reporter, cells were sorted by Fluorescence Activated Cell Sorting (FACS) using an Influx High-Speed sorter (BD Biosciences). Luciferase activity was quantified *in vitro* using d-luciferin (150 μg/mL) and the IVIS bioluminescence system (Xenogen Co.). To produce tumors in nude mice, sub-confluent cultures of labeled UM-UC3 were lifted with trypsin, mixed with 10% FBS MEM, centrifuged at 1,200 rpm for 5 min, washed in PBS, and resuspended in HBSS. Cells were then injected orthotopically into the bladder wall at a concentration of 5×10^5/50μL using a lower laparotomy. Mice bearing metastases were euthanized 5 to 8 weeks after tumor cell injection, the lymph node and distant metastases were excised, cut into small pieces using scalpels, exposed to 1% trypsin for 20 minutes, centrifuged (1,200 rpm for 5 min), and cultured in 10% supplemented MEM. After FACS sorting, the recycled cells were sub-confluently cultured and re-injected at a concentration of 2×10^5/50μL HBSS as described

above. Thus, tumor cell recycling was performed three times in order to select a highly metastatic UM-UC3 subpopulation which develops metastases in ~75% of mice. For our therapy experiment, we injected the 4^{th} cycle of recycled UM-UC3 at a concentration of 2×10^5/50µL. Mice with detectable tumor growth at the time of the first imaging (5 days after injection) were randomized into two groups (n = 7/group) and immediately were administrated either vehicle control (1% Tween-80) or BGJ-398 (12.5 mg/kg) once daily by oral gavage.

2.16. *In vivo* bioluminescence imaging

Bioluminescence imaging was conducted on an IVIS 100 imaging system with Living Image software (Xenogen) as described elsewhere (citation). In brief, animals were anesthetized with a 2.5% isoflurane/air mixture before imaging and injected s.c. with 15 mg/mL of luciferin potassium salt in PBS at a dose of 150 mg/kg. A digital gray-scale animal image was acquired and a pseudo-colored image was overlaid representing the spatial distribution of detected photons emerging from active luciferase. Signal intensity was quantified as the sum of all detected photons within the region of interest per second, separately counting each primary tumor and each metastatic site.

2.17. Collection of primary tumors and circulating tumor cells

Forty days after injection, when animals in the control group became moribund, mice were anesthetized with isoflurane as described above. To

measure the number of circulating tumor cells (CTCs), the maximal amount of blood (600-1200µl) was collected by cardiac puncture using 1 ml syringe, 22 gauge needle, and heparin-coated collection tubes as described previously. Mice were then euthanized with carbon monoxide. For further blood processing, red blood cells were lysed twice for 5 min with 10ml ACK lysis buffer (Invitrogen), and centrifuged for 5 min at 1200 rpm in Eppendorf tubes. The pellet was finally lysed and further processed for total RNA isolation using the mirVANA^{TM} miRNA Isolation kit (Ambion, Life Science). To quantify the CTCs, absolute quantification of real-time PCR analysis (Step One; Applied Biosystems) was used to generate cycle threshold (CT) values for human specific HLA-C primer (Hs00740298_g1) for each sample. RT-PCR analysis of the blood samples was run alone with standard isolates (0, 2, 20, 200, 2000, and 20,000 UM-UC3 cells in 100µl mouse blood). CT values of the standards were used to create a standard curve for UM-UC3 CTCs, and the number of CTCs of each blood sample was calculated accordingly.

2.18. Statistics

Statistical analysis was performed using GraphPad Prism Software (GraphPad). As appropriate, raw data or percentages were compared by unpaired Student's t-test. Tumor growth curves in xenografts were analyzed using Two-Way ANOVA with Bonferroni multiple comparisons. Statistical significance was set at $p < 0.05$.

CHAPTER 3. FGFR1 AND FGFR3 MEDIATE DISTINCT FUNCTIONS IN HUMAN BLADDER CANCER GROWTH AND METASTASIS

3.1. Results

3.1.1. Genome wide expression profiling of FGFRs and correlation with EMT markers.

Our previous studies [115,147] revealed a binary pattern of heterogeneity in a panel of 30 urothelial cancer cells. More specifically, it was shown that UC cells can be grouped into two major categories in terms of biomarker expression, forming: “epithelial” and “mesenchymal” subsets. In this study, we first analyzed the expression of all four FGF receptors and the dominant cancer-associated FGF ligand, FGF2/basic FGF, at the mRNA level in the panel of 30 cell lines using whole genome expression profiling (Illumina HT12V4 Platform) and compared the pattern of FGFR/bFGF expression to markers of the “epithelial” and “mesenchymal” subsets. The expression of FGFR3 correlated with E-cadherin and p63 [148-150], which suggested FGFR3 was expressed by “epithelial” UC cells. In contrast, the expression of FGFR1 and FGF2 directly correlated with vimentin, a “mesenchymal” marker (Figure 3.1). To more accurately define the “epithelial” and “mesenchymal” subsets within the panel of UC cells, we then used quantitative real-time reverse transcriptase PCR (RT-PCR) to measure the expression of two “epithelial” markers (E-cadherin and p63) and two “mesenchymal” markers (Zeb-1 and vimentin) in the cells. As shown in the Figure 3.2, the expression of E-cadherin directly correlated with p63 expression while inversely correlating with expression of Zeb-1

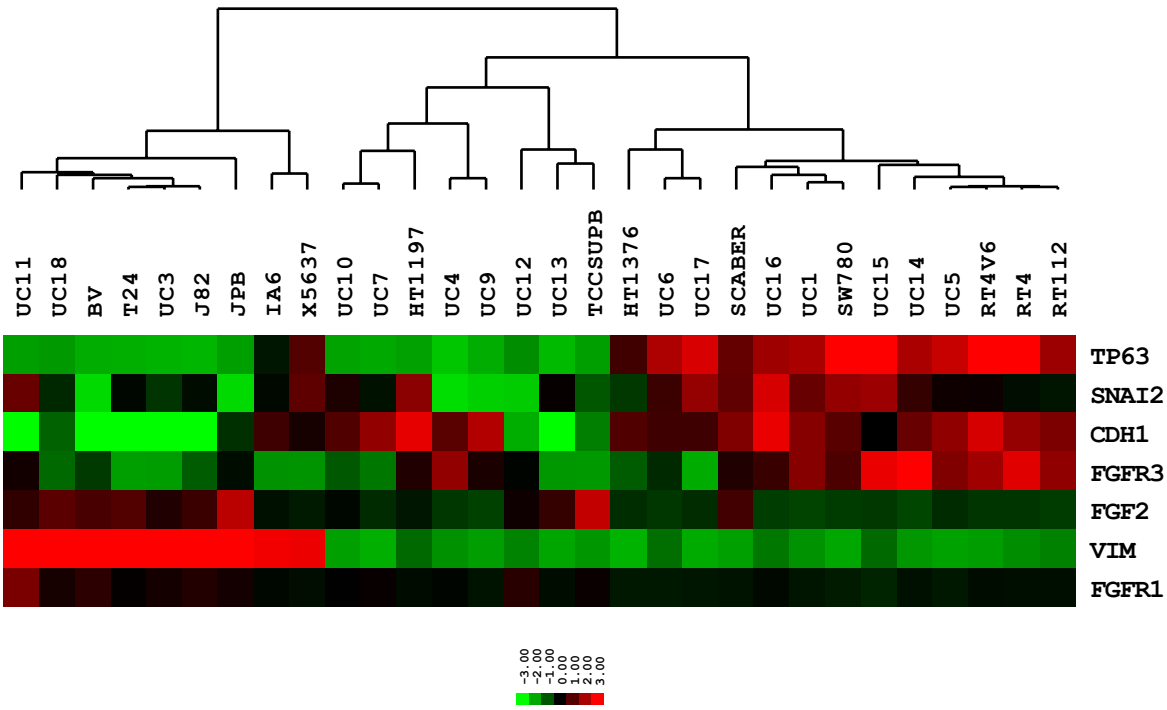

Figure 3.1 Expression of FGFR1, FGFR3 and bFGF in distinct subsets of human urothelial cancer cells. Correlation of FGFR1, FGFR3 and bFGF with canonical EMT markers. mRNA levels were measured by whole genome mRNA expression profiling (Illumina). The heatmap illustrate the expression of FGFR1, FGFR3, FGF2, p63 (TP63), E-cadherin (CDH1), Slug (SNAI2) and vimentin (VIM).

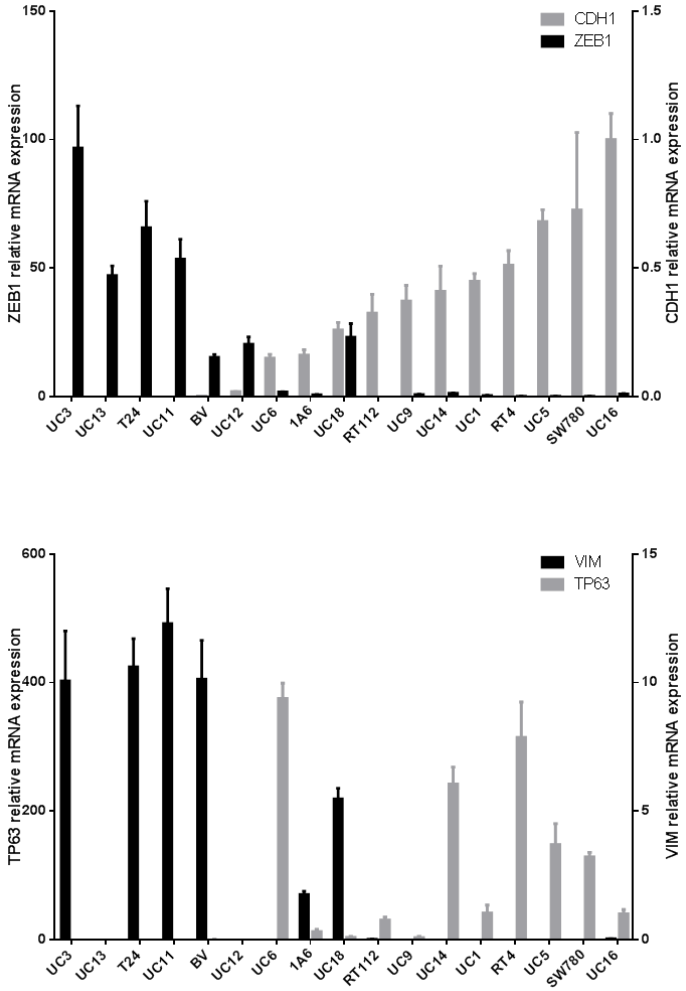

Figure 3.2 Expression of EMT markers measured by RT-PCR. Relative levels of “epithelial” markers E-cadherin (CDH1) and p63 (TP63), and “mesenchymal” markers Zeb-1 (ZEB1) and vimentin (VIM) were measure by RT-PCR. Expression levels were normalized to UM-UC16.

and vimentin. These data indicated that the “epithelial” and “mesenchymal” markers are expressed in a non-overlapping manner among the majority of UC cell panel in that only two cell lines (UM-UC18 and 1A6) co-expressed “epithelial” and “mesenchymal” markers (Figure 3.2).

3.1.2. Correlation between E-cadherin and FGFR/bFGF expression in urothelial cancer cells.

To fully understand the relationship between EMT markers and FGFR/bFGF expression, we first examined expression of FGFRs1-4 and bFGF (FGF-2) by RT-PCR. In line with the gene expression profiling data, the expression of FGFR1 and FGF-2 were enriched in the “mesenchymal” subset (UM-UC3, UM-UC13, T24, BV and UM-UC12), whereas FGFR3 was primarily expressed within “epithelial” subset (RT4, UM-UC14, RT112 and SW780) (Figure 3.3). Although FGFR2 expression also appeared to be concentrated within the “epithelial” subset and FGFR4 expression in “mesenchymal” subset respectively, their levels of expression were lower than the levels of FGFR3, FGFR1 or bFGF, which is consistent with recent studies [103]. We then used nonparametric correlation analyses to confirm that expression of FGFR3 correlated strongly with E-cadherin expression (Spearman $r=0.8155$, $p<0.0001$, Figure 3.4) but inversely with expression of “mesenchymal” markers (Table 3.1). On the contrary, expression of FGFR1 and bFGF correlated strongly and directly with Zeb-1 expression

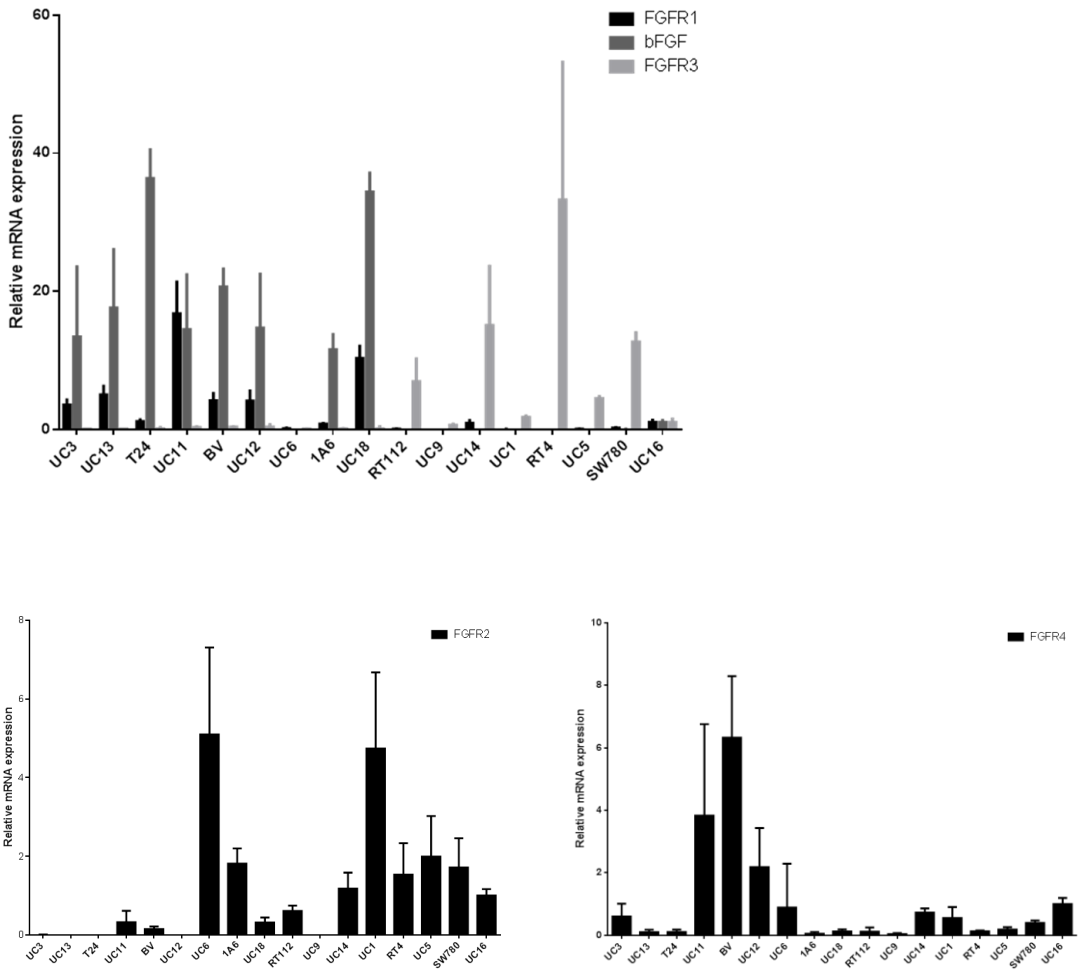

Figure 3.3 Expression of FGFRs 1-4 and bFGF. The relative mRNA levels were measured by quantitative real-time RT-PCR. The cell lines in each panel are organized by relative E-cadherin expression (low to high, from left to right, refer to Figure 3.2).

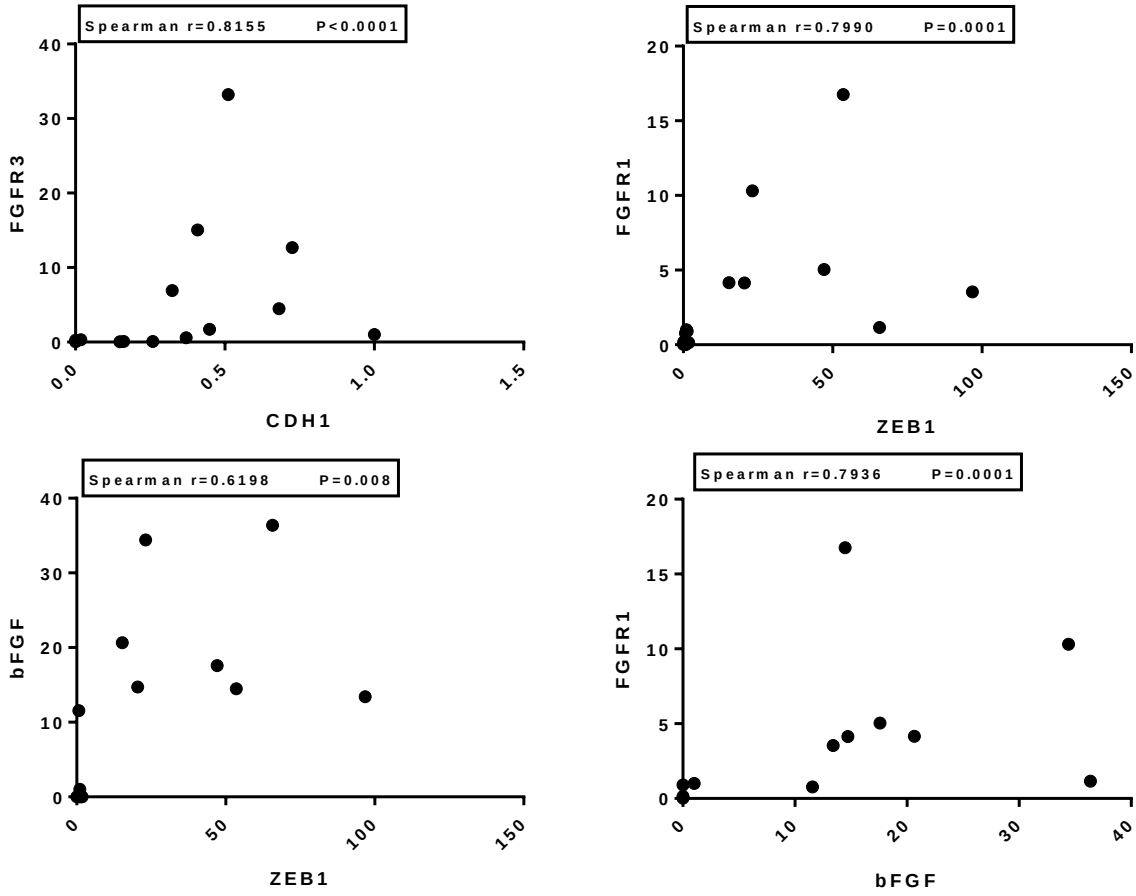

Figure 3.4 Relationship beteween FGFR/bFGF and EMT markers.

Scatterplots depicting the relationships between expression of FGFR3, bFGF, FGFR1, and EMT markers. Nonparametric correlation analyses were used to evaluate the relationships between FGFR3 and E-cadherin (CDH1) expression, FGFR1 and ZEB1 expression, bFGF and ZEB1 expression, and bFGF and FGFR1 expression. Correlation coefficients and p values are indicated on the figure.

	bFGF	FGFR1	FGFR3
TP63	-0.7494 0.0005	-0.6225 0.0076	0.6005 0.0108
CDH1	-0.6527 0.0045	-0.6242 0.0074	0.8155 0.0001
ZEB1	0.8606 0.0026	0.7990 0.0001	-0.8015 0.0001
VIM	0.6118 0.0091	0.6029 0.0104	-0.2426 0.3480

	FGFR3
FGFR1	-0.5858 0.0135

Spearman correlation *R value, #P value

Table 3.1 Correlation between FGFR/bFGF and EMT markers. The figure displays the results of the nonparametric correlation analyses. Correlation coefficients are displayed in red, and corresponding p values are depicted in black. Negative correlation coefficients indicate the presence of an inverse relationship between markers.

(Spearman r=0.799, p=0.0001 for FGFR1 and r=0.6198, p=0.008 for bFGF, Figure 3.4). In addition, FGFR1 and bFGF correlated directly with each other as we expected (Figure 3.4). We then investigated whether the pattern of differences observed in mRNA level could be translated into protein level in a subset of the cell lines by immunoblotting. We found that FGFR3 but not FGFR1 was expressed in “epithelial” cell lines UM-UC14, RT112 and RT4. Conversely, FGFR1 but not FGFR3 was expressed in “mesenchymal” cell lines UM-UC3, UM-UC12 and UM-UC13. Although bFGF was expressed in all 6 cell lines, “mesenchymal” cell lines (UM-UC3, UM-UC12 and UM-UC13) indeed expressed more bFGF than “epithelial” cell lines (UM-UC14, RT112 and RT4) (Figure 3.5). Together, these data suggested that FGFR1/bFGF and FGFR3 probably drive separate functions in non-overlapping “mesenchymal” and “epithelial” UC cells.

3.1.3. Effects of BGJ-398 on proliferation.

Recent studies indicated that FGFR inhibition blocks cell proliferation in human UC cells [104,126]. We therefore examined the effects of BGJ-398 on proliferation in 17 UC cell lines to characterize the scale of heterogeneity of drug sensitivity. Cells was incubated with increasing concentration of BGJ-398 for 48 hours and then subjected to MTT assay to measure drug induced cytotoxicity and/or growth arrest. We identified 4 cell lines (UM-UC14, SW780, RT4 and RT112) that were drug sensitive as ≥50% growth inhibition at concentrations of 1μM or lower (Figure 3.6A).

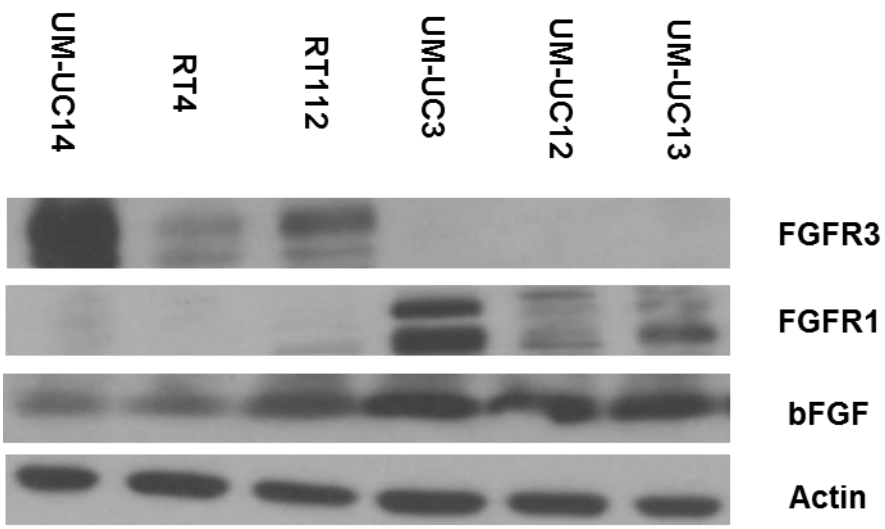

Figure 3.5 Baseline expression of FGFR1, FGFR3 and bFGF proteins in subsets of epithelial and mesenchymal UC cells. FGFR1, FGFR3 and bFGF in 3 representative “epithelial” (UM-UC14, RT4 and RT112) and 3 “mesenchymal” (UM-UC3, UM-UC12 and UM-UC13) cell lines were measured by immunoblotting.

A.

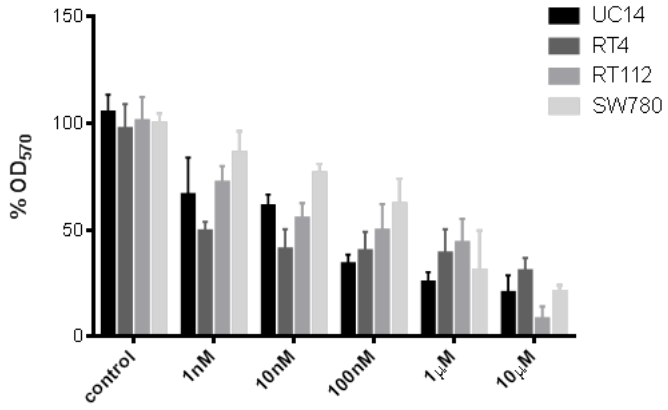

B.

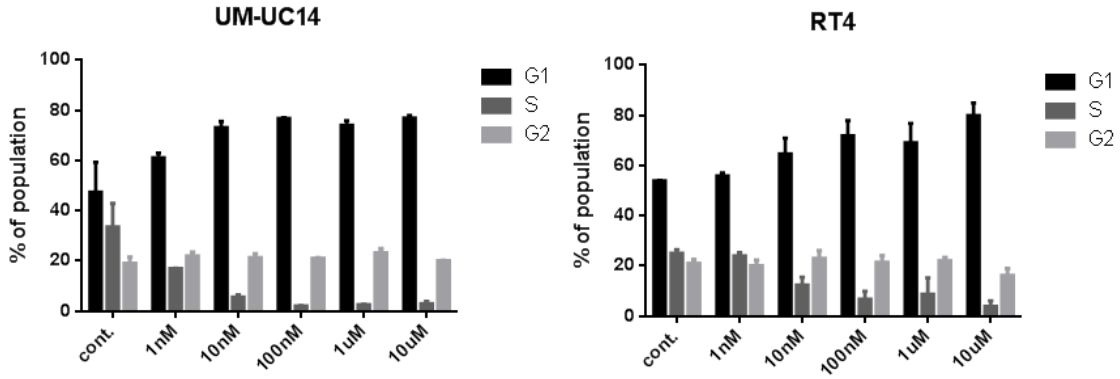

Figure 3.6 Effects of BGJ-398 on cell proliferation in the drug-sensitive cells. A. cells were incubated for 48 h in the presence of the indicated concentrations of BGJ-398 and cell growth was measured by MTT reduction. Mean ± SEM, n = 6. B. UM-UC14 or RT4 cells were incubated with the indicated concentrations of BGJ-398 and the percentages of cells within each cell cycle quadrant were quantified by propidium iodide staining and FACS analysis. Mean ± SEM, n = 3.

To further determine the relative contribution of cell death versus growth arrest to these effects, we directly measured cell cycle arrest and apoptosis by propidium iodide (PI) staining and FACS analysis after exposing UM-UC14 and RT4 cells to increasing concentration of BGJ-398 for 48 hours. We observed increases in percentage of cells in G1 phase whereas a decreases in percentage of cells in S phase in both cell lines with increasing concentrations of BGJ-398. More specifically, the percentage of cells in G1 phase increased from 47.5% and 54% to 74.2% and 69.1%, and in parallel the percentages of cells in S phase decreased from 33.5% and 25% to 2.7% and 8.8%, in the BGJ-398 treated UM-UC14 and RT4 respectively (Figure 3.6B). On the contrary, BGJ-398 exposure did not cause any apoptosis at concentration lower than 10 μM in either of the cell lines (data not shown). These data indicated that BGJ-398 induced cytostatic effects on UC cells *in vitro*.

Recent studies revealed FGFR3 activating mutations and overexpression as potential mechanisms contributing to response to FGFR antagonist [64,151]. We therefore examined the relationship between BGJ-398 sensitivity and the presence of activating FGFR3 mutations. We first identified 5 cell lines (UM-UC6, UM-UC14, UM-UC15, UM-UC16 and UM-UC17) that contained activating FGFR3 mutations within our panel by exon sequencing (Table 3.2). Strikingly, only one of the 5 cell lines was BGJ-398 sensitive. However, FGFR3 mRNA expression correlated strongly with drug sensitivity using nonparametric correlation analysis

Summary of FGFR3 Mutation

Cell line	Exon	Condon	Amino-acid Change
UC6	7	248	R248C
UC14	7	249	S249C
UC15	7	249	S249C
	10	375	Y375C
UC16	7	249	S249C
UC17	7	249	S249C

Table 3.2 FGFR3 mutation status in human bladder cancer cells. The presence of activating FGFR3 mutations was determined by exon sequencing. Note that among the 5 cell lines within the panel that contain activating mutations, only one (UM-UC14) is sensitive to BGJ-398.

(Spearman r=0.7247 p=0.01, Figure 3.7), whereas no clear correlation was observed between FGFR1 mRNA expression and sensitivity to BGJ-398 (Spearman r=-0.2931 p=0.2536, Figure 3.9)

Given the non-overlapping pattern of FGFR3 and FGFR1 expression, the indicated results suggested that FGFR3 was more essential than FGFR1 in driving cell proliferation in “epithelial” UC cells. We then used RNAi to directly test this hypothesis. BGJ-398 sensitive cells were transfected with either FGFR3 or FGFR1 siRNAs to knock down the targeted gene and cell proliferation was measured by MTT assay. Quantitative PCR confirmed FGFR3 knockdown efficiencies of 50% and >80% in the RT4 and UM-UC14 with FGFR3 siRNAs compared to non-specific siRNA control, respectively. The result was also confirmed by Immunoblotting at protein level (Figure 3.8). The corresponding effect of FGFR3 silencing was very similar to BGJ-398 exposure. Cell proliferation was reduced by 60% and >90% in RT4 and UM-UC14 cells transfected with FGFR3 siRNA, respectively (Figure 3.9). Cell cycle analyses revealed that FGFR3 knockdown increased the percentage of cells in G1 phase and decreased the percentage of cells in G2 phase, which is consistent with the MTT results. However, FGFR1 silencing had no significant effect on proliferation and cell cycle in both RT4 and UM-UC14(Figure 3.10).

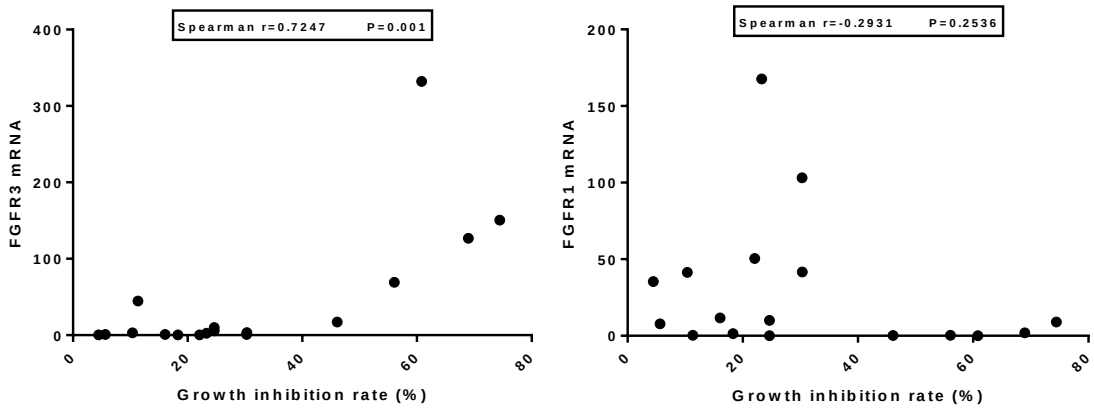

Figure 3.7 Sensitivity to the anti-proliferative effects of BGJ-398 correlates with FGFR3 expression but not with the presence of activating FGFR3 mutations. The level of growth inhibition observed after 48 h exposure to 1 μM BGJ-398 (as measured by MTT assays) was correlated with the relative level of FGFR3 (left panel) or FGFR1 (right panel) mRNA expression in a panel of 17 human BC cell lines.

A.

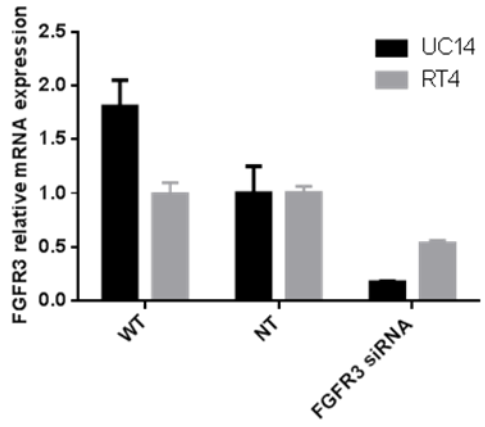

B.

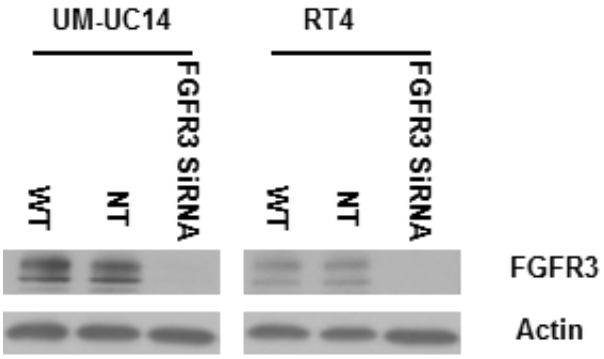

Figure 3.8 Efficiency of FGFR3 silencing measured by quantitative RT-PCR and immunoblotting. A. measurement of FGFR3 silencing efficiency by quantitative PCR. B. measurement of FGFR3 silencing efficiency by immunoblotting.

A.

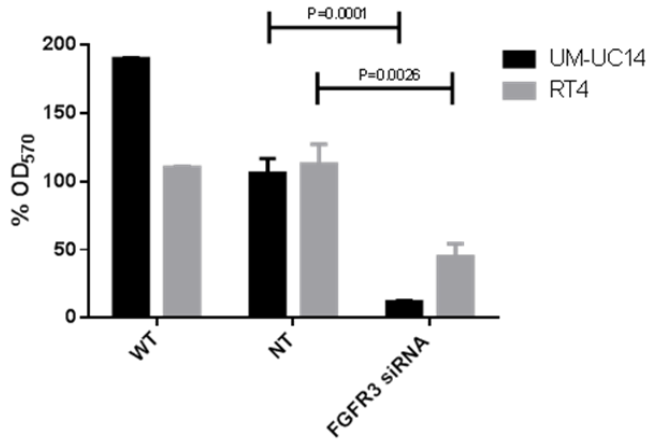

B.

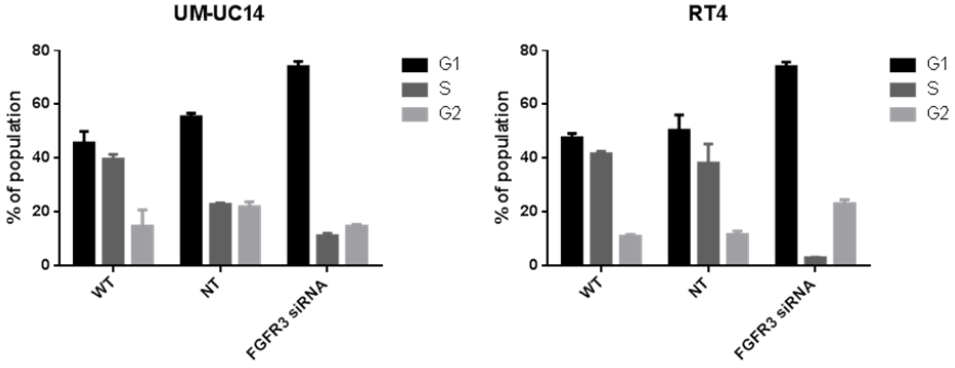

Figure 3.9 Effects of FGFR3 knockdown on cell proliferation. UM-UC14 or RT4 cells were transiently transfected with either non-targeting (NT) or FGFR3-specific siRNAs and, A. cell growth was measured at 48 h by MTT reduction. Mean ± SEM, n = 6. B. percentages of cells within each phase of the cell cycle were quantified by propidium iodide staining and FACS analysis. Mean ± SEM, n = 3.

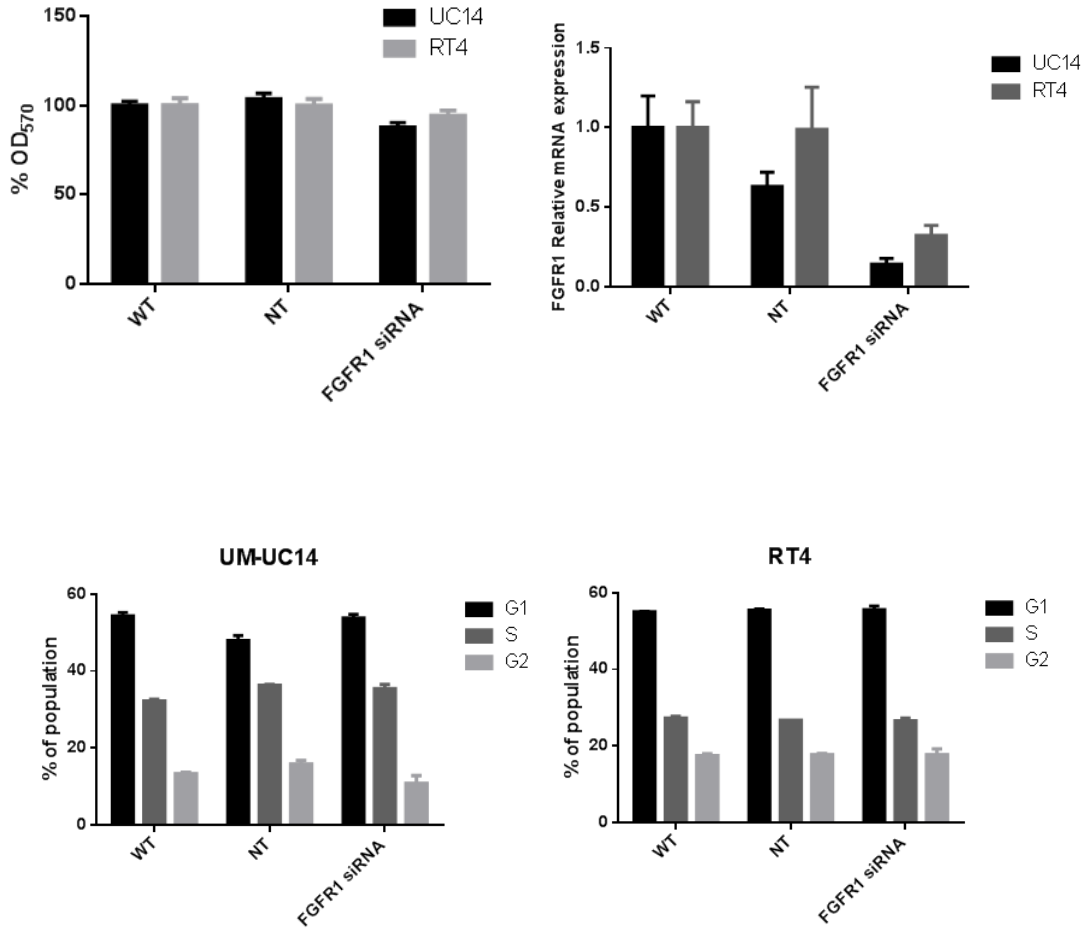

Figure 3.10 Effects of FGFR1 knockdown on FGFR1 expression and proliferation in RT4 and UM-UC14 cells. UM-UC14 or RT4 cells were transiently transfected with either non-targeting (NT) or FGFR1-specific siRNAs and, cell growth was measured at 48 h using MTT. Mean ± SEM, n = 8. And, the percentages of cells within each phase of the cell cycle were quantified by propidium iodide staining and FACS analysis. Mean ± SEM, n = 3.

3.1.4. Effects of BGJ-398 on invasion.

Our data indicated the “mesenchymal” UM-UC3 and UM-UC13 were resistant to the growth arrest effect of BGJ-398 (Figure 3.11A) although both of they expressed relatively high levels of FGFR1. Given that migration, invasion and metastasis are key characters of “mesenchymal” cells [150], we examined the effects of BGJ-398 on invasion in UM-UC3 and UM-UC13 while two “epithelial” BGJ-398 resistant cells (UM-UC6 and UM-UC9) were used as controls. The cells were exposed to increasing concentrations of BGJ-398 and invasion was measured using modified Boyden chambers. BGJ-398 effectively inhibited invasion in the “mesenchymal” UM-UC3 and UM-UC13 cells in a concentration dependent manner but not in the “epithelial” UM-UC6 and UM-UC9 cells (Figure 3.11B).

Because our previous data suggested a direct correlation between bFGF/FGFR1 and “mesenchymal” markers (Figure 3.3), we then hypothesized that bFGF/FGFR1 are involved in the regulation of invasion in “mesenchymal” cells. To directly test the hypothesis, we first transfected UM-UC3 and UM-UC13 cells with lentiviral shRNAs to stably silenced the expression of either bFGF or FGFR1. The efficiency of targeted knockdown was confirmed by both quantitative PCR at mRNA level and immunoblotting at protein level (Figure 3.12). We then quantified invaded cells in these bFGF/FGFR1 stably silenced cells and compared it to the results from non-specific control and parental cells using modified Boyden

A.

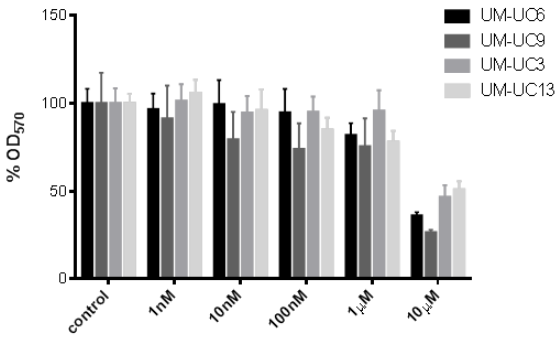

B.

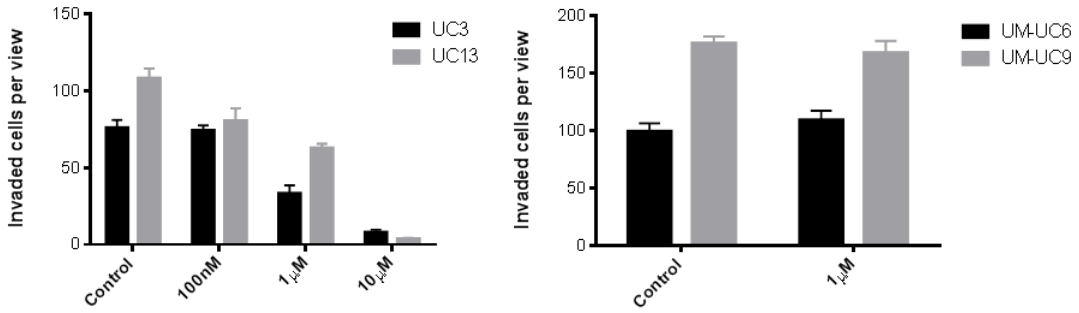

Figure 3.11 Effects of BGJ-398 on cell growth and invasion in two "mesenchymal' (UM-UC3, UM-UC13) and two "epithelial" (UM-UC6, UM-UC9) cell lines. Growth inhibition was measured at 48 h by MTT reduction. Mean ± SEM, n = 6. Invasion was measured using modified Boyden chambers and standard light microscopy as described in Materials and Methods. Mean ± SEM, n = 3.

A.

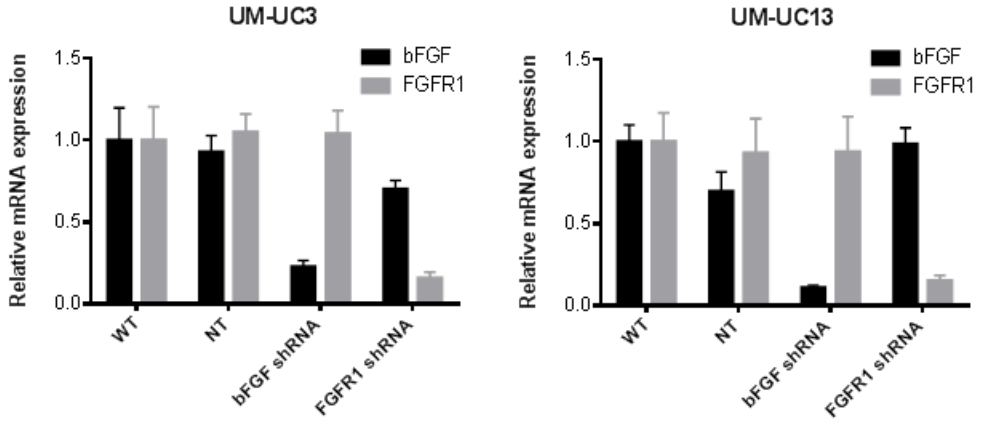

B.

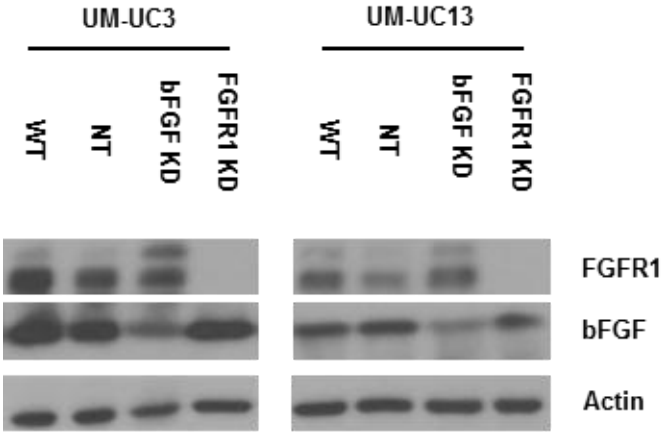

Figure 3.12 FGFR1 or bFGF silencing in cells transduced with lentiviral shRNAs. A. Relative mRNA levels were measured by quantitative real-time RT-PCR and B. protein levels were measured by immunoblotting.

chambers and confocal microscopy. In UM-UC3 cells, the percentage of invading cells was reduced from 85% in the parental cells or cells transduced with a control lentiviral construct to 54.5% in bFGF KD cells (P=0.0029) and 63.8% in FGFR1 KD cells (P=0.0038), respectively. Similarly, in UM-UC13 cells, the levels of invasion were reduced from 82% in parental cells or cells transduced with the non-targeting lentivirus to 64.8% in the bFGF KD cells (P=0.0146) and 52.4% in FGFR1 KD cells (P=0.0018) (Figure 3.13). Together, the data confirmed that bFGF and FGFR1 both promoted invasion in “mesenchymal” BC cells.

3.1.5. Effects of BGJ-398 on tumor growth and metastasis.

Although *in vitro* models are excellent tools for studying molecular mechanisms, the process of cancer metastasis is regulated by tumor-stromal interactions that cannot be modeled well *in vitro*. Therefore, in order to better define the effects of BGJ-398 on primary tumor growth versus metastasis in “mesenchymal” BC cells, we first isolated a highly metastatic form of UM-UC3 using orthotopic “recycling” in nude mice [152]. We transduced the cells with a lentiviral vector encoding luciferase and red fluorescent protein (RFP), which enabled us to monitor primary tumor growth and metastasis non-invasively by luciferase imaging and to isolate circulating tumor cells (CTCs) by cell sorting. After 3 rounds of recycling, the UM-UC3 cells formed orthotopic tumors in 100% of mice and consistently produced metastases to lymph nodes, lungs, and bone in over 70% of mice. We then implanted 200,000 of the recycled UM-UC3

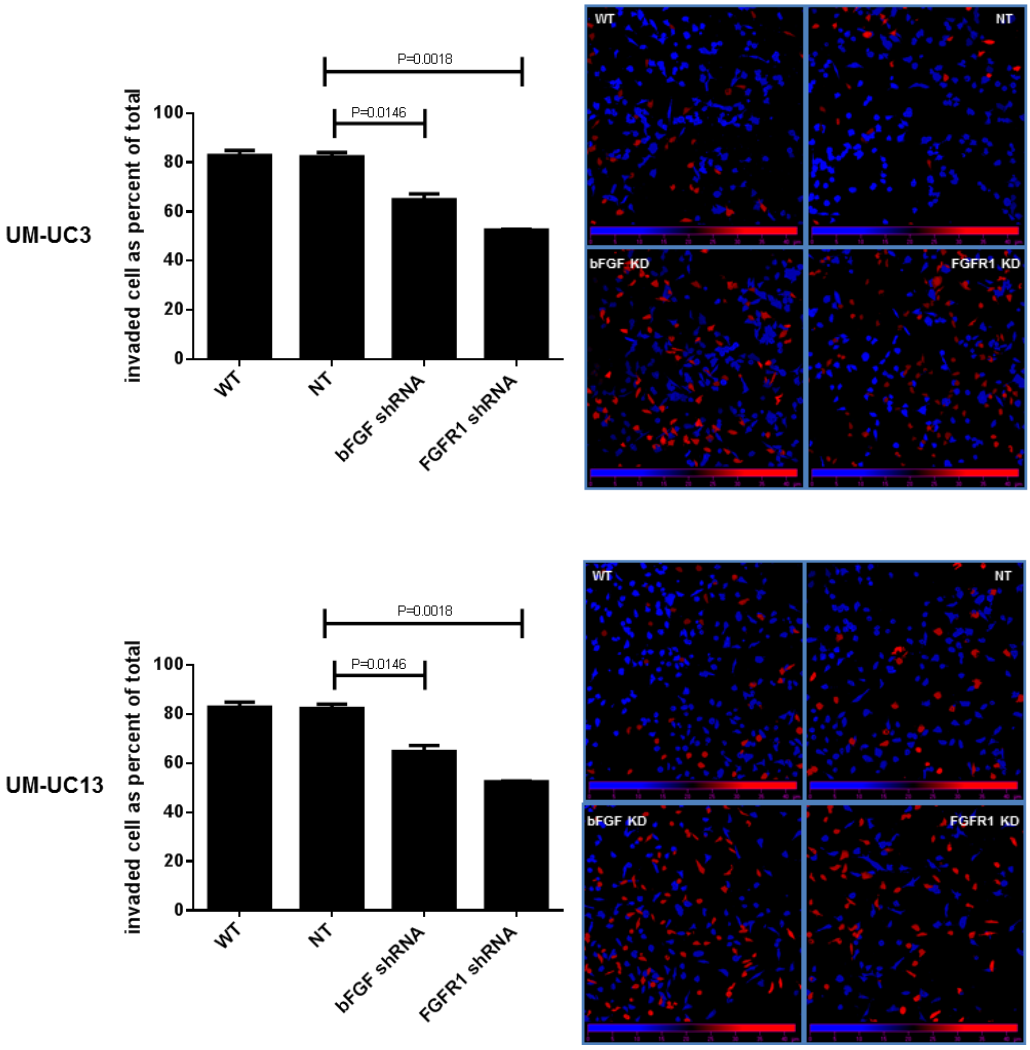

Figure 3.13 Effects of FGFR1 or bFGF silencing on invasion. The percentages of cells that invaded through Matrigel in modified Boyden chambers were quantified by propidium iodide staining and confocal microscopy. Representative confocal images were displayed at right panel where the nuclei of the cells that invaded are pseudo-colored blue and the cells that did not invade are depicted in red.

cells orthotopically in nude mice and initiated therapy with BGJ-398 or vehicle (via oral gavage) once primary tumors were well established (on day 8), monitoring tumor growth and metastasis biweekly by IVIS imaging (Figure 3.14; 3.15). Interestingly, primary tumors in the mice treated with BGJ-398 appeared to grow slightly faster than controls, although the differences in growth rates were not statistically significant (Figure 3.14; $P>0.05$). In contrast, BGJ-398 strongly inhibited the development of metastases and CTCs. Specifically, 5 out of 7 mice within the control group developed lymph node metastasis by day 15, and two of these subsequently developed bone and lung metastasis at day 36 (Fig. 3.15 right panel). However, we detected only 1 lymph node metastasis in the 7 animals within the BGJ-398 treatment group. When we quantified total metastatic burden using luciferase imaging, the differences between the vehicle and BGJ-398 treatment groups were highly significant (Figure 3.15; $p = 0.0078$). Finally, we quantified the numbers of circulating tumor cells in the mice at the time of sacrifice on day 40 by measuring human HLA-C levels in whole peripheral blood by quantitative PCR. CTC numbers within the control group ranged from 325 to 336,008 cells (mean = 158,977), whereas CTC numbers in the treated group ranged from 160 to 370 (mean = 243.6) (Figure 3.16; $p < 0.01$). Together, the results demonstrated that BGJ-398 had no inhibitory effect on the growth of UM-UC3 primary tumors but did block tumor cell extravasation into the vasculature (as measured by CTC production) and metastasis.

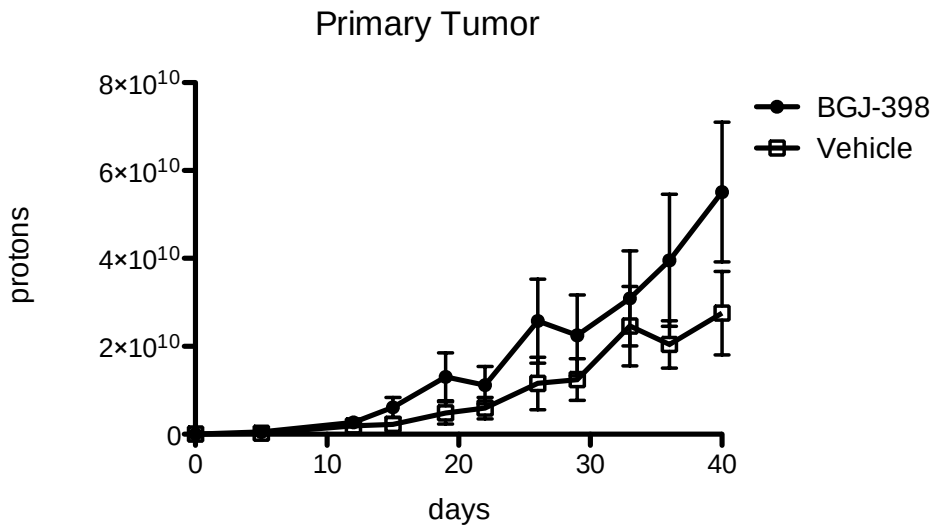

Figure 3.14 Effects of BGJ-398 on primary tumor growth in mice bearing orthotopic UM-UC3 xenografts. Luciferase-labelled, orthotopically recycled UM-UC3 cells were implanted into the bladders of nude mice, and tumors were allowed to grow for 8 days prior to initiating therapy with BGJ-398 (daily via oral gavage). Tumor growth was measured biweekly by luciferase imaging. Mean ± SEM from 6 (control) or 7 (treated) mice per group.

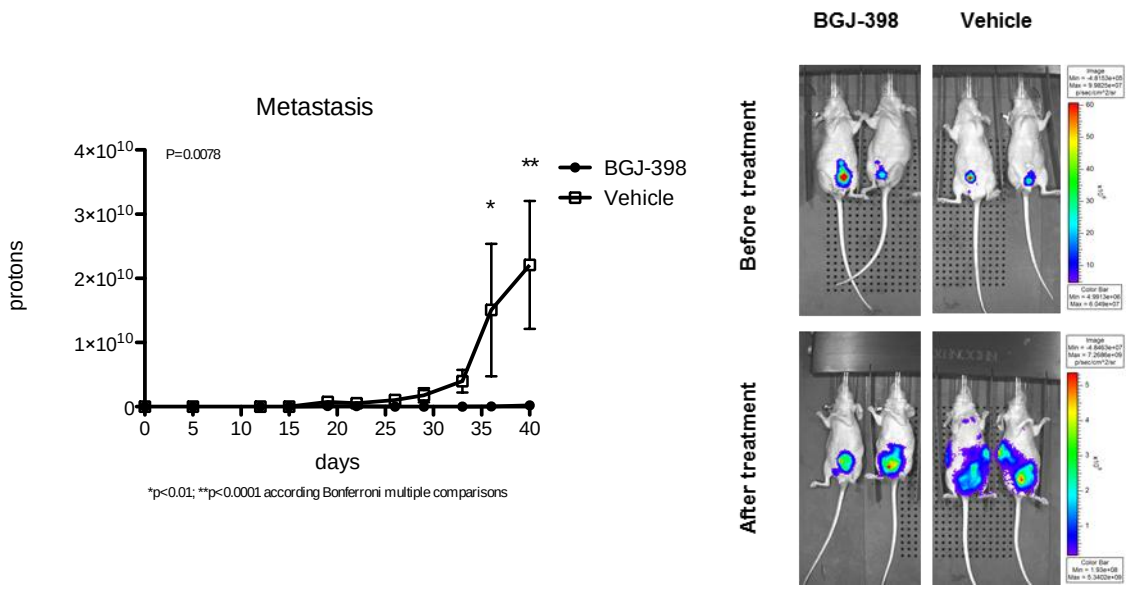

Figure 3.15 Effects of BGJ-398 on metastasis in mice bearing orthotopic UM-UC3 xenografts. Whole animal metastatic burdens were determined non-invasively by luciferase imaging. Mean ± SEM, n = 6 (control mice) or 7 (treated mice). Representative whole body luciferase images taken just prior to the initiation of therapy and at the conclusion of the experiment were displayed at right panel.

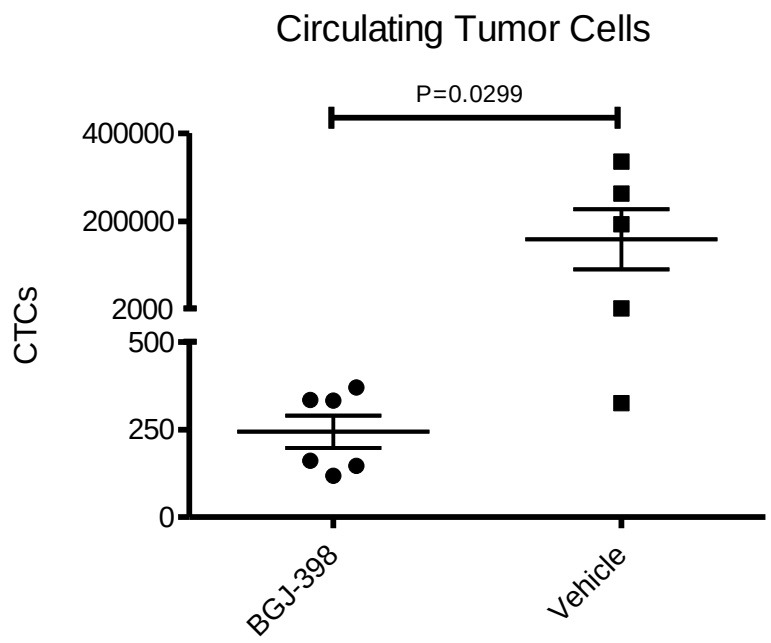

Figure 3.16 Effects of BGJ-398 on UM-UC3 CTC production. CTC numbers were estimated by measuring human HLA levels in isolated whole blood by quantitative PCR; cell numbers were determined using a UM-UC3 standard curve. The scatterplot displays the results obtained from each animal; the lines denote the mean values for each group.

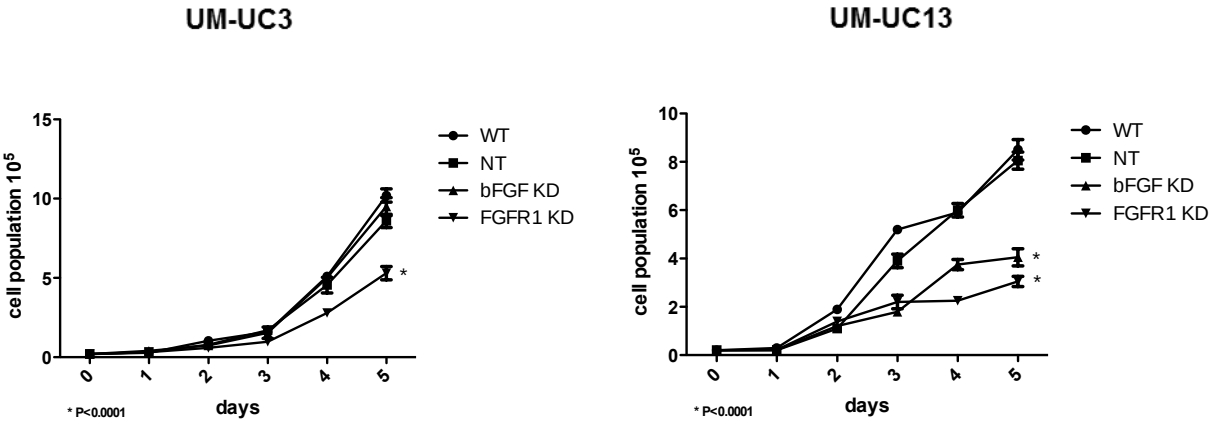

Figure 3.17 Effects of bFGF or FGFR1 silencing in long-term proliferation assays. MTT results obtained in 5-day assays. Mean ± SEM, n = 6. *p<0.05.

3.2. Discussion

FGFR3 is frequently activated by mutation [42,151,153] in both muscle invasive and non-invasive urothelial cancers, where it appears to drive cell proliferation [101,102]. Recent studies also revealed the prevalence of FGFRs overexpression, specifically overexpression of FGFR1 [103] and FGFR3 [154,155], which may identify as oncogenic addiction in urothelial cancer. Taken together, these data identify FGFR1 and FGFR3 as two of the most attractive targets in clinical development in bladder cancer [105,154]. However, there exists a significant heterogeneity in response to FGFR inhibitors [64,156-158] in BC cells based on the results published to date, and it is presently unclear what factors are driving sensitivity to FGFR inhibitors. The heterogeneity and the unclear underlying mechanisms could significantly jeopardize the identification of the appropriate subset of BC patients who could benefit markedly from the FGFR targeted therapy.

Based on recent studies, it is likely that FGFR3 activating mutation (i.e. S249C) determines the FGFR3 dependency which drives the sensitivity to selective and non-selective FGFR inhibitors. However, in this study, our data demonstrated that the presence of an FGFR3 activating mutation alone does not predict sensitivity to BGJ-398 in a panel of human UC cells. Conversely, FGFR3 mRNA expression levels did correlate well with the sensitivity to BGJ-398 (Figure 3.7), suggesting a link between FGFR3 overexpression and FGFR3 dependency. More specifically, among BC

cell lines bearing FGFR3 activating mutations, the majority of them were not sensitive to BGJ-389 in this study (UM-UC6, UM-UC15, UM-UC16, UM-UC17) or other FGFRs inhibitors (94-10, 97-18, J82) [156,158], though only two of them were highly sensitive to BGJ-398 or other inhibitors [156,157]. In contrast, at least one FGFR3 wild-type cell line (UM-UC1) was as sensitive to BGJ-398 as the most sensitive FGFR3 mutant cells [156]. In addition, two other cell lines (RT4, RT112) bearing the FGFR3-TACC3 translocation were among the cell lines that are sensitive to BGJ-398. Although little is unknown about the underlying mechanism regarding this heterogeneity, a recent study provided a possible explanation, where FGFR3 mutant cells exhibited an escape mechanism through pathway redundancy to rescue the proliferation refractory from FGFR inhibition [132].

More importantly, our results indicated a non-overlapping pattern between FGFR3 and FGFR1 expression in the panel of human BC cells we studied, and interesting, cells with high expression level of FGFR1 were all relatively resistant to BGJ-398. Collectively, these data demonstrated that FGFR3 expression is a more important determinant than FGFR1 expression in driving cell proliferation in the specific cells we studied. In addition, our data demonstrated that the primary effects of FGFR inhibition by BGJ-398 are cytostatic rather than cytotoxic, which indicated the potential value of FGFR inhibition lies in the combination with conventional chemotherapy or radiation therapy in clinical development. Indeed, in

future studies we are going to examine the hypothesis that FGFR inhibition could improve the effect of conventional chemotherapy or radiation therapy by promoting their cytotoxic effects. With respect to clinical development, it is worth noting that all of the human UC cell lines with a possible exception of RT4 are derived from muscle invasive UC. Due to this limitation, it is possible that the cell line studies underestimate the potential efficacy of FGFR3 inhibition in non-muscle invasive UCs. In fact, a majority of non-muscle invasive BC contain FGFR3 activating mutations, strongly suggesting that FGFR antagonists could have strong clinical activity in them.

Interestingly, our data also demonstrated that FGFR1 played a significant role in cell invasion and tumor metastasis even though FGFR1 was less important than FGFR3 in promoting cell proliferation. More specifically, FGFR1 signaling repression by either BGJ-398 or specific FGFR1 silencing led to reduced cell invasion *in vitro* (Figure 3.11, 3.13). In addition, BGJ-398 inhibited CTC production and metastasis without decreasing primary tumor growth *in vivo* (Figure 3.14, 3.15, 3.16), which seems to contradict a recent study suggesting the role of FGFR1 in driving both cell proliferation *in vitro* and tumor growth *in vitro*. However, our conclusion that FGFR1 did not drive cell proliferation in some "mesenchymal" UC cells was based on MTT assay to measure short-term effects of BGJ-398. We reached to the same conclusion that was advanced in previous work (blocking FGFR1 impaired cell proliferation)

when we measured long-term effects of stable silencing FGFR1 using colony formation assays (Figure 3.17), which indicated the importance of FGFR1 for initiation but not maintenance of cell proliferation in UC cells. Furthermore, our *in vivo* experiment was based on FGFR targeted therapy by BGJ-398 in mice with established orthotopic tumors whereas the previous work relied on stable silencing of FGFR1, consistent with the idea that FGFR1 is important for tumor initiation but may be not for maintenance of tumor growth. It is also worth noting that several other studies also suggested a role of FGFR1 in cell invasion and tumor metastasis [104].

Finally, our results demonstrated distinct effects of FGFR inhibition, in that FGFR3 inhibition blocked cell proliferation, whereas FGFR1 inhibition suppressed cell invasion and metastasis. It is presently unclear why the differential effects exist given that the effects on proliferation and invasion were clearly linked to inhibition of the same signal transduction pathway (MAPK/Erk signaling) [47,49,104]. One possible explanation was that the different effects are a consequence of the distinct biological difference between the epithelial and mesenchymal phenotype. Our data suggested a non-overlapping expression pattern of FGFR1 versus FGFR3 in UC cell lines in that FGFR1 primarily expressed in mesenchymal phenotype, whereas FGFR3 correlated well in epithelial phenotype (Figure 3.1, 3.2, 3.3). It is highly possible that the “epithelial” cells are more dependent on autocrine growth factors for G1/S transition and proliferation than

“mesenchymal” cells, whereas the “mesenchymal” cells rely on growth factors for invasion rather than other cell functions. Our results also shed the light on possible clinical translation in muscle invasive urothelial tumors or where a subset of low grade non-muscle invasive urothelial tumors progress into muscle-invasive tumors. FGFRs inhibition in conjunction with conventional chemotherapy could be valuable to target these tumors and benefit patient sub-groups if appropriate biomarkers can be identified and deployed to pinpoint the subsets of tumors.

CHAPTER 4. A PPARγ-FABP4 TRANSCRIPTIONAL COMPLEX REGULATES EGFR DEPENDENCY IN HUMAN BLADDER CANCER CELLS

4.1. Result

4.1.1. Sensitivity to EGFR or FGFR inhibitors is confined to the "epithelial" subset of bladder cancer (BC) cell lines

Previous studies showed that 5 urothelial cancer (UC) cell lines (UM-UC4, UM-UC5, UM-UC7, UM-UC9 and UM-UC16) were sensitive to EGFR inhibitor gefitinib at clinically relevant concentration (≤ 1μM) in a panel of 25 human urothelial cancer cell lines [115,147]. A recent screening of the FGFR inhibitor BGJ-398 in the same panel also identified 4 different cell lines (UM-UC14, SW780, RT4 and RT112) that were sensitive at clinically relevant concentration (≤ 1μM) [70]. We first confirmed that the same cell lines were sensitive to the structurally distinct FGFR inhibitor AZD4547 but not EGFR inhibitor gefitinib using both MTT assay (Figure 4.1) and thymidine incorporation assay (Figure 4.2). We also confirmed that the other 4 UC cell lines (UM-UC4, UM-UC5, UM-UC7, UM-UC9) were still sensitive to the EGFR inhibitor gefitinib but not FGFR inhibitor AZD4547 as measured by both MTT assay (Figure 4.1) and thymidine incorporation assay (Figure 4.2). In addition, we also tested drug responses *in vivo* to further verify the observation. We found that UM-UC9 subcutaneous xenografts were sensitive to gefitinib and that UM-UC14 subcutaneous xenografts were sensitive to AZD4547 *in vivo*. The *in vivo* effects of the drugs were associated with decreased proliferation as measured by Ki-67 immunohistochemistry (Figure 4.3).

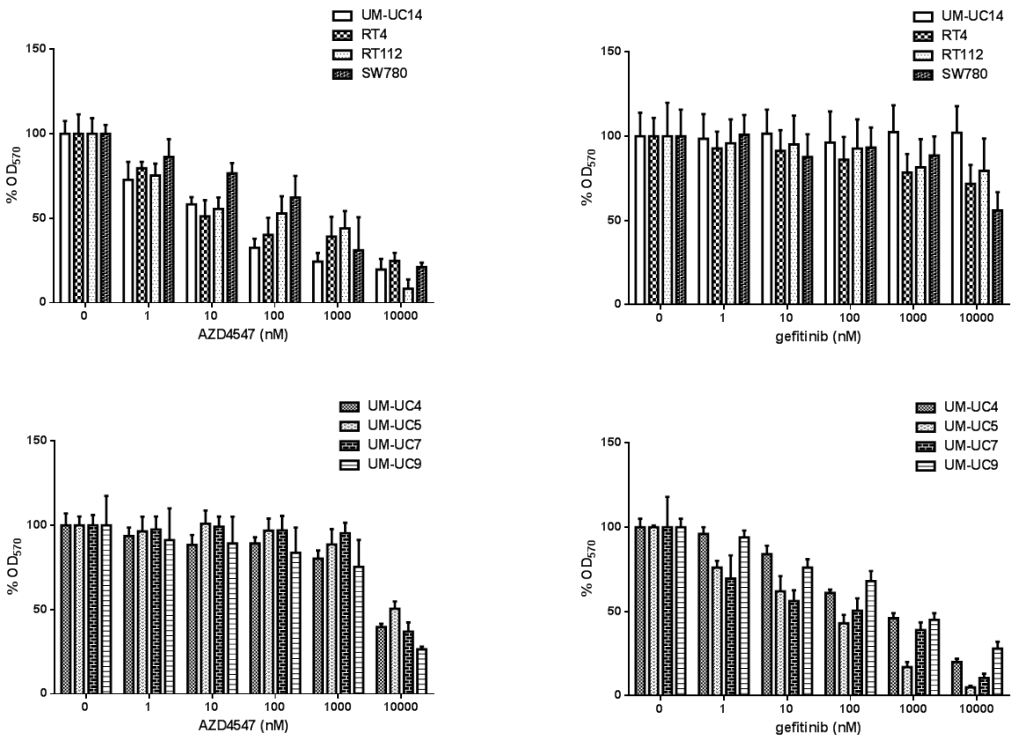

Figure 4.1 Differential effects of the FGFR inhibitor AZD4547 and the EGFR inhibitor gefitinib in human UC cells. The human UC lines UM-UC4, UM-UC5, UM-UC7, UM-UC9, UM-UC14, RT4, RT112, and SW780 were exposed to either AZD4547 or gefitinib at the indicated concentrations, and cell proliferation was measured by MTT assays, normalized to controls (mean ± SEM).

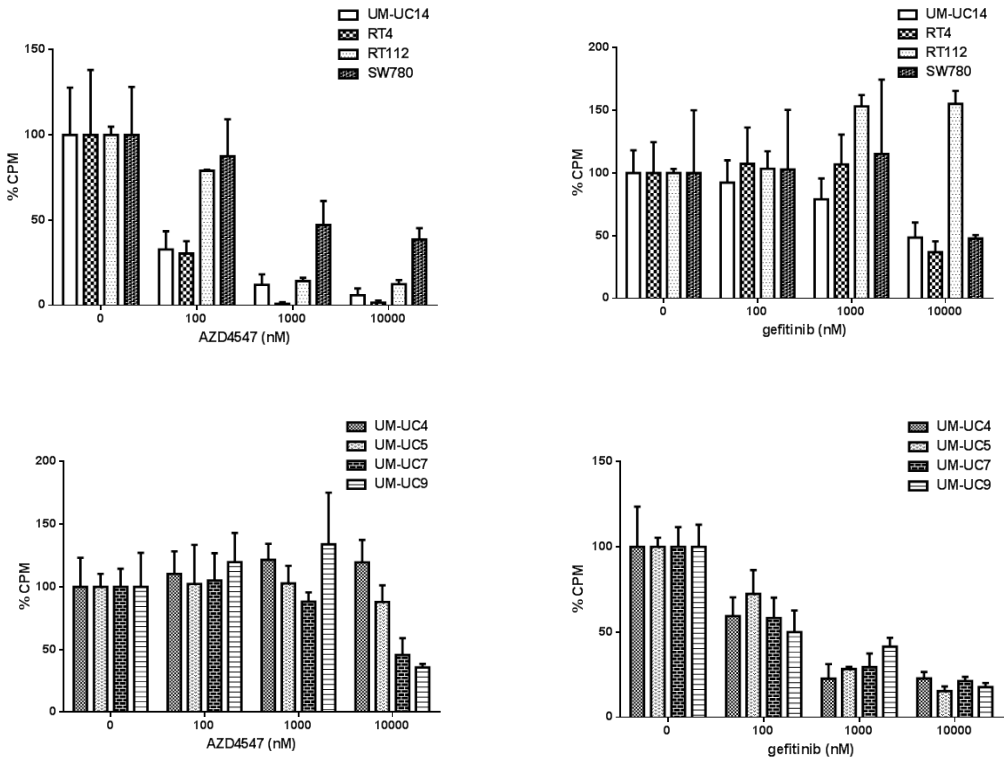

Figure 4.2 Differential effects of the FGFR inhibitor AZD4547 and the EGFR inhibitor gefitinib in human UC cells. The human UC lines UM-UC4, UM-UC5, UM-UC7, UM-UC9, UM-UC14, RT4, RT112, and SW780 were exposed to either AZD4547 or gefitinib at the indicated concentrations, and cell proliferation was measured by thymidine incorporation assay, normalized to controls (mean ± SEM).

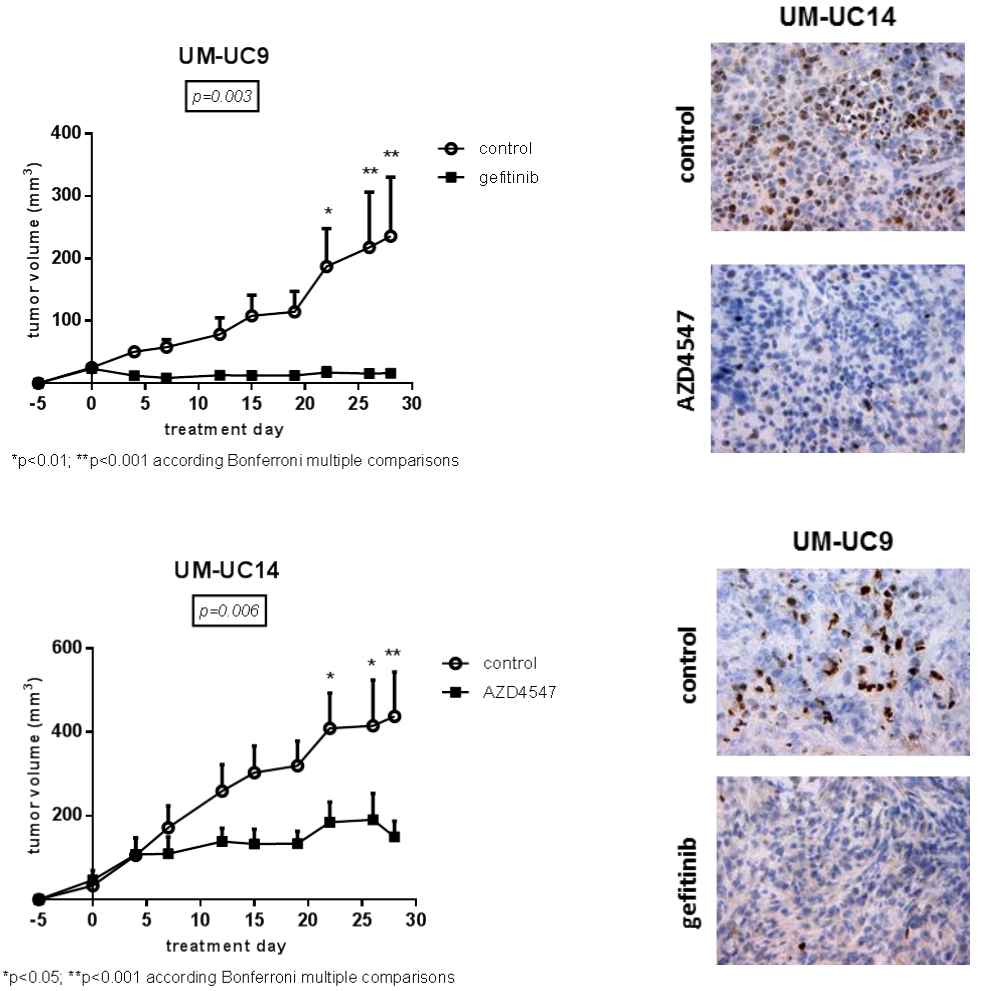

Figure 4.3 Growth inhibition of gefitinib or AZD4547 in subcutaneous xenograft models. UM-UC9 and UM-UC14 cells were injected subcutaneously into nude mice. Tumors were allowed to establish for 5 days prior to treatment with either vehicle (control) or gefitinib (UM-UC9; n = 12 / group) or AZD4547 (UM-UC14; n = 9 / group) via oral gavage. Tumor volumes (mm3) were calculated using the formula width^2 x length / 2, and depicted as means ± SEMs. Tumor tissue was harvested, fixed and stained for Ki-67 using immunohistochemistry.

These results suggested that sensitivity to either gefitinib or AZD4547 were confined to an ‘epithelial’ subset of UC cell lines characterized by high levels of E-cadherin expression (an epithelial marker) [70,147] and that sensitivity to either drug was mutually exclusive. Specifically, all of the cell lines that were sensitive to gefitinib were resistant to AZD4547, and all of the cell lines that were sensitive to AZD4547 were resistant to gefitinib (Figure 4.1 and 4.2). We then confirmed these *in vitro* results using orthotopic *in vivo* models by conducting four-arm studies in UM-UC9 (n =11 / group) and UM-UC14 (n = 9 / group) tumor-bearing nude mice. Consistent with the *in vitro* results, we found that once-daily oral administration of gefitinib (12.5 mg/kg) produced strong tumor growth inhibition in UM-UC9. On the contrary, AZD4547 (12.5 mg/kg) had no effect on tumor growth by itself. In addition, the combination of gefitinib and AZD4547 (each at 12.5 mg/kg) did not result in any additional effect (Figure 4.4, upper left panel). Conversely, AZD4547 but not gefitinib (each at 12.5 mg/kg) produced strong growth inhibition in the orthotopic UM-UC14 tumors. In addition, combination of AZD4547 and gefitinib produced no added benefit as compare to single agent therapy with AZD4547 (Figure 4.4, lower left panel). Measurements of tumor weights at sacrifice (after 4 weeks of therapy) confirmed the imaging results (Figure 4.4, right panel). Together, these date indicated sensitivity to either EGFR or FGFR inhibitor is non-overlapping and mutually exclusive both *in vitro* and *in*

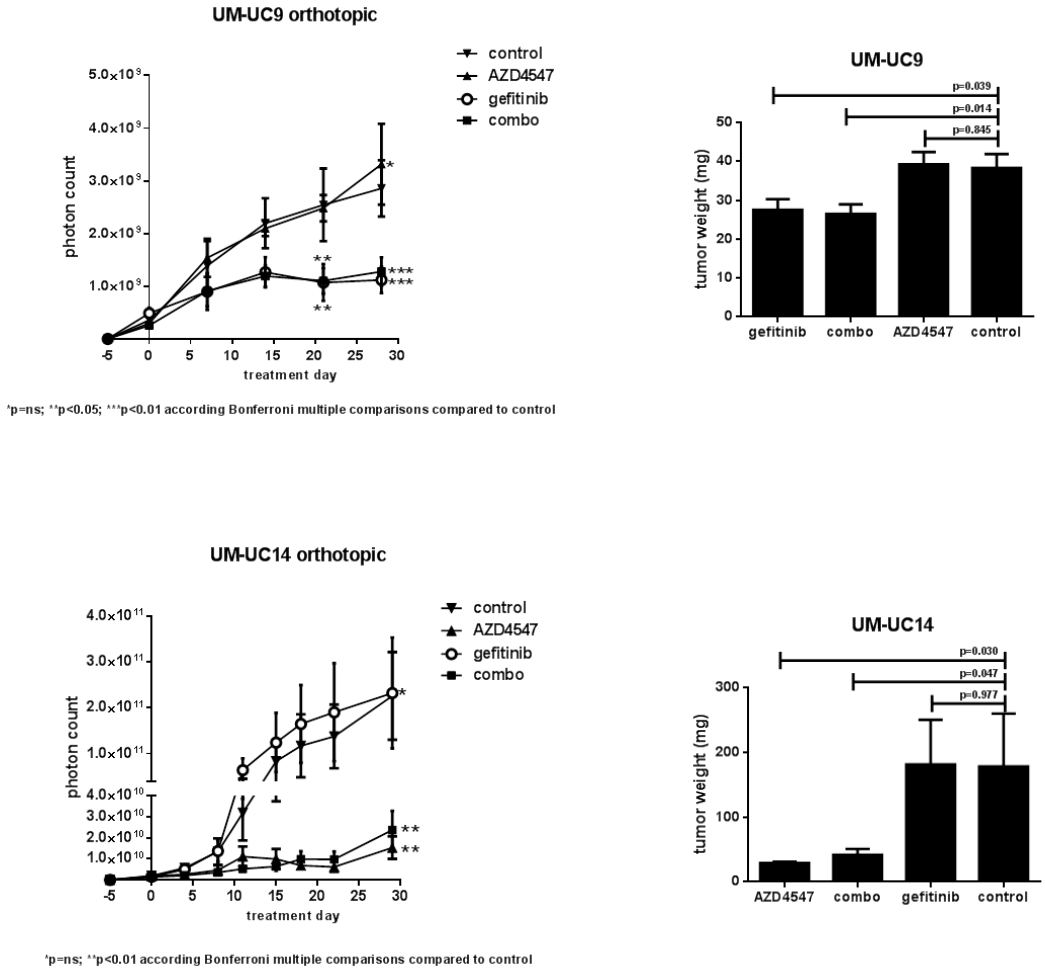

Figure 4.4 Effects of AZD4547, gefitinib, and AZD4547 plus gefitinib on the tumor growth of orthotopic xenografts. Luciferase-labeled UM-UC9 and UM-UC14 were orthotopically implanted into the bladders of nude mice. Tumors were allowed five days to establish prior to treatment. Animals were given AZD4547 (12.5mg/kg), gefitinib (12.5mg/kg), or a combination of both TKIs (12.5mg/kg each), or vehicle control (1% Tween 80, 99% deionized water) once daily for four weeks by oral gavage (n = 9 / group). Tumor growth was repeatedly measured non-invasively by *in vivo* bioluminescence imaging. The results are expressed as photon counts

(mean ± SEM). In addition, UM-UC9 and UM-UC14 primary tumors were harvested at sacrifice and weighed after four weeks of treatment. Tumor weights (mg) are indicated as means ± SEM.

vivo. Therefore, we identified 4 UC cell lines (UM-UC14, SW780, RT4 and RT112) as FGFR dependent and another discrete 4 cell lines (UM-UC4, UM-UC5, UM-UC7, UM-UC9) EGFR dependent within the panel.

We also noticed that several of the UC cell lines that contain activating FGFR3 mutations are resistant to FGFR inhibitors *in vitro* such as UM-UC6 [70]. Since three-dimensional growth and/or the tumor microenvironment could have major effects on drug sensitivity [159], we examined the effects of AZD4547 on orthotopic tumors (n = 8 mice / group) derived from the 'epithelial' UM-UC6 cells, which contain an activating S249C mutation but are resistant to FGFR inhibitors *in vitro* [70]. We observed that AZD4547 alone had no effect on tumor growth (Figure 4.5), confirming and extending our previous conclusion that FGFR3 mutational status alone is not predictive of FGFR inhibitor sensitivity [70].

4.1.2. Sensitivity to AZD4547 correlates with A-FABP/FABP4 expression

To determine the biological mechanisms underlying the differential sensitivities of UC cells to AZD4547 and gefitinib, we performed mRNA expression profiling using the Illumina platform (Human HT-12 V 4.0) to compare the baseline mRNA expression profiles in the FGFR- and EGFR-dependent UC cells. We found that several of the top genes that were differentially expressed between them were components of the PPARγ transcriptional pathway (Figure 4.6). Specifically, high baseline expression

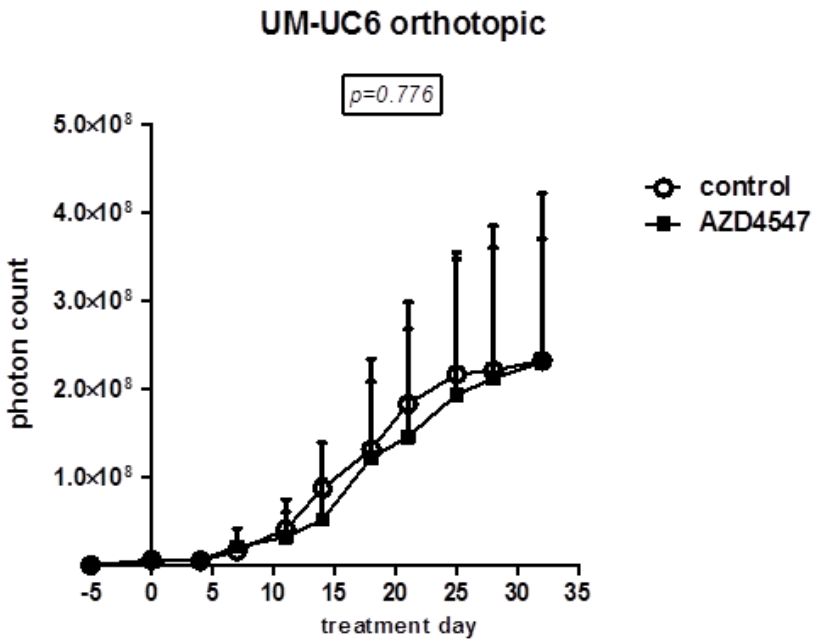

Figure 4.5 Effects of AZD4547 in orthotopic UM-UC6 tumors. UM-UC6 cells were orthotopically implanted into the bladder. Tumors were allowed five days to establish prior to treatment. Animals were given either vehicle or AZD4547 (12.5 mg/kg) via oral gavage (n = 8 / group). Primary tumor growth was continuously measured by non-invasive *in vivo* bioluminescence imaging. Photon counts are indicated as mean ± SEM.

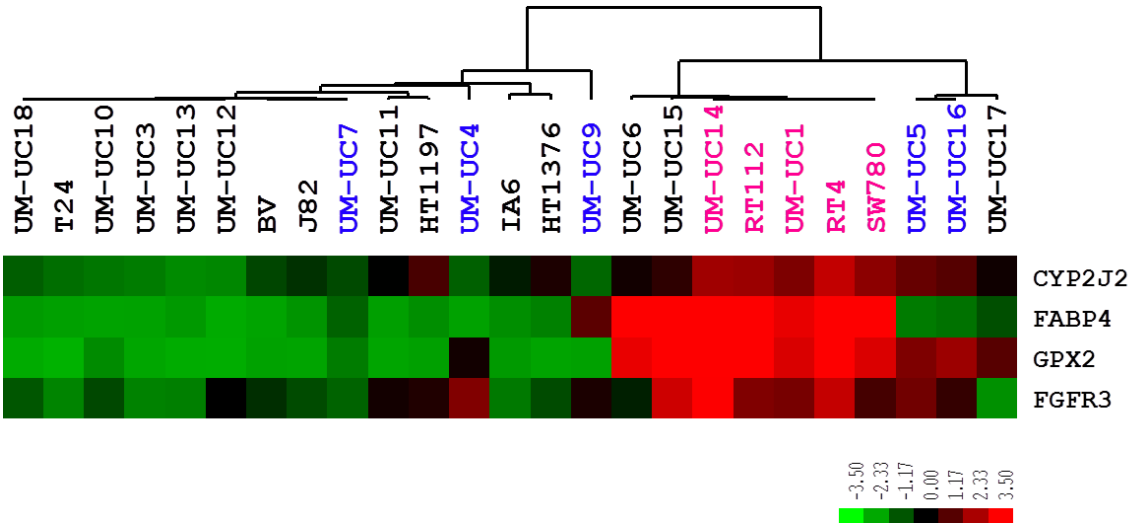

Figure 4.6 Differential expression of FABP4, CYP2J2, GPX2 and FGFR3 in a panel of urothelial cancer cell lines (n = 25). Whole genome mRNA expression profiling (Illumina platform) was used to measure mRNA expression. The heat map depicts the expression of CYP2J2, FABP4, GPX2 and FGFR3. Urothelial cancer cell lines are color-coded according to the corresponding sensitivity to gefitinib (blue) or AZD4547 (red).

of fatty acid binding protein 4 (FABP4, Adipocyte-FABP), characterized the FGFR-dependent cell lines, whereas FABP4 was essentially undetectable in the EGFR-dependent cells (a 55-fold difference) (Figure 4.6). We confirmed these findings by both quantitative PCR and Immunoblotting (Figure 4.7). Additionally, the FGFR-dependent cells expressed high levels of CYP2J2 (7-fold difference), the cytochrome P450 isoform that produces PPAR ligands [160], and GPX2 (18 fold difference), a known downstream target of PPARγ signaling [160,161] (Figure 4.6). These results were also confirmed by quantitative PCR (Figure 4.8). To further validate that the FGFR-dependent cells displayed baseline gene expression patterns consistent with PPARγ activation, we then used a hepatocyte-derived PPARγ gene set [162] to conduct gene set enrichment analyses (GSEA) to test degree of PPARγ signal enrichment in the FGFR-dependent cells as compared to the EGFR-dependent cells. The results indicated that PPARγ regulating genes were enriched in the FGFR-dependent cells with a normalized enrichment score (NES) of 1.83 (Figure 4.9, P=0.002). Together, these results suggested a strong correlation between PPARγ activation, more specifically constitutive expression of FABP4

4.1.3. PPARγ modulates FABP4 expression in UC cells

FABP4 functions as a specific co-activator for PPARγ by binding PPARγ ligands in the cytosol, transferring and facilitating ligand binding to PPARγ via a mechanism that has been termed “ligand tunneling”, and promoting

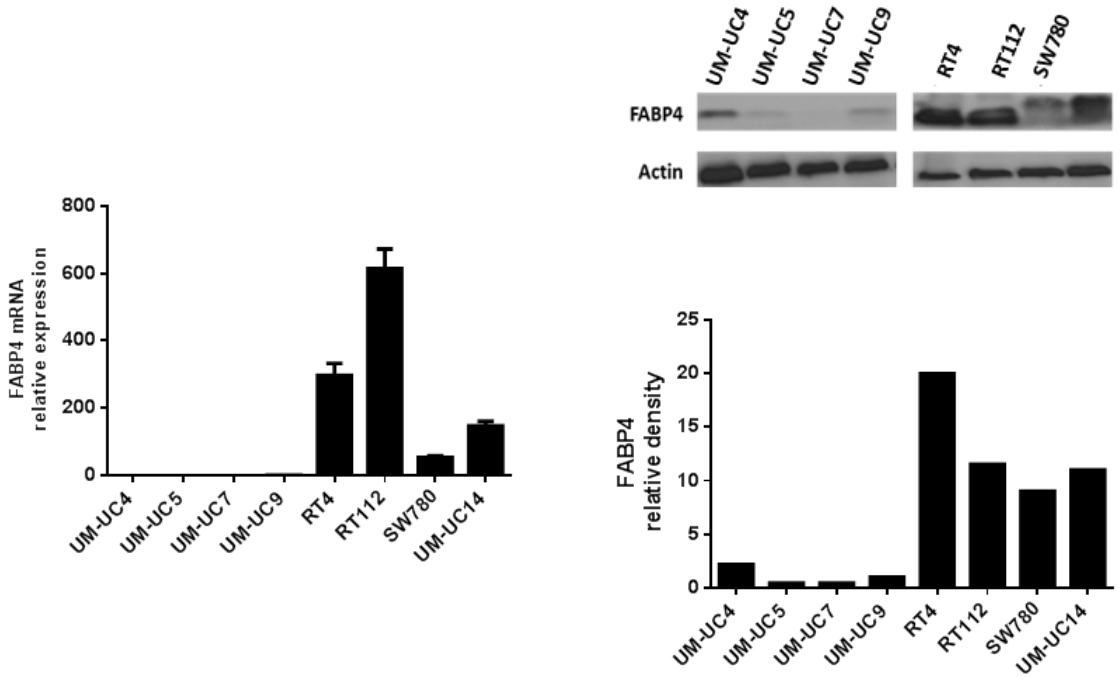

Figure 4.7 Confirmation of differential FABP4 expression in the panel of UC cells. FABP4 mRNA and protein expression were measured by quantitative PCR and immunobloting respectively.

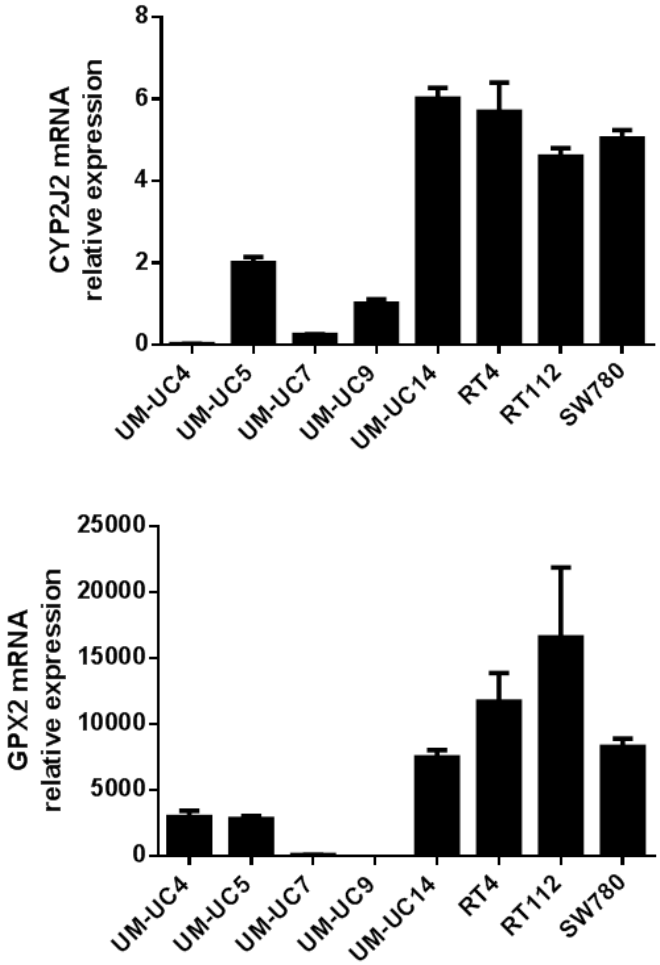

Figure 4.8 Expression of CYP2J2 and GPX2 in the EGFR (UM-UC4, UM-UC5, UM-UC7, UM-UC9) and FGFR (UM-UC14, RT4, RT112, SW780) dependent UC cell lines. CYP2J2 and GPX2 mRNA expression was measured by quantitative PCR and normalized to UM-UC9.

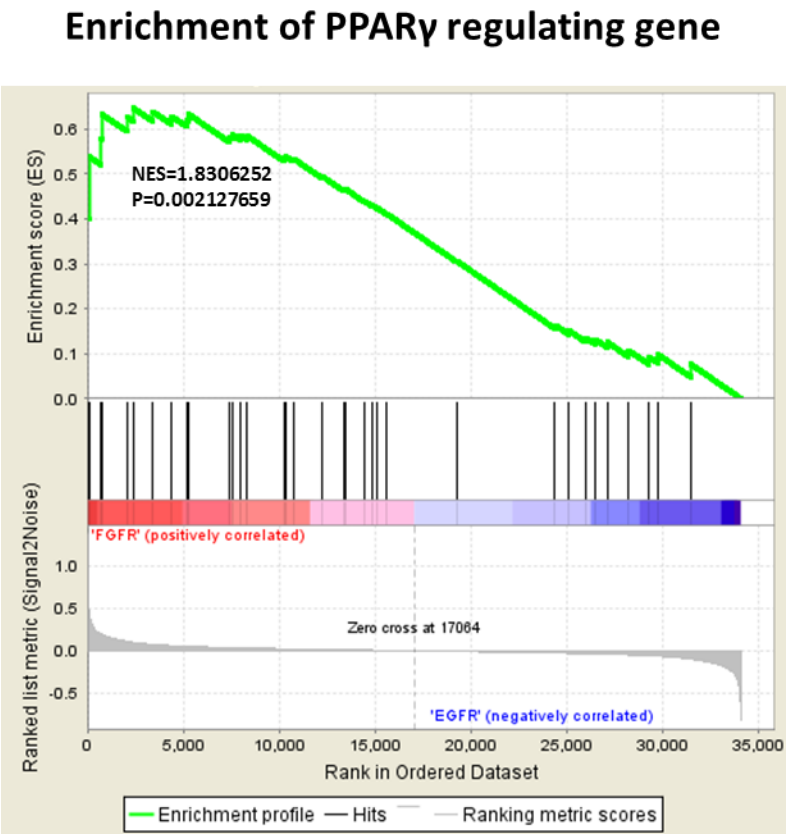

Figure 4.9 Hepatocyte-derived PPARγ gene set is enriched in FGFR3-dependent cells. Gene set enrichment analyses were performed to compare PPARγ pathway gene expression in the four FGFR3-dependent (UM-UC14, RT4, RT112, SW780; red color coded) and the four EGFR-dependent (UM-UC4, UM-UC5, UM-UC7, UM-UC9; blue color coded) cell lines using the whole genome mRNA expression profiling data.

PPARγ translocation to the nucleus [163,164]. Although GSEA indicated the activation of PPARγ transcriptional pathway in FGFR dependent UC cells that were featured constitutive expression of FABP4, it was unclear whether PPARγ was in fact responsible for this constitutive FABP4 expression in the FGFR dependent cells because of the fact that all three PPAR isoforms (α, β, γ) interact with similar DNA response elements [165]. Therefore, we first used isoform-specific chemical agonists to determine this. Exposure to the PPARγ-selective agonist rosiglitazone but not the α- and β-isoform agonists Wy14643 and L-165,041 resulted in strong induction of FABP4 in the EGFR-dependent cells (Figure 4.10 upper panel). We observed similar but less substantial effects in the FGFR dependent cells, most likely because they expressed higher levels of FABP4 at baseline (Figure 4.10 lower panel). None of the three isoform-selective antagonists had any effects on FABP4 expression in the absence of ligand (data shown for PPARγ, Figure 4.10). However, siRNA mediated silencing of PPARγ (but not the other isoforms) inhibited basal FABP4 expression in the FGFR dependent cell lines UM-UC14 and RT4 (Figure 4.11). Taken together, these data suggested that the constitutive high-level expression of FABP4 observed in the FGFR dependent UC cells is caused by constitutive PPARγ activation.

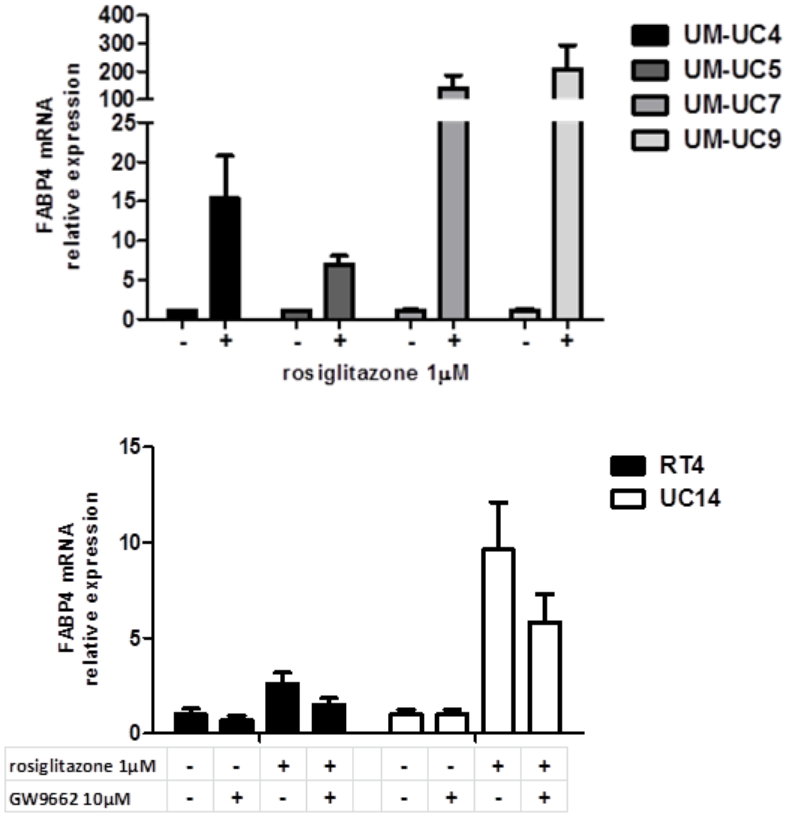

Figure 4.10 FABP4 expression is regulated by PPARγ. EGFR dependent bladder cancer cells (UM-UC4, UM-UC5, UM-UC7, UM-UC9) were exposed to the selective PPARγ agonist rosiglitazone and FABP4 mRNA expression was measured by quantitative RT-PCR. Modulation of FABP4 mRNA levels by the PPARγ agonist rosiglitazone and the PPARγ antagonist GW9662 in FGFR3 dependent bladder cancer cells (UM-UC14, RT4).

A.

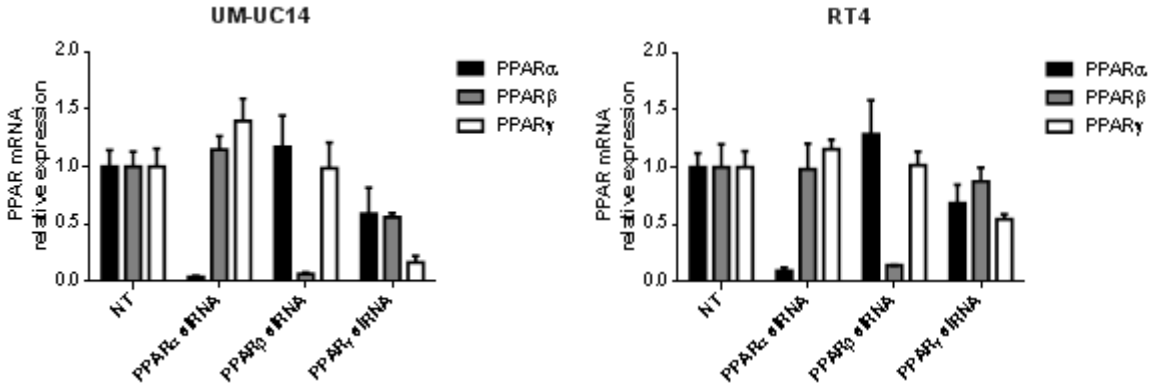

B.

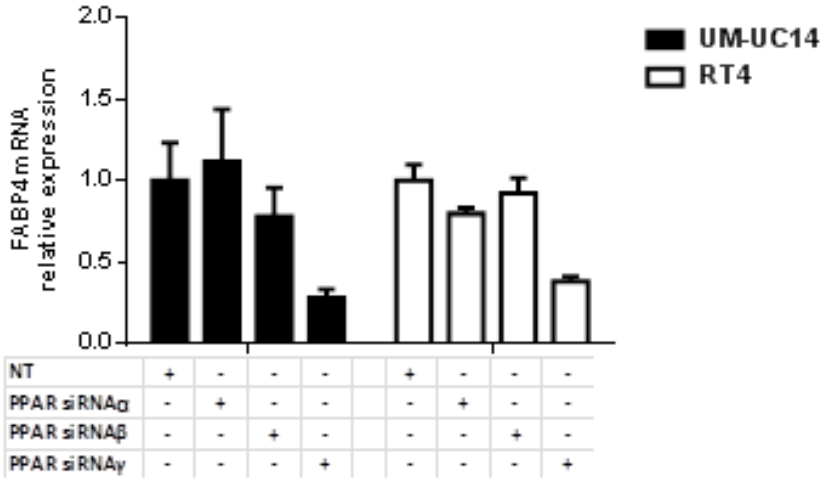

Figure 4.11 Effects of silencing PPARα, β or γ isoform on FABP4 expression. A. Knockdown efficacy of siRNAs specific for different PPAR isoforms. B. FABP4 expression after PPARα, β or γ knockdown. Relative mRNA expression was measured by quantitative PCR.

4.1.4. Modulation of FABP4 affects EGFR sensitivity

Recent publication suggests that FABP4 is an obligate co-activator for PPARγ activation, in that FABP4 binds and delivers PPARγ ligands from cytosol to nucleus, therefore facilitating the ligation and enhancing the transcriptional activity of PPARγ [163,164]. Additionally, our data revealed that FGFR dependent cells are characterized by the constitutive PPARγ activation, whereas little/low level of PPARγ activation marks the EGFR-dependent cells. Therefore, we tried to determine whether PPARγ activation affected FGFR and/or EGFR inhibitor sensitivity. We first exposed the EGFR dependent cell lines to rosiglitazone with or without gefitinib and measured growth inhibition using 5-day MTT assays. We observed that rosiglitazone alone had no effects on cell proliferation (data not shown). However, it actually prevented the growth inhibition that was induced by gefitinib in EGFR dependent cells (Figure 4.12). These data appeared to contradict previous studies, which concluded that PPARγ agonists inhibit proliferation and/or induce apoptosis in bladder cancer cells [166,167]. However, these previous studies used very high concentrations (≥ 100μM) of the PPARγ agonists compared to our study, and we concluded that rosiglitazone had no effects on cell proliferation by itself in any of the cell lines at concentrations that induced strong FABP4 expression. Furthermore, stable FABP4 knockdown (gene knockdown efficacy shown in figure 4.13 lower panel) blocked the gefitinib resistance induced by rosiglitazone in the EGFR dependent cell lines (UM-UC4, UM-

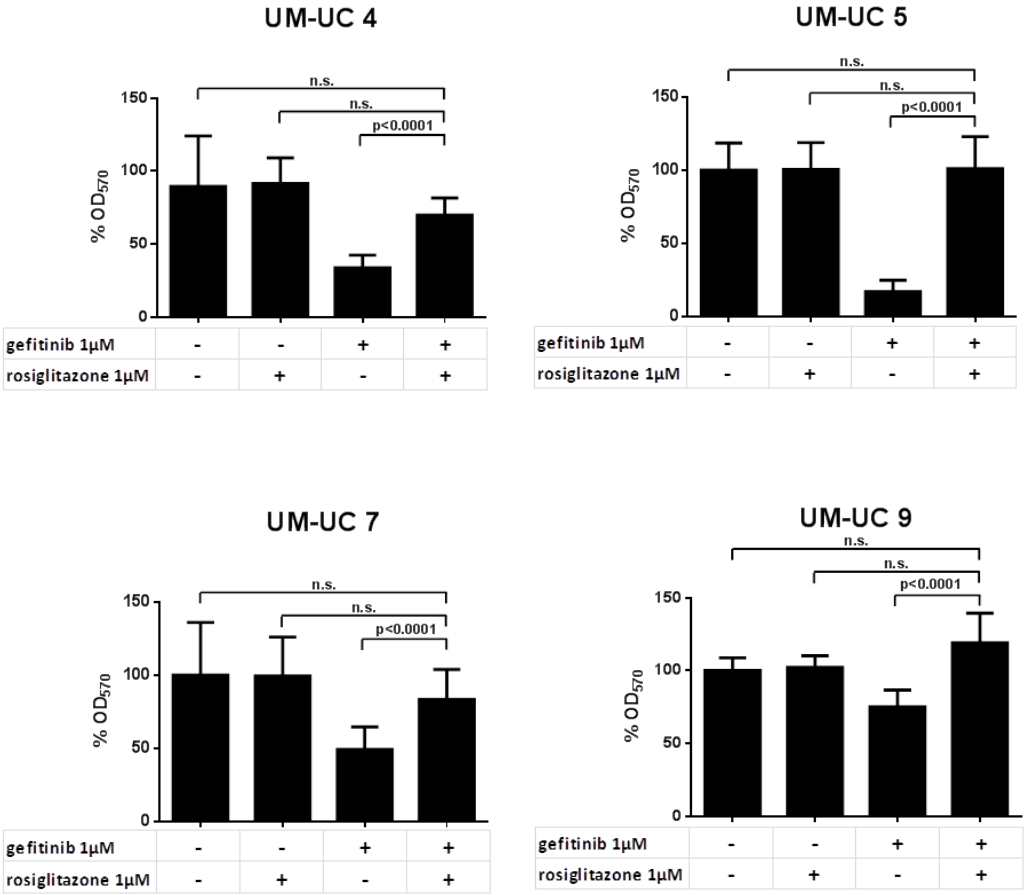

Figure 4.12 Activation of the PPARγ signaling pathway blocks EGFR dependency. The EGFR-dependent UM-UC4, UM-UC5, UM-UC7, and UM-UC9 cells were exposed to rosiglitazone (1μM), gefitinib (1μM), or a combination of both (1μM each) at days 0 and 2, and cell proliferation was measured at day 5 using MTT assays. Data are normalized to controls and indicated as means ± SEM.

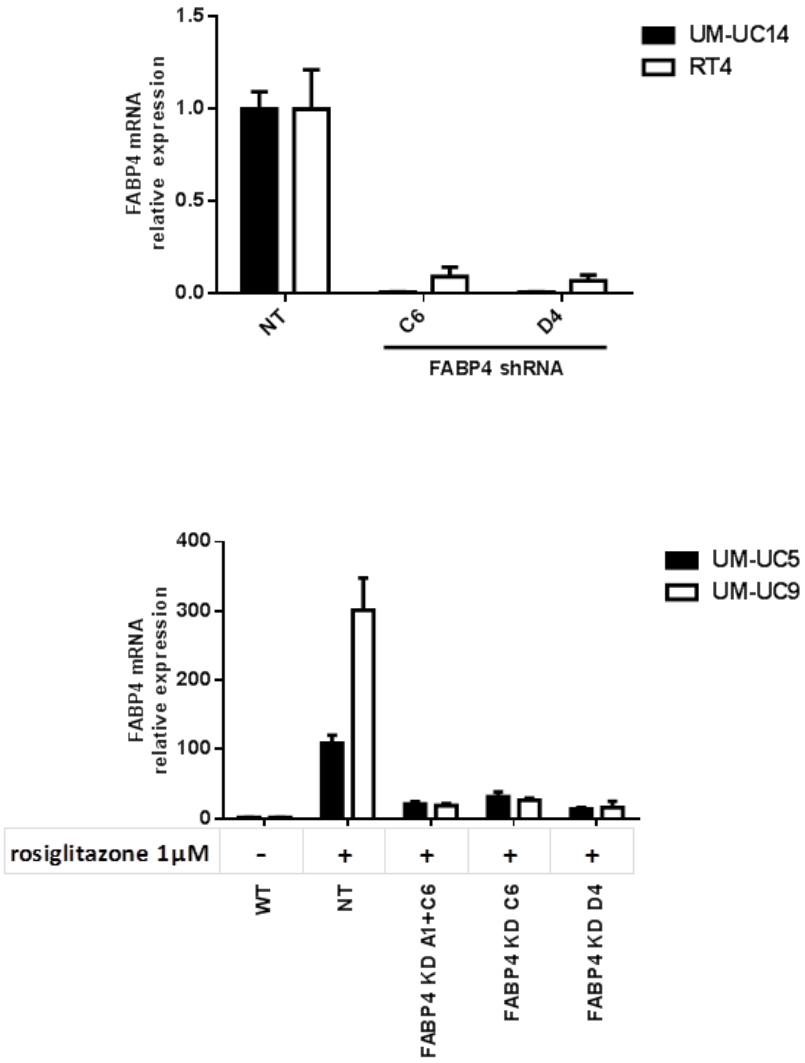

Figure 4.13 Efficiency of FABP4 silencing in FGFR dependent (UM-UC14 and RT4) and EGFR dependent (UM-UC5 and UM-UC9) cells.

Cells were transfected with FABP4 shRNA constructs (C6 or D4) along in FGFR dependent cells or in the presence of absence of PPARγ agonist rosiglitazone in the EGFR dependent cells. FABP4 mRNA expression was measured by quantitative PCR.

UC5, UM-UC7 and UM-UC9) (Figure 4.14). Specifically, rosiglitazone induced resistance to gefitinib in these EGFR dependent cells (Figure 4.12). However, exposure to rosiglitazone didn't prevent growth inhibition induced by gefitinib when FABP4 was stably silenced (Figure 4.14).

Given that our data suggested induction of FABP4 expression promoted resistance to gefitinib in EGFR dependent cells, it is presently unclear whether FABP4 modulation altered sensitivity to EGFR inhibitor gefitinib in FGFR dependent cells. Therefore, we first stably knocked down FABP4 in FGFR dependent cell lines UM-UC14 and RT4. Gene silencing efficacy was measured by PCR analysis (Figure 4.13 upper panel). We then exposed the stable FABP4-knockdown UM-UC14 and RT4 with gefitinib to test whether decreased FABP4 increased sensitivity to gefitinib. Cell growth data revealed that FABP4 silencing induced concentration dependent response to gefitinib in FGFR dependent cells UM-UC14 and RT4, whereas the counterpart NT controls remained resistance to gefitinib (Figure 4.15). Overall, we could conclude that sensitivity to EGFR inhibitor gefitinib could be affected by PPARγ activation, specifically modulation of FABP4.

4.1.5. CHOP acts downstream of PPARγ (Preliminary data)

To identify the downstream transcriptional targets of PPARγ that controlled EGFR dependency, we performed whole genome gene

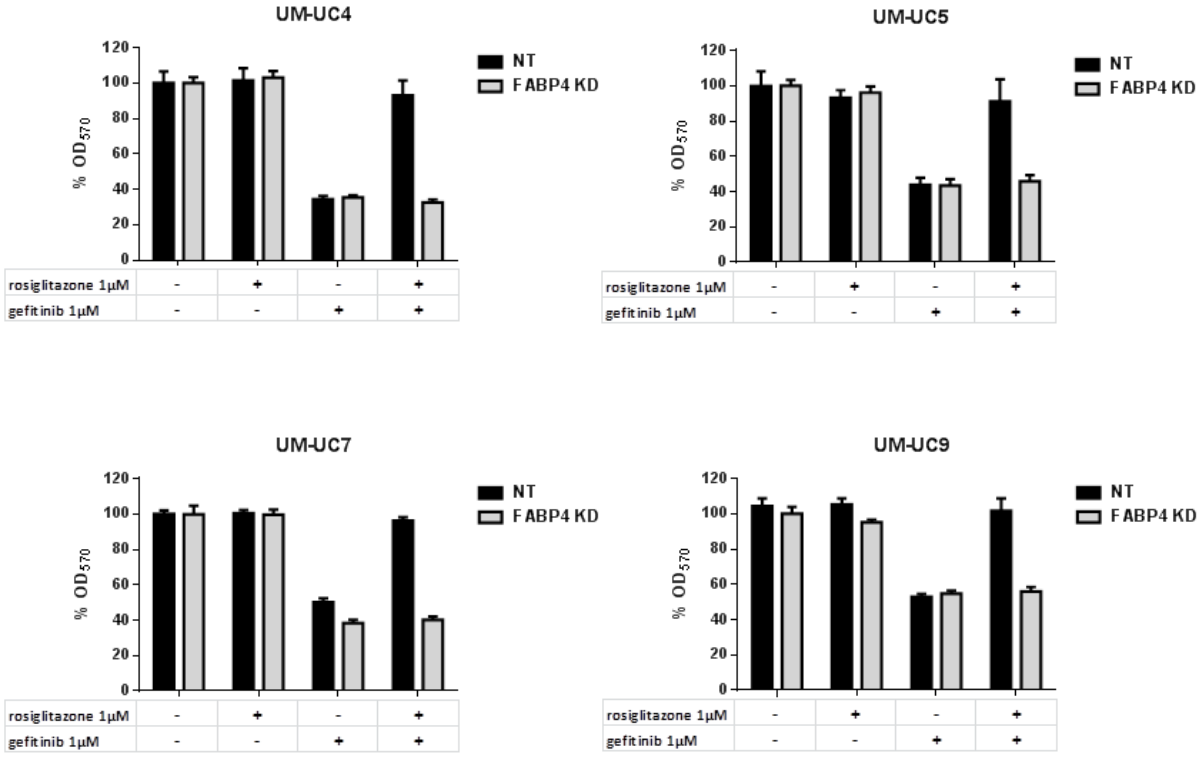

Figure 4.14 FABP4 silencing blocks rosiglitazone-induced gefitinib resistance. EGFR dependent cells (UM-UC4, UM-UC5, UM-UC7, and UM-UC9) were stably transduced with the FABP4-specific or non-targeting shRNA constructs. Cells were then exposed to rosiglitazone (1μM), gefitinib (1μM), or a combination of both (1μM each) for 5 days, and cell proliferation was measured using MTT assays. Data were normalized to NT controls and indicated as mean ± SEM.

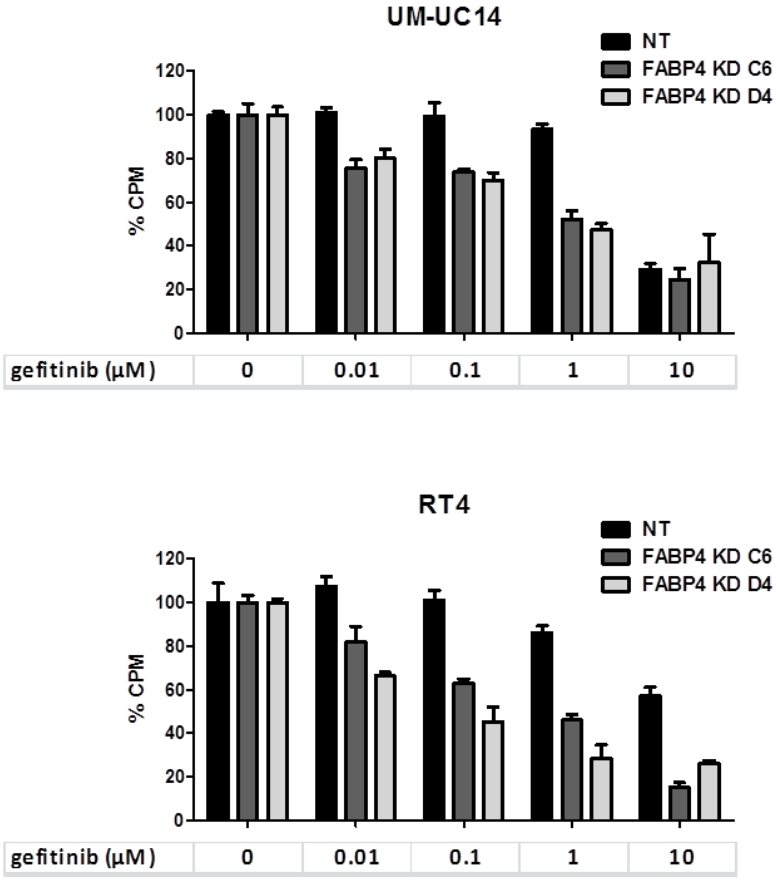

Figure 4.15 Down-regulation of FABP4 promotes gefitinib sensitivity in FGFR-dependent cells. UM-UC14 and RT4 were stably transduced with two different FGFR3-specific lentiviral shRNA constructs (C6 or D4) or a non-targeting (NT) control. Cells were then exposed to the indicated concentrations of either AZD4547 or gefitinib, and cell proliferation was measured after 48 hours using thymidine incorporation assays. Data were normalized to NT control and indicated as mean ± SEM.

expression profiling of the EGFR dependent UM-UC9 cells incubated with or without rosiglitazone (in triplicate). We also performed the gene expression profiling of the FGFR dependent UM-UC14 cells transduced with non-targeting or FABP4-specific shRNA constructs (in triplicate). We then performed class comparison analyses using BRB Array Tools to extract the significantly differentially expressed genes in each cell line group ($p<0.001$ with FDR <0.1) and subjected the genes to Ingenuity Pathway Analyses (IPA). These analyses identified the known PPARγ target FABP4 as one of top 5 activated genes in the rosiglitazone-treated UM-UC9 cells and one of top 5 suppressed genes in the FABP4 silenced UM-UC14 cells, which was expected and served as a positive control. Other than FABP4, the endoplasmic reticular (ER) stress-responsive transcription factor GADD153/CHOP (DDIT3) was the only other gene that was shared among the top 5 altered genes in both models (Table 4.1). Furthermore, using the IPA Upstream Regulators function, the CHOP pathway was identified as the one that was most strongly down-regulated in the FABP4 silenced UM-UC14 cells and most strongly up-regulated pathway in the rosiglitazone-treated UM-UC9 cells. In addition, 4 out of 4 CHOP targeted molecules defined by IPA changed in the same direction as CHOP did in FABP4 silenced UM-UC14 cells (Figure 16 left panel). Among these 4 genes, GADD34, ERO1L also changed in the same direction as CHOP did in rosiglitazone-treated UM-UC9 cells (Figure 16 right panel). Interestingly, the cyclic AMP-dependent transcription factor

		UM-UC14				
		Non-targeting	FABP4 Knockdown	Fold change	FDR	Parametric p value
UP-REGULATED	S100A8	6.79	8.94	4.44	0.000131	1.00E-07
	KRT6A	6.45	8.35	3.73	< 1e-07	< 1e-07
	CALML3	6.05	7.79	3.33	0.00104	3.40E-06
	PMEPA1	8.45	9.93	2.78	0.0247	0.000939
	MT1X	9.37	10.83	2.75	0.000448	7.00E-07
DOWN-REGULATED	GDF15	13.50	9.58	0.066	< 1e-07	< 1e-07
	FABP4	14.03	10.34	0.078	< 1e-07	< 1e-07
	LCN2	12.45	9.15	0.1	< 1e-07	< 1e-07
	DDIT3	11.97	8.80	0.11	0.00069	1.40E-06
	ORL1	9.38	6.86	0.17	< 1e-07	< 1e-07

		UM-UC9				
		Vehicle	rosigalitazone	Fold change	FDR	Parametric p value
UP-REGULATED	HMGCS2	5.78	10.09	19.89	< 1e-07	< 1e-07
	DDIT3	7.17	10.95	13.73	< 1e-07	< 1e-07
	FABP4	10.96	14.59	12.41	< 1e-07	< 1e-07
	BBOX1	8.36	11.91	11.7	< 1e-07	< 1e-07
	HPGD	9.05	12.44	10.5	< 1e-07	< 1e-07
DOWN-REGULATED	SPRR2D	11.39	8.06	0.099	< 1e-07	< 1e-07
	OSBP2	9.38	6.12	0.1	< 1e-07	< 1e-07
	IL11	10.00	6.83	0.11	< 1e-07	< 1e-07
	OAS2	10.02	6.98	0.12	< 1e-07	< 1e-07
	IFI44L	10.09	7.06	0.12	< 1e-07	< 1e-07

Table 4.1 Identification of GADD153/CHOP/DDIT3 as a PPARγ target gene. List of differentially expressed genes that were shared in FABP4 knockdown UM-UC14 cells compared to non-targeting (NT) controls, and rosiglitazone-treated UM-UC9 cells versus controls.

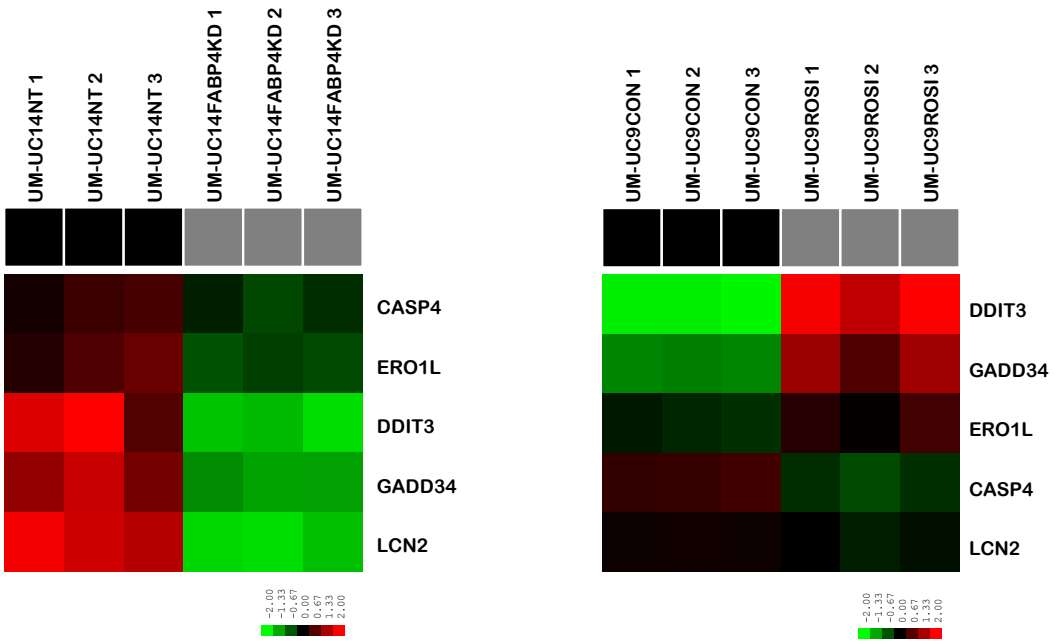

Figure 4.16 Identification of GADD153/CHOP/DDIT3 as a PPARγ target gene. Heatmap depicts CHOP (DDIT3) expression and expression of its IPA-defined downstream targets (HSPE1, CASP4, ERO1L, GADD34, LCN2) in the UM-UC14 and UM-UC9 experimental sets.

ATF-3 (ATF3), which acts downstream of CHOP, was also among the top IPA “upstream regulators” as measured by log ratio change in both subsets (data not shown).

4.2. Discussion

Previous work has revealed the existence of subsets of human bladder cancer cells that are either EGFR [115,147] or FGFR3 [70,156] dependent for cell proliferation and tumor growth. However, little is known regarding the underlying mechanism of such EGFR or FGFR3 dependency in human urothelial cancer cells. Although recent studies have provided some indirect explanation, including pathway redundancy and impaired negative feedback loops [132], much is left to be discovered. In this study, we directly demonstrated for the first time that EGFR and FGFR3 dependency are non-overlapping and mutually exclusive in human urothelial cancer. Furthermore, our data suggested that this mutually exclusive EGFR or FGFR3 dependency is tightly regulated by PPARγ signaling both in human urothelial cancer cells and in orthotopic xenograft. PPARγ, a member of peroxisome proliferator activated receptors active in nucleus, is a intracellular transcription factor well known for its important role in adipogenesis and tissue differentiation [168-171]. On the other hand, CHOP is also a transcription factor that is extensively studied for its role in the response to ER stress [172]. Although their roles in controlling

of growth factor receptor dependency in human cancer have not been reported, previously a few studies have demonstrated that C/EBP protein family acts as co-activators with PPARγ to promote the transcription of genes involved in adipogenesis and adiopocyte differentiation [169,171,173]. A recent chromatin immunoprecipitaiton sequencing study revealed that C/EBP binding motifs were located in the vicinity of PPAR binding site, and both C/EBP proteins and PPARγ binding to specific DNA motifs were required for robust adipocyte gene expression. Collectively, our data suggested for the first time that PPARγ potentially coordinate with CHOP to control EGFR dependency. To verify this hypothesis that CHOP acts downstream of PPARγ to regulate EGFR sensitivity, we are planning to directly silence CHOP in UM-UC14 and RT4 and test whether silencing of CHOP sensitize these cells to EGFR antagonist gefitinib. Moreover, we also planning to overexpress CHOP in original EGFR dependent cells (UM-UC4, UM-UC5, UM-UC7 and UM-UC9) and test whether activation of PPARγ by overexpression of CHOP will block the sensitivity to EGFR inhibitor gefitinib. If our hypothesis is tested to be true, we are going to further investigate whether PPARγ-CHOP signaling regulate EGFR dependency through mechanisms that directly interact with the receptor.

Previous work suggested that pathway redundancy provided escape mechanisms for acquired resistance to EGFR TKIs [132,145], which indicated a direct interaction between EGFR and FGFR on the receptor level. Furthermore, given the high level of downstream signal transduction

redundancy between EGFR and FGFR3 signaling [115,156], it is possible that PPARγ signaling employs mechanisms that directly interact with the respective receptors rather than with downstream signaling components to modulate EGFR or FGFR3 dependency. MIG6, one of the four EGFR inducible feedback inhibitors, is a cytosolic protein that is induced through EGFR activation and attenuates EGFR signaling following its activation [174]. MIG6 contains a centrally located ErbB binding region (ERB) that allows for specific binding to EGFR kinase domain to lock EGFR molecules in a catalytically inactive configuration, which prevents signal generation and transduction [174]. Moreover, MIG6 also has the capability to rapidly down-regulate EGFR molecules and route them to lysosome for degradation [175,176]. Overexpression of MIG6 is sufficient to abrogate EGFR phosphorylation and activation, EGFR mediated downstream signaling transduction, and EGFR regulated biological and cellular function [174,177]. Given that, we are planning to directly test the hypothesis that MIG6 (ERRFI1 or RALT) acts as a downstream target of PPARγ signaling to inhibit EGFR dependency though MIG6's direct interaction between MIG6 and respective receptors without interfering with the downstream MAPK/Erk and PI3K pathways, which are also used to mediate FGFR3 dependency.

While our data revealed that PPARγ-CHOP signaling modulated EGFR dependency, it is still unclear whether PPARγ-CHOP controls FGFR3 dependency. Therefore, we are planning to examine the linkage between

PPARγ-CHOP and FGFR3 dependency. Although preliminary data suggested that rosiglitazone alone did not increase sensitivity to the FGFR inhibitor AZD4547 in EGFR dependent cell line UM-UC9 (data not shown), it was possible that FGFR3 dependency required high level expression of surface FGFR3, which was evidenced by our previous study [70,156]. Hence, we are going to direct test this hypothesis using exogenous expression of FGFR3 in UM-UC9. Moreover, we are also planning to examine whether PPARγ-CHOP controls FGFR3 dependency in cells natively responding to FGFR3 inhibitors.

FGFR substrate 2α (FRS2) is a docking/scaffolding adaptor protein that functions downstream of certain receptor tyrosine kinases to promote signal transduction [178]. Specifically, emerging evidence indicated that FRS2α acts as a control center for FGFR intracellular signaling. It becomes tyrosine phosphorylation on several residues followed by FGFR activation, which creates binding sites for SH2 domain of Grb2 adaptor protein. The activated Grb2 recruits multiple adaptor proteins including SOS that finally leads to strong activation of Ras/MAPK/Erk pathway [179]. Interestingly and more importantly, FRS2α selectively binds some receptor tyrosine kinases over the others, which is one of the unique characters of this adaptor protein [178]. A good example is that It acts downstream of FGFRs but not EGFR. Therefore, we could further hypothesize that PPARγ-CHOP signaling controls FGFR3 dependency via the induction of FRS2α without interfering with EGFR-mediated signaling,

and we are going to test it using exogenous expression of CHOP in UM-UC9 cells. Furthermore, exploring the link between PPARγ-CHOP and FRS2α would provide direct mechanistic explanation as to why PPARγ-CHOP regulates FGFR3 dependency.

CHAPTER 5. FINAL CONCLUSIONS AND FUTURE DIRECTIONS

5.1. Final conclusions

5.1.1. FGFR3 regulates human urothelial cancer growth

In summary, we have demonstrated that the levels of FGFR3 expression correlate with FGFR3 dependency, and that FGFR3 is more important than FGFR1 in driving proliferation in human urothelial cancer cells. Specifically, FGFR3 expression correlated well with the sensitivity to the FGFR antagonist (BGJ-398) in a panel of 17 urothelial cancer cell lines. Furthermore, silencing of FGFR3 simulates the effects of BGJ-398 exposure in both UM-UC14 and RT4 cells *in vitro*. Additionally, both exposure to BGJ-398 and FGFR3 specific knockdown using an RNAi based strategy produced cell cycle arrest, which indicate that FGFR inhibitors induce cytostatic but not cytotoxic in human bladder cancer cells. Our data together with other recent studies [102,154,156] support the ongoing development of FGFR specific inhibitors for clinical targeted therapy, particularly in combination with chemotherapy or radiation therapy due to their cytostatic effects. However, human urothelial cancer cells display a remarkable heterogeneity in sensitivity to FGFR inhibitors as revealed both in this study and previous work [156]. It is still unclear what mechanisms drive the intrinsic sensitivity to FGFR inhibitors, though several mechanisms have been proposed including FGFR3 activating mutations, the presence of TACC3-FGFR3 translocation, and high level of FGFR3 expression. The predictive value of these markers must now be determined in urothelial cancer patients so that it is practically possible to

identify the appropriate subset of bladder cancer patients who could benefit markedly from the FGFR targeted therapy. Therefore, tremendous efforts from clinical research are needed in the future to uncover the mechanisms that could lead to successful development of biomarkers to identify the patient population for FGFR3 targeted therapy.

5.1.2. FGFR1 mediates human urothelial cancer metastasis

More importantly, our study indicates that FGFR1 mediates cell invasion and tumor metastasis in human urothelial cancer. Specifically, FGFR1 repression by either FGFR antagonist (BGJ-398) or direct FGFR1 silencing severely reduced cell invasion *in vitro*. In addition, exposure to BGJ-398 inhibited metastasis and circulating tumor cells production without affecting primary tumor growth in orthotopic tumor xenografts. Consistent with our conclusion, a recent study also supports the role of FGFR1 in promoting epithelial-to-mesenchymal transition, which results in increased levels of invasion and metastasis [104]. Although the same study suggested that FGFR1 promotes cell migration and invasion through cyclooxygenase-2 (COX-2) activation, much more is left to be determined. Further investigation utilizing global gene expression profiling and pathway analysis would be performed to address the cause-effect questions of what signaling pathways and transcriptional factors acting downstream of FGFR1 to promote cell invasion and tumor metastasis. Furthermore, our study also provides a rationale for targeting FGFR, specifically FGFR1, to prevent invasion and treat metastasis. Clinically, ~20% of the non-muscle

invasive bladder cancers progress to become muscle invasive and metastatic, which accounts for the bulk of patient mortality. If appropriate biomarkers could be developed to identify the right patient subset, FGFR1 targeted therapy combined with conventional chemotherapy could be beneficial to this sub-group of patients. Therefore, future effects should focus on the development of clinically relevant biomarkers to prospectively identify patients who are more likely to benefit from FGFR targeted therapy as well as testing the efficacy of FGFR targeted therapy in a metastatic setting.

5.1.3. Heterogeneous sensitivity to FGFR antagonist in "epithelial" bladder cells

Finally, our study suggests that there is profound heterogeneity of FGFR3 dependency. Specifically, although some of the urothelial cell lines that contain activating mutations were highly sensitive to FGFR inhibitors, the majority of FGFR3-mutant cell lines remained resistant to FGFR inhibitor (BGJ-398). Previously, several studies have uncovered the mechanisms how FGFR3 activating mutations drive proliferation in human bladder cancer cells. However, our data suggest the existence of more complicated biological interaction that urothelial cells possess, which require further investigate to elucidate and validate. Recently, several studies highlight the EGFR and FGFR interaction as one of the mechanisms that cells escape from the pressure of FGFR antagonist, which provide a direction to elucidate the mechanism of intrinsic and

acquired resistance. We plan to further investigate the FGFR3-mutant cell lines that are resistant to FGFR inhibitor to uncover the escape mechanisms, with hopes of identifying the best strategies to appropriately utilize FGFR targeted therapy to benefit patient clinically.

5.1.4. Discrete EGFR dependency is controlled by PPARγ-FABP4 transcriptional complex

We demonstrate for the first time that EGFR and FGFR3 dependency are non-overlapping and mutually exclusive to each other in human urothelial cancer. More specifically, we have identified 4 cell lines (UM-UC4, UM-UC5, UM-UC7 and UM-UC9) that were sensitive to EGFR antagonist gefitinib but not to FGFR antagonist AZD4547 at the clinical relevant concentration (≤ 1μM). We also identify different 4 cell lines (UM-UC14, SW780, RT4 and RT112) that were sensitive to FGFR inhibitor AZD4547 but not to EGFR inhibitor gefitinib. Our data indicated the possibility that human urothelial cancer cells depends primarily on one single growth factor receptor for growth and proliferation. However, this idea needs extensive research to test and validate.

Furthermore, the observation that PPARγ signaling pathway controls this mutually exclusive biological phenotype extends our knowledge of molecular mechanism that mediates EGFR dependent proliferation. More specifically, PPARγ signal activation is enriched in FGFR3 dependent (but EGFR inhibitor resistant) urothelial cells, whereas EGFR dependent (but

FGFR inhibitor resistant) urothelilal cells lack PPARγ activation. In addition, up-regulation of FABP4 forces EGFR dependent cells becoming resistance to EGFR antagonist while down-regulation of FABP4 promotes sensitivity to EGFR inhibitor in FGFR3 dependent cells. Overall, we for the first time have shown that PPARγ activation, specifically via FABP4, represses EGFR dependency that is exclusive to FGFR3 dependency in urothelilal cancer.

5.2. Future directions

5.2.1. FGFR1 and cell invasion

In this study, we have demonstrated that FGFR1 inhibition blocks cell invasion and tumor metastasis. More specifically, direct FGFR1 silencing decreased cell invasion *in vitro*, and the FGFR antagonist BGJ-398 reduced tumor metastasis in orthotopic UM-UC3 metastatic xenografts *in vivo*. However, these interesting findings present at least two important avenues that require further research and elucidation. First, our data suggests that FGFR1 but not FGFR3 is responsible for cell invasion in “mesenchymal” UM-UC3 and UM-UC13 cells. However, our *in vivo* data don’t necessarily show that FGFR1 but not FGFR -2 or -3 regulated tumor metastasis because we used BGJ-398, a pan FGFR1-3 antagonist, instead of a direct FGFR1 inhibitor to conduct the animal study. Given the similarity of protein sequence among FGFRs, it is very difficult to develop

a specific FGFR1 antagonist. However, we could resolve this problem using FGFR1 gene silencing. Specifically, we could conduct a three arm *in vivo* study to directly test the hypothesis, with one arm for wild-type metastatic UM-UC3, the second arm transduced with non-targeting scramble shRNA, and the third arm transduced with FGFR1 specific shRNA.

Secondly, our study and a recent publication [104] suggest the role of FGFR1 in cell invasion and possible epithelial-to-mesenchymal transition. However, it is presently unclear that how FGFR1 regulates cell invasion, what molecules act downstream of FGFR1 pathway to mediate cell invasion and whether such a regulation involves EMT. To address these questions, we could start with gene expression profiling study to identify differential expressed genes by directly comparing the expression profile between non-targeting and FGFR1 knockdown in UM-UC3 and UM-UC13. Following upon the identification of differential expressed genes, we could use Ingenuity Pathway Analysis to dissect differential expressed genes to pinpoints candidates for further investigation. Finally, we could test the hypothesis that the candidate genes acts downstream of FGFR1 and are directly responsible for cell invasion and/or epithelial-to-mesenchymal transition.

5.2.2. Discrete EGFR dependency and PPARγ-FABP4 axis

In this study, we have identified the non-overlapping and mutually exclusive FGFR3 and EGFR dependency in urothelial cancer cells. The observation prompts us to propose the hypothesis that urothelial cancer cells or even cancer cells in genenral depends primarily on one single growth factor receptor for cell proliferation and tumor growth [180]. Therefore, we are going to evaluate various TKIs *in vitro* for their effects on proliferation of human urothelial cancer cells with the purpose to identify cell lines that are dependent on one primary growth factor receptor other than pre-defined EGFR and FGFR3 dependent cells in this study. The proposed study would elucidate the tendency whether one primary growth factor receptor drives proliferation in given cancer cells, which would pave the way to investigate and develop molecular signatures that would be ultimately used in clinic to improve personalized medicine. Furthermore, it will be helpful to investigate the molecular mechanism of such a dependency in order to identify relevant biomarkers/signatures for clinical translation. Given that the downstream signal transduction pathways controlled by the growth factor receptors are highly redundant, it is more likely that the molecular signatures that are responsible for such dependency lie in genes mediating growth factor receptor internalization, cytoplasmic trafficking, or controlling negative feedback loop mechanism. We plan to utilize genomic wide gene expression profiling to directly test these hypotheses. Presently, multiple studies have suggested the role of

pathway redundancy as one of the mechanisms cells employing to escape from TKIs. With this context in mind, we are going to directly examine the hypothesis that activating alternative growth factor receptors contributes to the resistance to FGFR or EGFR inhibition, which could help us to understand the mechanisms of intrinsic or acquired resistance.

Additionally, we demonstrate that the PPARγ signaling regulates the EGFR dependency. These important findings present at least two opportunities upon further experimental examination and validation. Firstly, we have established throughout our study that PPARγ signaling promotes CHOP expression in EGFR dependent urothelial cancer cells. However, our data does not provide details with respect to how PPARγ interacts with FABP4 to stimulate CHOP expression. Previously, FABP4 was shown to function as a specific co-activator for PPARγ through “ligand tunneling”, which facilitates PPARγ ligands transferring and binding to PPARγ receptor, and then promotes PPARγ translocation to nucleus. To specific address this question, we plan to investigate the PPARγ-FABP4 protein to protein interaction in FGFR3 dependent cells, examine the CHOP promoter area to identify potential PPARγ binding sites, and design chromatin immunoprecipitation (ChIP) experiment to confirm the binding of PPARγ-FABP4 complex to CHOP promoter.

Secondly, we identified several potential signatures, including high level of FGFR3 expression, FGFR3 activating mutation, and activation of PPARγ signaling, in the FGFR3 dependent cells although we haven’t established

the cause-effect link between PPARγ activation and FGFR3 dependency. We would further investigate this hypothesis by testing whether modulation of PPARγ activation affects FGFR3 dependency. Furthermore, if the hypothesis could be proven true, these findings could pave the way for uncovering clinical biomarkers to prospectively identify appropriate subset of patients who could benefit from FGFR3 targeted therapy. However, further clinical research in a large scale is needed to verify the correlation between FGFR and PPARγ-FABP4 signaling, and obtain the biomarker profiling to support the prospective identification of patient subset. We would also direct test the predictive power of these presumed biomarkers (PPARγ, FABP4, FGFR3 and its mutation) in clinical trials that are primarily designed to testing selective FGFR inhibitors in patients.

REFERENCES

1. Itoh N, Ornitz DM (2004) Evolution of the Fgf and Fgfr gene families. Trends Genet 20: 563-569.

2. Olsen SK, Garbi M, Zampieri N, Eliseenkova AV, Ornitz DM, et al. (2003) Fibroblast growth factor (FGF) homologous factors share structural but not functional homology with FGFs. J Biol Chem 278: 34226-34236.

3. Goldfarb M, Schoorlemmer J, Williams A, Diwakar S, Wang Q, et al. (2007) Fibroblast growth factor homologous factors control neuronal excitability through modulation of voltage-gated sodium channels. Neuron 55: 449-463.

4. Itoh N, Ornitz DM (2011) Fibroblast growth factors: from molecular evolution to roles in development, metabolism and disease. J Biochem 149: 121-130.

5. Kharitonenkov A (2009) FGFs and metabolism. Curr Opin Pharmacol 9: 805-810.

6. Mohammadi M, Olsen SK, Ibrahimi OA (2005) Structural basis for fibroblast growth factor receptor activation. Cytokine Growth Factor Rev 16: 107-137.

7. Johnson DE, Lu J, Chen H, Werner S, Williams LT (1991) The human fibroblast growth factor receptor genes: a common structural arrangement underlies the mechanisms for generating receptor forms that differ in their third immunoglobulin domain. Mol Cell Biol 11: 4627-4634.

8. Orr-Urtreger A, Bedford MT, Burakova T, Arman E, Zimmer Y, et al. (1993) Developmental localization of the splicing alternatives of fibroblast growth factor receptor-2 (FGFR2). Dev Biol 158: 475-486.

9. Schlessinger J, Plotnikov AN, Ibrahimi OA, Eliseenkova AV, Yeh BK, et al. (2000) Crystal structure of a ternary FGF-FGFR-heparin complex reveals a dual role for heparin in FGFR binding and dimerization. Mol Cell 6: 743-750.

10. Wu DQ, Kan MK, Sato GH, Okamoto T, Sato JD (1991) Characterization and molecular cloning of a putative binding protein for heparin-binding growth factors. J Biol Chem 266: 16778-16785.

11. Ibrahimi OA, Yeh BK, Eliseenkova AV, Zhang F, Olsen SK, et al. (2005) Analysis of mutations in fibroblast growth factor (FGF) and a

pathogenic mutation in FGF receptor (FGFR) provides direct evidence for the symmetric two-end model for FGFR dimerization. Mol Cell Biol 25: 671-684.

12. Hacker U, Nybakken K, Perrimon N (2005) Heparan sulphate proteoglycans: the sweet side of development. Nat Rev Mol Cell Biol 6: 530-541.

13. Eswarakumar VP, Lax I, Schlessinger J (2005) Cellular signaling by fibroblast growth factor receptors. Cytokine Growth Factor Rev 16: 139-149.

14. Altomare DA, Testa JR (2005) Perturbations of the AKT signaling pathway in human cancer. Oncogene 24: 7455-7464.

15. Klint P, Claesson-Welsh L (1999) Signal transduction by fibroblast growth factor receptors. Front Biosci 4: D165-177.

16. Peters KG, Marie J, Wilson E, Ives HE, Escobedo J, et al. (1992) Point mutation of an FGF receptor abolishes phosphatidylinositol turnover and Ca2+ flux but not mitogenesis. Nature 358: 678-681.

17. Thien CB, Langdon WY (2001) Cbl: many adaptations to regulate protein tyrosine kinases. Nat Rev Mol Cell Biol 2: 294-307.

18. Casci T, Vinos J, Freeman M (1999) Sprouty, an intracellular inhibitor of Ras signaling. Cell 96: 655-665.

19. Hacohen N, Kramer S, Sutherland D, Hiromi Y, Krasnow MA (1998) sprouty encodes a novel antagonist of FGF signaling that patterns apical branching of the Drosophila airways. Cell 92: 253-263.

20. Tsang M, Friesel R, Kudoh T, Dawid IB (2002) Identification of Sef, a novel modulator of FGF signalling. Nat Cell Biol 4: 165-169.

21. Zhao Y, Zhang ZY (2001) The mechanism of dephosphorylation of extracellular signal-regulated kinase 2 by mitogen-activated protein kinase phosphatase 3. J Biol Chem 276: 32382-32391.

22. Thisse B, Thisse C (2005) Functions and regulations of fibroblast growth factor signaling during embryonic development. Dev Biol 287: 390-402.

23. Beenken A, Mohammadi M (2009) The FGF family: biology, pathophysiology and therapy. Nat Rev Drug Discov 8: 235-253.

24. Turner N, Grose R (2010) Fibroblast growth factor signalling: from development to cancer. Nat Rev Cancer 10: 116-129.

25. Meyers EN, Lewandoski M, Martin GR (1998) An Fgf8 mutant allelic series generated by Cre- and Flp-mediated recombination. Nat Genet 18: 136-141.

26. Colvin JS, White AC, Pratt SJ, Ornitz DM (2001) Lung hypoplasia and neonatal death in Fgf9-null mice identify this gene as an essential regulator of lung mesenchyme. Development 128: 2095-2106.

27. Sekine K, Ohuchi H, Fujiwara M, Yamasaki M, Yoshizawa T, et al. (1999) Fgf10 is essential for limb and lung formation. Nat Genet 21: 138-141.

28. Tekin M, Ozturkmen Akay H, Fitoz S, Birnbaum S, Cengiz FB, et al. (2008) Homozygous FGF3 mutations result in congenital deafness with inner ear agenesis, microtia, and microdontia. Clin Genet 73: 554-565.

29. Wiedemann HR (1997) Salivary gland disorders and heredity. Am J Med Genet 68: 222-224.

30. van der Walt JM, Noureddine MA, Kittappa R, Hauser MA, Scott WK, et al. (2004) Fibroblast growth factor 20 polymorphisms and haplotypes strongly influence risk of Parkinson disease. Am J Hum Genet 74: 1121-1127.

31. Wang G, van der Walt JM, Mayhew G, Li YJ, Zuchner S, et al. (2008) Variation in the miRNA-433 binding site of FGF20 confers risk for Parkinson disease by overexpression of alpha-synuclein. Am J Hum Genet 82: 283-289.

32. Webster MK, Donoghue DJ (1997) FGFR activation in skeletal disorders: too much of a good thing. Trends Genet 13: 178-182.

33. Kannan K, Givol D (2000) FGF receptor mutations: dimerization syndromes, cell growth suppression, and animal models. IUBMB Life 49: 197-205.

34. Abuharbeid S, Czubayko F, Aigner A (2006) The fibroblast growth factor-binding protein FGF-BP. Int J Biochem Cell Biol 38: 1463-1468.

35. Beer HD, Bittner M, Niklaus G, Munding C, Max N, et al. (2005) The fibroblast growth factor binding protein is a novel interaction partner of FGF-7, FGF-10 and FGF-22 and regulates FGF activity: implications for epithelial repair. Oncogene 24: 5269-5277.

36. Su SC, Mendoza EA, Kwak HI, Bayless KJ (2008) Molecular profile of endothelial invasion of three-dimensional collagen matrices: insights into angiogenic sprout induction in wound healing. Am J Physiol Cell Physiol 295: C1215-1229.

37. Antoine M, Wirz W, Tag CG, Mavituna M, Emans N, et al. (2005) Expression pattern of fibroblast growth factors (FGFs), their receptors and antagonists in primary endothelial cells and vascular smooth muscle cells. Growth Factors 23: 87-95.

38. Antoine M, Wirz W, Tag CG, Gressner AM, Wycislo M, et al. (2006) Fibroblast growth factor 16 and 18 are expressed in human cardiovascular tissues and induce on endothelial cells migration but not proliferation. Biochem Biophys Res Commun 346: 224-233.

39. Barrientos S, Stojadinovic O, Golinko MS, Brem H, Tomic-Canic M (2008) Growth factors and cytokines in wound healing. Wound Repair Regen 16: 585-601.

40. Grose R, Werner S (2004) Wound-healing studies in transgenic and knockout mice. Mol Biotechnol 28: 147-166.

41. Greenman C, Stephens P, Smith R, Dalgliesh GL, Hunter C, et al. (2007) Patterns of somatic mutation in human cancer genomes. Nature 446: 153-158.

42. Cappellen D, De Oliveira C, Ricol D, de Medina S, Bourdin J, et al. (1999) Frequent activating mutations of FGFR3 in human bladder and cervix carcinomas. Nat Genet 23: 18-20.

43. Rosty C, Aubriot MH, Cappellen D, Bourdin J, Cartier I, et al. (2005) Clinical and biological characteristics of cervical neoplasias with FGFR3 mutation. Mol Cancer 4: 15.

44. Hernandez S, de Muga S, Agell L, Juanpere N, Esgueva R, et al. (2009) FGFR3 mutations in prostate cancer: association with low-grade tumors. Mod Pathol 22: 848-856.

45. Knights V, Cook SJ (2010) De-regulated FGF receptors as therapeutic targets in cancer. Pharmacol Ther 125: 105-117.

46. Naski MC, Wang Q, Xu J, Ornitz DM (1996) Graded activation of fibroblast growth factor receptor 3 by mutations causing achondroplasia and thanatophoric dysplasia. Nat Genet 13: 233-237.

47. di Martino E, L'Hote CG, Kennedy W, Tomlinson DC, Knowles MA (2009) Mutant fibroblast growth factor receptor 3 induces intracellular signaling and cellular transformation in a cell type- and mutation-specific manner. Oncogene 28: 4306-4316.

48. Munro NP, Knowles MA (2003) Fibroblast growth factors and their receptors in transitional cell carcinoma. J Urol 169: 675-682.

49. Lopez-Knowles E, Hernandez S, Malats N, Kogevinas M, Lloreta J, et al. (2006) PIK3CA mutations are an early genetic alteration associated with FGFR3 mutations in superficial papillary bladder tumors. Cancer Res 66: 7401-7404.

50. Platt FM, Hurst CD, Taylor CF, Gregory WM, Harnden P, et al. (2009) Spectrum of phosphatidylinositol 3-kinase pathway gene alterations in bladder cancer. Clin Cancer Res 15: 6008-6017.

51. Byron SA, Gartside MG, Wellens CL, Mallon MA, Keenan JB, et al. (2008) Inhibition of activated fibroblast growth factor receptor 2 in endometrial cancer cells induces cell death despite PTEN abrogation. Cancer Res 68: 6902-6907.

52. Nord H, Segersten U, Sandgren J, Wester K, Busch C, et al. (2010) Focal amplifications are associated with high grade and recurrences in stage Ta bladder carcinoma. Int J Cancer 126: 1390-1402.

53. Jacquemier J, Adelaide J, Parc P, Penault-Llorca F, Planche J, et al. (1994) Expression of the FGFR1 gene in human breast-carcinoma cells. Int J Cancer 59: 373-378.

54. Reis-Filho JS, Simpson PT, Turner NC, Lambros MB, Jones C, et al. (2006) FGFR1 emerges as a potential therapeutic target for lobular breast carcinomas. Clin Cancer Res 12: 6652-6662.

55. Freier K, Schwaenen C, Sticht C, Flechtenmacher C, Muhling J, et al. (2007) Recurrent FGFR1 amplification and high FGFR1 protein expression in oral squamous cell carcinoma (OSCC). Oral Oncol 43: 60-66.

56. Gorringe KL, Jacobs S, Thompson ER, Sridhar A, Qiu W, et al. (2007) High-resolution single nucleotide polymorphism array analysis of epithelial ovarian cancer reveals numerous microdeletions and amplifications. Clin Cancer Res 13: 4731-4739.

57. Simon R, Richter J, Wagner U, Fijan A, Bruderer J, et al. (2001) High-throughput tissue microarray analysis of 3p25 (RAF1) and 8p12 (FGFR1) copy number alterations in urinary bladder cancer. Cancer Res 61: 4514-4519.

58. Kunii K, Davis L, Gorenstein J, Hatch H, Yashiro M, et al. (2008) FGFR2-amplified gastric cancer cell lines require FGFR2 and Erbb3 signaling for growth and survival. Cancer Res 68: 2340-2348.

59. Takeda M, Arao T, Yokote H, Komatsu T, Yanagihara K, et al. (2007) AZD2171 shows potent antitumor activity against gastric cancer over-expressing fibroblast growth factor receptor 2/keratinocyte growth factor receptor. Clin Cancer Res 13: 3051-3057.

60. Nakazawa K, Yashiro M, Hirakawa K (2003) Keratinocyte growth factor produced by gastric fibroblasts specifically stimulates proliferation of cancer cells from scirrhous gastric carcinoma. Cancer Res 63: 8848-8852.

61. Li Z, Zhu YX, Plowright EE, Bergsagel PL, Chesi M, et al. (2001) The myeloma-associated oncogene fibroblast growth factor receptor 3 is transforming in hematopoietic cells. Blood 97: 2413-2419.

62. Otsuki T, Yamada O, Yata K, Sakaguchi H, Kurebayashi J, et al. (1999) Expression of fibroblast growth factor and FGF-receptor family genes in human myeloma cells, including lines possessing t(4;14)(q16.3;q32. 3) and FGFR3 translocation. Int J Oncol 15: 1205-1212.

63. Onwuazor ON, Wen XY, Wang DY, Zhuang L, Masih-Khan E, et al. (2003) Mutation, SNP, and isoform analysis of fibroblast growth factor receptor 3 (FGFR3) in 150 newly diagnosed multiple myeloma patients. Blood 102: 772-773.

64. Qing J, Du X, Chen Y, Chan P, Li H, et al. (2009) Antibody-based targeting of FGFR3 in bladder carcinoma and t(4;14)-positive multiple myeloma in mice. J Clin Invest 119: 1216-1229.

65. Trudel S, Stewart AK, Rom E, Wei E, Li ZH, et al. (2006) The inhibitory anti-FGFR3 antibody, PRO-001, is cytotoxic to t(4;14) multiple myeloma cells. Blood 107: 4039-4046.

66. Xiao S, Nalabolu SR, Aster JC, Ma J, Abruzzo L, et al. (1998) FGFR1 is fused with a novel zinc-finger gene, ZNF198, in the t(8;13) leukaemia/lymphoma syndrome. Nat Genet 18: 84-87.

67. Roumiantsev S, Krause DS, Neumann CA, Dimitri CA, Asiedu F, et al. (2004) Distinct stem cell myeloproliferative/T lymphoma syndromes induced by ZNF198-FGFR1 and BCR-FGFR1 fusion genes from 8p11 translocations. Cancer Cell 5: 287-298.

68. Yagasaki F, Wakao D, Yokoyama Y, Uchida Y, Murohashi I, et al. (2001) Fusion of ETV6 to fibroblast growth factor receptor 3 in peripheral T-cell lymphoma with a t(4;12)(p16;p13) chromosomal translocation. Cancer Res 61: 8371-8374.

69. Williams SV, Hurst CD, Knowles MA (2013) Oncogenic FGFR3 gene fusions in bladder cancer. Hum Mol Genet 22: 795-803.

70. Cheng T, Roth B, Choi W, Black PC, Dinney C, et al. (2013) Fibroblast growth factor receptors-1 and -3 play distinct roles in the regulation of bladder cancer growth and metastasis: implications for therapeutic targeting. PLoS One 8: e57284.

71. Mendelsohn J, Baselga J (2006) Epidermal growth factor receptor targeting in cancer. Semin Oncol 33: 369-385.

72. Mendelsohn J, Baselga J (2003) Status of epidermal growth factor receptor antagonists in the biology and treatment of cancer. J Clin Oncol 21: 2787-2799.

73. Yarden Y, Sliwkowski MX (2001) Untangling the ErbB signalling network. Nat Rev Mol Cell Biol 2: 127-137.

74. Olayioye MA, Neve RM, Lane HA, Hynes NE (2000) The ErbB signaling network: receptor heterodimerization in development and cancer. EMBO J 19: 3159-3167.

75. Ennis BW, Lippman ME, Dickson RB (1991) The EGF receptor system as a target for antitumor therapy. Cancer Invest 9: 553-562.

76. Hubbard SR (2005) EGF receptor inhibition: attacks on multiple fronts. Cancer Cell 7: 287-288.

77. Burgess AW, Cho HS, Eigenbrot C, Ferguson KM, Garrett TP, et al. (2003) An open-and-shut case? Recent insights into the activation of EGF/ErbB receptors. Mol Cell 12: 541-552.

78. Franklin MC, Carey KD, Vajdos FF, Leahy DJ, de Vos AM, et al. (2004) Insights into ErbB signaling from the structure of the ErbB2-pertuzumab complex. Cancer Cell 5: 317-328.

79. Salomon DS, Brandt R, Ciardiello F, Normanno N (1995) Epidermal growth factor-related peptides and their receptors in human malignancies. Crit Rev Oncol Hematol 19: 183-232.

80. Schlessinger J (2000) Cell signaling by receptor tyrosine kinases. Cell 103: 211-225.

81. Lewis TS, Shapiro PS, Ahn NG (1998) Signal transduction through MAP kinase cascades. Adv Cancer Res 74: 49-139.

82. Chan TO, Rittenhouse SE, Tsichlis PN (1999) AKT/PKB and other D3 phosphoinositide-regulated kinases: kinase activation by phosphoinositide-dependent phosphorylation. Annu Rev Biochem 68: 965-1014.

83. Vivanco I, Sawyers CL (2002) The phosphatidylinositol 3-Kinase AKT pathway in human cancer. Nat Rev Cancer 2: 489-501.

84. Mendelsohn J (2002) Targeting the epidermal growth factor receptor for cancer therapy. J Clin Oncol 20: 1S-13S.

85. Masui H, Kawamoto T, Sato JD, Wolf B, Sato G, et al. (1984) Growth inhibition of human tumor cells in athymic mice by anti-epidermal growth factor receptor monoclonal antibodies. Cancer Res 44: 1002-1007.

86. Gill GN, Kawamoto T, Cochet C, Le A, Sato JD, et al. (1984) Monoclonal anti-epidermal growth factor receptor antibodies which are inhibitors of epidermal growth factor binding and antagonists of epidermal growth factor binding and antagonists of epidermal growth factor-stimulated tyrosine protein kinase activity. J Biol Chem 259: 7755-7760.

87. Nicholson RI, Gee JM, Harper ME (2001) EGFR and cancer prognosis. Eur J Cancer 37 Suppl 4: S9-15.

88. Goldstein NI, Prewett M, Zuklys K, Rockwell P, Mendelsohn J (1995) Biological efficacy of a chimeric antibody to the epidermal growth factor receptor in a human tumor xenograft model. Clin Cancer Res 1: 1311-1318.

89. Kawamoto T, Sato JD, Le A, Polikoff J, Sato GH, et al. (1983) Growth stimulation of A431 cells by epidermal growth factor: identification of high-affinity receptors for epidermal growth factor by an anti-receptor monoclonal antibody. Proc Natl Acad Sci U S A 80: 1337-1341.

90. Hirsch FR, Varella-Garcia M, Bunn PA, Jr., Di Maria MV, Veve R, et al. (2003) Epidermal growth factor receptor in non-small-cell lung carcinomas: correlation between gene copy number and protein expression and impact on prognosis. J Clin Oncol 21: 3798-3807.

91. Savas P, Hughes B, Solomon B (2013) Targeted therapy in lung cancer: IPASS and beyond, keeping abreast of the explosion of targeted therapies for lung cancer. J Thorac Dis 5: S579-S592.

92. Sharma SV, Bell DW, Settleman J, Haber DA (2007) Epidermal growth factor receptor mutations in lung cancer. Nat Rev Cancer 7: 169-181.

93. Gan HK, Kaye AH, Luwor RB (2009) The EGFRvIII variant in glioblastoma multiforme. J Clin Neurosci 16: 748-754.

94. Jutten B, Rouschop KM (2014) EGFR signaling and autophagy dependence for growth, survival, and therapy resistance. Cell Cycle 13: 42-51.

95. Ferlay J, Shin HR, Bray F, Forman D, Mathers C, et al. (2010) Estimates of worldwide burden of cancer in 2008: GLOBOCAN 2008. Int J Cancer 127: 2893-2917.

96. Siegel R, Naishadham D, Jemal A (2012) Cancer statistics, 2012. CA Cancer J Clin 62: 10-29.

97. Iyer G, Milowsky MI (2013) Fibroblast growth factor receptor-3 in urothelial tumorigenesis. Urol Oncol 31: 303-311.

98. Dinney CP, McConkey DJ, Millikan RE, Wu X, Bar-Eli M, et al. (2004) Focus on bladder cancer. Cancer Cell 6: 111-116.

99. Morgan TM, Keegan KA, Clark PE (2011) Bladder cancer. Curr Opin Oncol 23: 275-282.

100. McConkey DJ, Lee S, Choi W, Tran M, Majewski T, et al. (2010) Molecular genetics of bladder cancer: Emerging mechanisms of tumor initiation and progression. Urol Oncol 28: 429-440.

101. Bernard-Pierrot I, Brams A, Dunois-Larde C, Caillault A, Diez de Medina SG, et al. (2006) Oncogenic properties of the mutated forms of fibroblast growth factor receptor 3b. Carcinogenesis 27: 740-747.

102. Tomlinson DC, Hurst CD, Knowles MA (2007) Knockdown by shRNA identifies S249C mutant FGFR3 as a potential therapeutic target in bladder cancer. Oncogene 26: 5889-5899.

103. Tomlinson DC, Lamont FR, Shnyder SD, Knowles MA (2009) Fibroblast growth factor receptor 1 promotes proliferation and survival via activation of the mitogen-activated protein kinase pathway in bladder cancer. Cancer Res 69: 4613-4620.

104. Tomlinson DC, Baxter EW, Loadman PM, Hull MA, Knowles MA (2012) FGFR1-induced epithelial to mesenchymal transition through MAPK/PLCgamma/COX-2-mediated mechanisms. PLoS One 7: e38972.

105. Knowles MA (2007) Role of FGFR3 in urothelial cell carcinoma: biomarker and potential therapeutic target. World J Urol 25: 581-593.

106. Mellon JK, Cook S, Chambers P, Neal DE (1996) Transforming growth factor alpha and epidermal growth factor levels in bladder cancer and their relationship to epidermal growth factor receptor. Br J Cancer 73: 654-658.

107. Chow NH, Liu HS, Yang HB, Chan SH, Su IJ (1997) Expression patterns of erbB receptor family in normal urothelium and transitional cell carcinoma. An immunohistochemical study. Virchows Arch 430: 461-466.

108. Ruck A, Jakobson E, Bjorkman S, Paulie S (1994) Adaptation of human bladder carcinoma cell lines to serum-free growth. Evidence for autocrine growth stimulation. Anticancer Res 14: 55-60.

109. Ruck A, Paulie S (1997) The epidermal growth factor receptor is involved in autocrine growth of human bladder carcinoma cell lines. Anticancer Res 17: 1925-1931.

110. Ciardiello F, Caputo R, Bianco R, Damiano V, Pomatico G, et al. (2000) Antitumor effect and potentiation of cytotoxic drugs activity in human cancer cells by ZD-1839 (Iressa), an epidermal growth factor receptor-selective tyrosine kinase inhibitor. Clin Cancer Res 6: 2053-2063.

111. Sriplakich S, Jahnson S, Karlsson MG (1999) Epidermal growth factor receptor expression: predictive value for the outcome after cystectomy for bladder cancer? BJU Int 83: 498-503.

112. Mellon K, Wright C, Kelly P, Horne CH, Neal DE (1995) Long-term outcome related to epidermal growth factor receptor status in bladder cancer. J Urol 153: 919-925.

113. Zhang ZT, Pak J, Shapiro E, Sun TT, Wu XR (1999) Urothelium-specific expression of an oncogene in transgenic mice induced the

formation of carcinoma in situ and invasive transitional cell carcinoma. Cancer Res 59: 3512-3517.

114. Kassouf W, Dinney CP, Brown G, McConkey DJ, Diehl AJ, et al. (2005) Uncoupling between epidermal growth factor receptor and downstream signals defines resistance to the antiproliferative effect of Gefitinib in bladder cancer cells. Cancer Res 65: 10524-10535.

115. Shrader M, Pino MS, Brown G, Black P, Adam L, et al. (2007) Molecular correlates of gefitinib responsiveness in human bladder cancer cells. Mol Cancer Ther 6: 277-285.

116. Li S, Schmitz KR, Jeffrey PD, Wiltzius JJ, Kussie P, et al. (2005) Structural basis for inhibition of the epidermal growth factor receptor by cetuximab. Cancer Cell 7: 301-311.

117. Ciardiello F, Caputo R, Bianco R, Damiano V, Fontanini G, et al. (2001) Inhibition of growth factor production and angiogenesis in human cancer cells by ZD1839 (Iressa), a selective epidermal growth factor receptor tyrosine kinase inhibitor. Clin Cancer Res 7: 1459-1465.

118. Busse D, Doughty RS, Ramsey TT, Russell WE, Price JO, et al. (2000) Reversible G(1) arrest induced by inhibition of the epidermal

growth factor receptor tyrosine kinase requires up-regulation of p27(KIP1) independent of MAPK activity. J Biol Chem 275: 6987-6995.

119. Moulder SL, Yakes FM, Muthuswamy SK, Bianco R, Simpson JF, et al. (2001) Epidermal growth factor receptor (HER1) tyrosine kinase inhibitor ZD1839 (Iressa) inhibits HER2/neu (erbB2)-overexpressing breast cancer cells in vitro and in vivo. Cancer Res 61: 8887-8895.

120. Bromberg JF, Wrzeszczynska MH, Devgan G, Zhao Y, Pestell RG, et al. (1999) Stat3 as an oncogene. Cell 98: 295-303.

121. Katoh M (2008) Cancer genomics and genetics of FGFR2 (Review). Int J Oncol 33: 233-237.

122. Paterson JL, Li Z, Wen XY, Masih-Khan E, Chang H, et al. (2004) Preclinical studies of fibroblast growth factor receptor 3 as a therapeutic target in multiple myeloma. Br J Haematol 124: 595-603.

123. Gust KM, McConkey DJ, Awrey S, Hegarty PK, Qing J, et al. (2013) Fibroblast growth factor receptor 3 is a rational therapeutic target in bladder cancer. Mol Cancer Ther 12: 1245-1254.

124. Fukuoka M, Yano S, Giaccone G, Tamura T, Nakagawa K, et al. (2003) Multi-institutional randomized phase II trial of gefitinib for previously

treated patients with advanced non-small-cell lung cancer (The IDEAL 1 Trial) [corrected]. J Clin Oncol 21: 2237-2246.

125. Kris MG, Natale RB, Herbst RS, Lynch TJ, Jr., Prager D, et al. (2003) Efficacy of gefitinib, an inhibitor of the epidermal growth factor receptor tyrosine kinase, in symptomatic patients with non-small cell lung cancer: a randomized trial. JAMA 290: 2149-2158.

126. Guagnano V, Furet P, Spanka C, Bordas V, Le Douget M, et al. (2011) Discovery of 3-(2,6-dichloro-3,5-dimethoxy-phenyl)-1-{6-[4-(4-ethyl-piperazin-1-yl)-phenylamin o]-pyrimidin-4-yl}-1-methyl-urea (NVP-BGJ398), a potent and selective inhibitor of the fibroblast growth factor receptor family of receptor tyrosine kinase. J Med Chem 54: 7066-7083.

127. Gavine PR, Mooney L, Kilgour E, Thomas AP, Al-Kadhimi K, et al. (2012) AZD4547: an orally bioavailable, potent, and selective inhibitor of the fibroblast growth factor receptor tyrosine kinase family. Cancer Res 72: 2045-2056.

128. Wakeling AE, Guy SP, Woodburn JR, Ashton SE, Curry BJ, et al. (2002) ZD1839 (Iressa): an orally active inhibitor of epidermal growth factor signaling with potential for cancer therapy. Cancer Res 62: 5749-5754.

129. Cohen MH, Johnson JR, Chattopadhyay S, Tang S, Justice R, et al. (2010) Approval summary: erlotinib maintenance therapy of advanced/metastatic non-small cell lung cancer (NSCLC). Oncologist 15: 1344-1351.

130. Thatcher N, Chang A, Parikh P, Rodrigues Pereira J, Ciuleanu T, et al. (2005) Gefitinib plus best supportive care in previously treated patients with refractory advanced non-small-cell lung cancer: results from a randomised, placebo-controlled, multicentre study (Iressa Survival Evaluation in Lung Cancer). Lancet 366: 1527-1537.

131. Nakata A, Gotoh N (2012) Recent understanding of the molecular mechanisms for the efficacy and resistance of EGF receptor-specific tyrosine kinase inhibitors in non-small cell lung cancer. Expert Opin Ther Targets 16: 771-781.

132. Herrera-Abreu MT, Pearson A, Campbell J, Shnyder SD, Knowles MA, et al. (2013) Parallel RNA Interference Screens Identify EGFR Activation as an Escape Mechanism in FGFR3-Mutant Cancer. Cancer Discov 3: 1058-1071.

133. Chell V, Balmanno K, Little AS, Wilson M, Andrews S, et al. (2013) Tumour cell responses to new fibroblast growth factor receptor tyrosine

kinase inhibitors and identification of a gatekeeper mutation in FGFR3 as a mechanism of acquired resistance. Oncogene 32: 3059-3070.

134. Kwak EL, Sordella R, Bell DW, Godin-Heymann N, Okimoto RA, et al. (2005) Irreversible inhibitors of the EGF receptor may circumvent acquired resistance to gefitinib. Proc Natl Acad Sci U S A 102: 7665-7670.

135. Kobayashi S, Boggon TJ, Dayaram T, Janne PA, Kocher O, et al. (2005) EGFR mutation and resistance of non-small-cell lung cancer to gefitinib. N Engl J Med 352: 786-792.

136. Yun CH, Mengwasser KE, Toms AV, Woo MS, Greulich H, et al. (2008) The T790M mutation in EGFR kinase causes drug resistance by increasing the affinity for ATP. Proc Natl Acad Sci U S A 105: 2070-2075.

137. Inukai M, Toyooka S, Ito S, Asano H, Ichihara S, et al. (2006) Presence of epidermal growth factor receptor gene T790M mutation as a minor clone in non-small cell lung cancer. Cancer Res 66: 7854-7858.

138. Vikis H, Sato M, James M, Wang D, Wang Y, et al. (2007) EGFR-T790M is a rare lung cancer susceptibility allele with enhanced kinase activity. Cancer Res 67: 4665-4670.

139. Mulloy R, Ferrand A, Kim Y, Sordella R, Bell DW, et al. (2007) Epidermal growth factor receptor mutants from human lung cancers exhibit enhanced catalytic activity and increased sensitivity to gefitinib. Cancer Res 67: 2325-2330.

140. Engelman JA, Zejnullahu K, Mitsudomi T, Song Y, Hyland C, et al. (2007) MET amplification leads to gefitinib resistance in lung cancer by activating ERBB3 signaling. Science 316: 1039-1043.

141. Bean J, Brennan C, Shih JY, Riely G, Viale A, et al. (2007) MET amplification occurs with or without T790M mutations in EGFR mutant lung tumors with acquired resistance to gefitinib or erlotinib. Proc Natl Acad Sci U S A 104: 20932-20937.

142. Kubo T, Yamamoto H, Lockwood WW, Valencia I, Soh J, et al. (2009) MET gene amplification or EGFR mutation activate MET in lung cancers untreated with EGFR tyrosine kinase inhibitors. Int J Cancer 124: 1778-1784.

143. Yano S, Wang W, Li Q, Matsumoto K, Sakurama H, et al. (2008) Hepatocyte growth factor induces gefitinib resistance of lung adenocarcinoma with epidermal growth factor receptor-activating mutations. Cancer Res 68: 9479-9487.

144. Turke AB, Zejnullahu K, Wu YL, Song Y, Dias-Santagata D, et al. (2010) Preexistence and clonal selection of MET amplification in EGFR mutant NSCLC. Cancer Cell 17: 77-88.

145. Ware KE, Marshall ME, Heasley LR, Marek L, Hinz TK, et al. (2010) Rapidly acquired resistance to EGFR tyrosine kinase inhibitors in NSCLC cell lines through de-repression of FGFR2 and FGFR3 expression. PLoS One 5: e14117.

146. Thomson S, Petti F, Sujka-Kwok I, Epstein D, Haley JD (2008) Kinase switching in mesenchymal-like non-small cell lung cancer lines contributes to EGFR inhibitor resistance through pathway redundancy. Clin Exp Metastasis 25: 843-854.

147. Black PC, Brown GA, Inamoto T, Shrader M, Arora A, et al. (2008) Sensitivity to epidermal growth factor receptor inhibitor requires E-cadherin expression in urothelial carcinoma cells. Clin Cancer Res 14: 1478-1486.

148. Choi W, Shah JB, Tran M, Svatek R, Marquis L, et al. (2012) p63 expression defines a lethal subset of muscle-invasive bladder cancers. PLoS One 7: e30206.

149. Marquis L, Tran M, Choi W, Lee IL, Huszar D, et al. (2012) p63 expression correlates with sensitivity to the Eg5 inhibitor ZD4877 in bladder cancer cells. Cancer Biol Ther 13: 477-486.

150. Polyak K, Weinberg RA (2009) Transitions between epithelial and mesenchymal states: acquisition of malignant and stem cell traits. Nat Rev Cancer 9: 265-273.

151. Billerey C, Chopin D, Aubriot-Lorton MH, Ricol D, Gil Diez de Medina S, et al. (2001) Frequent FGFR3 mutations in papillary non-invasive bladder (pTa) tumors. Am J Pathol 158: 1955-1959.

152. Dinney CP, Fishbeck R, Singh RK, Eve B, Pathak S, et al. (1995) Isolation and characterization of metastatic variants from human transitional cell carcinoma passaged by orthotopic implantation in athymic nude mice. J Urol 154: 1532-1538.

153. Sibley K, Stern P, Knowles MA (2001) Frequency of fibroblast growth factor receptor 3 mutations in sporadic tumours. Oncogene 20: 4416-4418.

154. Knowles MA (2008) Novel therapeutic targets in bladder cancer: mutation and expression of FGF receptors. Future Oncol 4: 71-83.

155. Tomlinson DC, Baldo O, Harnden P, Knowles MA (2007) FGFR3 protein expression and its relationship to mutation status and prognostic variables in bladder cancer. J Pathol 213: 91-98.

156. Lamont FR, Tomlinson DC, Cooper PA, Shnyder SD, Chester JD, et al. (2011) Small molecule FGF receptor inhibitors block FGFR-dependent urothelial carcinoma growth in vitro and in vivo. Br J Cancer 104: 75-82.

157. Gozgit JM, Wong MJ, Moran L, Wardwell S, Mohemmad QK, et al. (2012) Ponatinib (AP24534), a multitargeted pan-FGFR inhibitor with activity in multiple FGFR-amplified or mutated cancer models. Mol Cancer Ther 11: 690-699.

158. Miyake M, Ishii M, Koyama N, Kawashima K, Kodama T, et al. (2010) 1-tert-butyl-3-[6-(3,5-dimethoxy-phenyl)-2-(4-diethylamino-butylamino)-pyrido[2,3 -d]pyrimidin-7-yl]-urea (PD173074), a selective tyrosine kinase inhibitor of fibroblast growth factor receptor-3 (FGFR3), inhibits cell proliferation of bladder cancer carrying the FGFR3 gene mutation along with up-regulation of p27/Kip1 and G1/G0 arrest. J Pharmacol Exp Ther 332: 795-802.

159. Bindels EM, Vermey M, De Both NJ, van der Kwast TH (2001) Influence of the microenvironment on invasiveness of human bladder carcinoma cell lines. Virchows Arch 439: 552-559.

160. Wray JA, Sugden MC, Zeldin DC, Greenwood GK, Samsuddin S, et al. (2009) The epoxygenases CYP2J2 activates the nuclear receptor PPARalpha in vitro and in vivo. PLoS One 4: e7421.

161. Dewa Y, Nishimura J, Muguruma M, Jin M, Saegusa Y, et al. (2008) beta-Naphthoflavone enhances oxidative stress responses and the induction of preneoplastic lesions in a diethylnitrosamine-initiated hepatocarcinogenesis model in partially hepatectomized rats. Toxicology 244: 179-189.

162. Rogue A, Lambert C, Josse R, Antherieu S, Spire C, et al. (2011) Comparative gene expression profiles induced by PPARgamma and PPARalpha/gamma agonists in human hepatocytes. PLoS One 6: e18816.

163. Ayers SD, Nedrow KL, Gillilan RE, Noy N (2007) Continuous nucleocytoplasmic shuttling underlies transcriptional activation of PPARgamma by FABP4. Biochemistry 46: 6744-6752.

164. Gillilan RE, Ayers SD, Noy N (2007) Structural basis for activation of fatty acid-binding protein 4. J Mol Biol 372: 1246-1260.

165. Dreyer C, Krey G, Keller H, Givel F, Helftenbein G, et al. (1992) Control of the peroxisomal beta-oxidation pathway by a novel family of nuclear hormone receptors. Cell 68: 879-887.

166. Kassouf W, Chintharlapalli S, Abdelrahim M, Nelkin G, Safe S, et al. (2006) Inhibition of bladder tumor growth by 1,1-bis(3'-indolyl)-1-(p-substitutedphenyl)methanes: a new class of peroxisome proliferator-activated receptor gamma agonists. Cancer Res 66: 412-418.

167. Plissonnier ML, Fauconnet S, Bittard H, Lascombe I (2010) Insights on distinct pathways of thiazolidinediones (PPARgamma ligand)-promoted apoptosis in TRAIL-sensitive or -resistant malignant urothelial cells. Int J Cancer 127: 1769-1784.

168. Fajas L, Fruchart JC, Auwerx J (1998) Transcriptional control of adipogenesis. Curr Opin Cell Biol 10: 165-173.

169. Lefterova MI, Zhang Y, Steger DJ, Schupp M, Schug J, et al. (2008) PPARgamma and C/EBP factors orchestrate adipocyte biology via adjacent binding on a genome-wide scale. Genes Dev 22: 2941-2952.

170. MacDougald OA, Lane MD (1995) Transcriptional regulation of gene expression during adipocyte differentiation. Annu Rev Biochem 64: 345-373.

171. Tontonoz P, Hu E, Spiegelman BM (1995) Regulation of adipocyte gene expression and differentiation by peroxisome proliferator activated receptor gamma. Curr Opin Genet Dev 5: 571-576.

172. Tabas I, Ron D (2011) Integrating the mechanisms of apoptosis induced by endoplasmic reticulum stress. Nat Cell Biol 13: 184-190.

173. Siersbaek R, Nielsen R, Mandrup S (2012) Transcriptional networks and chromatin remodeling controlling adipogenesis. Trends Endocrinol Metab 23: 56-64.

174. Segatto O, Anastasi S, Alema S (2011) Regulation of epidermal growth factor receptor signalling by inducible feedback inhibitors. J Cell Sci 124: 1785-1793.

175. Frosi Y, Anastasi S, Ballaro C, Varsano G, Castellani L, et al. (2010) A two-tiered mechanism of EGFR inhibition by RALT/MIG6 via kinase suppression and receptor degradation. J Cell Biol 189: 557-571.

176. Ying H, Zheng H, Scott K, Wiedemeyer R, Yan H, et al. (2010) Mig-6 controls EGFR trafficking and suppresses gliomagenesis. Proc Natl Acad Sci U S A 107: 6912-6917.

177. Anastasi S, Baietti MF, Frosi Y, Alema S, Segatto O (2007) The evolutionarily conserved EBR module of RALT/MIG6 mediates suppression of the EGFR catalytic activity. Oncogene 26: 7833-7846.

178. Sato T, Gotoh N (2009) The FRS2 family of docking/scaffolding adaptor proteins as therapeutic targets of cancer treatment. Expert Opin Ther Targets 13: 689-700.

179. Kouhara H, Hadari YR, Spivak-Kroizman T, Schilling J, Bar-Sagi D, et al. (1997) A lipid-anchored Grb2-binding protein that links FGF-receptor activation to the Ras/MAPK signaling pathway. Cell 89: 693-702.

180. Stommel JM, Kimmelman AC, Ying H, Nabioullin R, Ponugoti AH, et al. (2007) Coactivation of receptor tyrosine kinases affects the response of tumor cells to targeted therapies. Science 318: 287-290.

Vitae

Tiewei Cheng was born in Wenzhou, China on August 5th, 1982, the son of Qiaosong Cheng and Aixiang Wu. Upon graduating from Wenzhou High School in 2000, he enrolled at Wenzhou Medical College from 2000 to 2005 and earned a doctoral degree in clinical medicine in 2005. He then began his residency at Shanghai Cancer Hospital, Fudan University during 2005 to 2008. In 2008, Tiewei enrolled at the Graduate School of Biomedical Sciences (GSBS) at The University of Texas Health Science Center/MD Anderson Cancer Center to pursue his PH.D. education. During his doctorate work, he worked in Dr. McConkey's lab to investigate FGFR and EGFR targeted therapy in human bladder cancer.